NASA TECHNICAL TRANSLATION NASA TT F-15,990

CARBON-FIBER-REINFORCED POLYMERS AND THEIR THERMAL DECOMPOSITION TO CARBON-CARBON COMPOSITES

A. Bürger

Translation of "Kohlenstoffaser-verstärkte Polymere und deren thermischer Abbau bis zu Kohlenstoff/Kohlenstoff-Verbundwerkstoffen," Karlsruhe University, Machine Building Department, Doctoral Dissertation, 1973, 193 pp.

NATIONAL AERONAUTICS AND SPACE ADMINISTRATION
WASHINGTON, D.C. 20546 OCTOBER 1974

STANDARD TITLE PAGE

1. Report No.	2. Government Accession No.	3. Recipient's Catalog No.
NASA TT F-15,990		

4. Title and Subtitle	5. Report Date
CARBON-FIBER-REINFORCED POLYMERS AND THEIR THERMAL DECOMPOSITION TO CARBON-CARBON COMPOSITES	October 1974
	6. Performing Organization Code
7. Author(s)	8. Performing Organization Report No.
A. Bürger, University of Karlsruhe, Machine Building Department	10. Work Unit No.
9. Performing Organization Name and Address	11. Contract or Grant No.
Leo Kanner Associates Redwood City, California, 94063	NASw-2481
	13. Type of Report and Period Covered
12. Sponsoring Agency Name and Address	Translation
National Aeronautics and Space Administration, Washington, D. C., 20546	14. Sponsoring Agency Code

15. Supplementary Notes

Translation of "Kohlenstoffaser-verstärkte Polymere and deren thermischer Abbau bis zu Kohlenstoff/Kohlenstoff-Verbundwerkstoffen", Karlsruhe University, Machine Building Department, Doctoral Dissertation, 1973, 193 pp.

16. Abstract

Carbon-fiber-reinforced composites with polymeric matrix materials have been developed for applications at higher temperatures. The chemical modification of conventional laminating resins was considered together with the application of new high-temperature resistant polymers and the thermal processing of polymers, taking into account a procedure involving a hardening of the material and a complete thermal decomposition leading to pure carbon. Attention is given to the study of unreinforced polymeric matrices and the preparation and testing of unidirectional fiber-reinforced composites.

17. Key Words (Selected by Author(s))	18. Distribution Statement
	Unclassified-Unlimited

19. Security Classif. (of this report)	20. Security Classif. (of this page)	21. No. of Pages	22. Price
Unclassified	Unclassified	142	

NASA-HQ

Annotation

The subject of this disseration is the development of a carbon-fiber-reinforced composite with a polymeric matrix for application at the highest possible temperatures. In addition to the chemical modification of conventional laminating resins (epoxy resins), the use of phenol and furfuryl alcohol resins not generally employed in lamination processes, and the application of new, high-stability polymers (polyimides), a special study is made of the thermal aftertreatment of these polymers, from curing to their complete decomposition to carbon.

In the first part of the experimental study, the curing and thermal decomposition of unreinforced polymeric matrices are studied and their properties (weight loss, shrinkage, strength, plasticity) in various thermal treatment stages are determined.

The second part of this work covers the production of composites reinforced unidirectionally with carbon fibers and their thermal aftertreatment, leading to the formation of carbon-carbon composites. The effects of the curing- and pyrolysis-shrinkage of matrix materials on the strength properties and the structural integrity of composite systems are studied, and various measures are taken to solve problems arising from matrix shrinkage.

The most important results from this work are summarized on pages 130-135.

This work was performed from May 1966 to July 1972 at the Institute of Chemical Engineering, Karlsruhe / Engineering University. I would like to thank the director of the Institute, Professor Dr. E. Fitzer, for providing the topic and for his valuable support in the performance of this work.

I would like to thank Dr. L. Albert, Director of the Institute of Electron Microscopy, Karlsruhe Engineering University, for his generous support in the preparation of electron micrographs.

I thank all of my colleagues and coworkers at the Institute for their assistance.

TABLE OF CONTENTS

CARBON-FIBER-REINFORCED POLYMERS AND THEIR THERMAL DECOMPOSITION TO CARBON-CARBON COMPOSITES

A. Burger

1. Introduction and research topic

1.1 Introduction to fiber-reinforced composites

The development of fiber-reinforced composites began early /1
in the 1940s with the study of the combined fiberglass/synthetic resin matrix in the U.S. [1]. Systematic further development gained a firm place among construction materials for this composite, which is now finding extensive application in various areas of engineering (e.g. production of equipment, vehicles and ships; aeronautics and astronautics).

Since glass fibers exhibit extremely high tensile strengths but a low modulus of elasticity [2], research work during the last 15 years has concentrated on those fiber materials which promised not only high strength but also a high modulus of elasticity. These primarily included fibers of the elements boron, carbon and beryllium, as well as carbides, nitrides, silicides and oxides. The rapid development of rigid fibers of high tensile strength based on these materials [2 - 4] satisfied conditions for extensive studies in the area of new high-strength, rigid fiber-reinforced composites during the 1960s.

At first, a return was made to the reinforcement of plastics here, making use of the technology of the production and processing of fiberglass-reinforced plastics. Since boron and carbon fibers proved to be of particular technical interest among the modern reinforcing fibers, the development of boron- and carbon-fiber-reinforced plastics was given special preference. Such composites are already being used technically [5]. Their application is limited primarily to aeronautics and astronautics, however, where high strength and low structural weight have such a decisive effect on performace limits that the considerably higher costs of a boron- or carbon-fiber-reinforced plastic mode of construction/2
relative to that of metal or fiberglass-reinforced plastic are considered acceptable.

Probably the most important goal now in the development of the new fiber-reinforced polymers is the raising of maximum permissible utilization temperature. For fiberglass-reinforced epoxy and polyester resins, this temperature is less than 150°C for continuous applications. The reason for this limit is the

---

[1] Numbers in the margin indicate pagination in the foreign text.

low long-term heat resistance of only about 80 - 130°C of the matrix materials [6]. These materials can take higher thermal stress for brief periods, but a further rise in the utilization temperature would also be limited by the glass fibers, since they rapidly lose strength with increasing temperature [2].

The development of the carbon-fiber-reinforced plastics does represent an important advance with regard to rigidity, but not an improvement in heat resistance. The carbon fibers themselves possess excellent mechanical properties up to temperatures of about 2500°C; however, the sustained-use temperature of carbon-fiber-reinforced composites is limited by the thermal stability of the matrix, just as in the case of fiberglass-reinforced plastics.

A matrix of increased thermal stability is required to make use of the high-temperature properties of carbon fibers. In the case of polymeric materials, this goal can be achieved only through either a chemical modification of the conventional laminating resins used to date or the application of new high-temperature-resistant polymers developed in recent years.

While fiber reinforcement was long restricted to plastics, increasing attention has been given in past years to the reinforcement of metallic and ceramic materials. Among the metals, the reinforcement of aluminum appeared to be of prime technical /3 interest because of its low specific gravity and its good electrical conductivity. The development of boron- [7,8] and carbon-fiber-reinforced [9, 10, 11] aluminum and other fiber-reinforced metals [12] is still in its initial stage, however.

Among the ceramic materials, the emphasis in earlier studies was placed on the development of a carbon composite reinforced with carbon fibers [13 - 26], in order to impart even better mechanical properties to carbon materials, with their many excellent physical properties such as low density, extremely high sublimation temperature, good electrical and thermal conductivity, and high resistance to thermal shock.

As can be seen from the above discussion, matrix materials are involved that exhibit different failure behavior. The best reinforcement effect is known to be obtained with ductal matrix materials (thermoplastics, plastically deformable metals). But even with brittle matrix materials we achieve appreciable reinforcing effects, particularly if the modulus of elasticity of the reinforcing component is orders of magnitude higher than that of the matrix component (boron-fiber reinforced epoxy resin). Reference may be made to the energy-consuming pull-out effect, which causes an appreciable obstruction of crack propagation and thus increases impact strength, even in a combination of brittle fibers in a brittle matrix with a small difference in the moduli of elasticity [27, 28]; see also Section 2.31.

1.2. Topic of this work

The topic of this work is the development of carbon-fiber-reinforced composites with polymeric matrix materials which can be used at the highest possible temperatures. The following potential alternatives are available for this: /4

a) chemical modification of conventional laminating resins,

b) application of new high-temperature-resistant polymers,

c) thermal aftertreatment of polymers in both groups.

The work is concerned especially with subproblem b) (polyimides) and particularly c). Thus the emphasis was on studying the thermal aftertreatment of polymers, from curing to their complete thermal decomposition to carbon.

We already know that wetted polymers shrink markedly during thermal aftertreatment. In the case of complete thermal decomposition to pure carbon, linear shrinkage amounts to up to 25%. Aside from the first partial results of this work already published [29, 30, 21], no detailed studies by other authors are available concerning the thermal decomposition of fiber-reinforced wetted polymers to produce carbon-fiber-reinforced articles of carbon, however. The matrix shrinkage accompanying the thermal decomposition of such composites and its effects on composite properties are therefore studied in this paper.

The following polymers were selected as matrices and matrix precursors for this study of carbon-fiber-reinforced polymers and their thermal decomposition to carbon-carbon deposits: epoxied resins, phenolic resin, furfuryl alcohol resins and polyimides.

a) Epoxy resins

The epoxy resins possess excellent room-temperature strength, good chemical and thermal stability, low curing shrinkage and excellent cementing properties. Thus they are already being given preference in technical applications for fiber-reinforced composites. Their properties can be varied within wide limits through the choice of epoxy/hardener components. In this /5 work, the thermal stability of commercial epoxy resins, in particular, was to be improved by modifying the hardener and suitably adapting curing conditions.

b) Phenolic resins

The phenolic resins are used technically primarily for moldable materials. They are generally not used for fiber-reinforced composites, since high molding pressures are needed to harden them without bubbles. To be sure, they are characterized

both by high strength and by good chemical and relatively high thermal stability. In addition, they are considerably less expensive than the epoxy resins and yield high coke residues in complete pyrolysis. These properties also make them appear promising as laminating resins and as matrix raw materials for carbon-fiber-reinforced carbon items. Phenolic resins will therefore be studied intently in this work.

c) Furfuryl alcohol resins

The furfuryl alcohol resins are characterized by their extremely good resistance to chemicals and high heat resistance. These resins are inexpensive and, like the phenolic resins, produce large coke residues upon complete pyrolysis. To date, they have been employed primarily as impregnants in the synthetic carbon industry [31] and as raw materials in the varnish industry [32], as well as for the production of glass-like carbon [33, 34, 35]. In this work, they are used only for comparison with the phenolic resins.

d) Polyimides

The polyimides are among the newly developed high-temperature-/6
resistant plastics and exhibit a sustained temperature resistance of 250 to 300°C. While most high-temperature-resistant plastics are insoluble and infusible and can be processed only with sintering techniques, polyimides can still be handled easily in the form of their soluble and fusible prepolymers. Like the phenolic and furfuryl alcohol resins, they produce high coke yields upon thermal degradation. Various types which recently have become commercially available have been studied both as matrix and as a precursor for the carbon matrix in this work.

Within the scope of this work, a check has primarily been made as to the extent to which the selected polymers are suitable, if at all, as matrices for carbon-fiber-reinforced composites. The following aspects will be taken into consideration here:

a) easy workability
b) good wetting behavior relative to carbon fibers
c) curing without pores

After this preliminary investigation, a special study will be made as to whether the thermal stability of fiber-reinforced polymers can be improved by thermal aftertreatment (aftercuring).

Finally, a study will be made as to whether carbon-fiber-reinforced carbon items can be produced from the composite systems through their complete thermal degradation, and possibilities for overcoming the problems to be expected from matrix shrinkage will be investigated.

2. General aspects of calculating and measuring mechanical properties of fiber-reinforced composites /7

2.1. Structure of fiber-reinforced composites

Fiber-reinforced composites are combined materials -- and consequently heterogeneous in terms of their structure and behavior -- which are taking the place of conventional materials more and more because of their excellent mechanical properties. While the fiber in a composite functions as a reinforcing and stiffening component, the matrix must fulfill the following tasks:

1. It supports and unites the fibers, which have little technical importance as an independent element.

2. It protects the reinforcing component from ambient effects.

3. It isolates the individual fibers from one another and thereby prevents their shearing one another, as well as the propagation of cracks in the brittle phase.

4. It transfers forces acting upon the object from outside to the fibers.

The mechanical properties of fiber-reinforced composites are primarily determined by their geometric and material structure. The partners involved in the structure of a composite must be matched both in their material properties and with regard to the interactions between them. High levels of reinforcement and stiffening can in principle be achieved only if fibers of high strength and high modulus of elasticity are imbedded in ductal matrix materials of low strength and low modulus of elasticity.

The prerequisites for an optimum interaction of matrix and fiber in the composite are, first of all, good matrix wetting behavior with respect to the reinforcing fibers and, secondly, good adhesion between the two components. Damage to the reinforcing material as the result of chemical reactions at the fiber/matrix phase interface or as the result of physical mass transport processes in areas close to the surface is undesirable, since the mechanical properties of the composite are then impaired. /8

The geometry of the heterogeneous structure of fiber-reinforced composites results from the way in which the fibers are imbedded in the matrix material and from the longitudinal extension of the reinforcing component in the composite. Accordingly, we differentiate between a random and an oriented arrangement of reinforcing material and between discontinuous and continuous fiber reinforcement.

Composites with continuous fiber reinforcement oriented parallel to the direction of load exhibit the highest degrees of

reinforcement and stiffening, since all fibers are made use of and the mechanical properties of the fibers are fully exploited because of their unlimited longitudinal extension within the composite.

While external forces can be absorbed and passed on by the fiber ends in the case of continuous fiber reinforcement, they must be transfered to the fibers with the aid of the matrix in the case of discontinuous fiber reinforcement. A condition for force transmission is adequate adhesion between matrix and fiber.

2.2. Prediction of the mechanical properties of composites reinforced unidirectionally with discontinuous and continuous fibers

The exact prediction of the strength behavior of composites with discontinuous fiber reinforcement is very difficult. Several /9
theories exist regarding longitudinal stress distribution in the matrix/fiber interface under an external tensile load in the direction of the fibers, the validity of which could be checked by studies performed on model composites. Holister and Thomas [36] and Broutmann and Krock [37] provide a summary of the basic papers.

Theory and practice indicate that a discontinuous fiber in the composite can be subjected to maximum tension only if its length is equal to or greater than a critical length. For the case of an elastically deformable fiber and matrix, according to Dow [38] and Sutton [39], critical fiber length l_{crit} is found to be

$$l_{crit} = 8.4 \frac{d_F}{B} \qquad (2\text{-}1)$$

where

$$B = \left[\frac{24 \, (G_F/E_F) \, [1 + (x_F/x_M) \, (E_F/E_M)]}{1 - 3(G_F/G_M) + 2(G_F/G_M) \, [(x_F^{-1.5} - 1)(x_F^{-1} - 1)]} \right]^{0.5}$$

and:

d_F = fiber diameter

G_F, F_M = shear moduli of fiber and matrix, resp.

E_F, E_M = moduli of elasticity of fiber and matrix

x_F, x_M = fractions, by volume, of fiber and matrix.

If the fiber deforms elastically and the matrix plastically, according to Kelly and Tyson [40], critical fiber length is found to be:

$$l_{crit} = \frac{\sigma_F \, d_F}{2 \tau} \, . \qquad (2\text{-}2)$$ /10

Where:

σ_F = tensile strength of fiber

d_F = fiber diameter

τ = shear strength between fiber and matrix.

The tensile strength and modulus of elasticity of continuously and discontinuously reinforced composites with a unidirectional arrangement of fibers are calculated by alligation from the relationships [41]:

$$\sigma_{V\,cont} = x_F \sigma_F + x_M \sigma_M^* \quad , \quad x_F > x_{F_{min}} \, , \tag{2-3}$$

$$\sigma_{V\,disc} = x_F \bar{\sigma}_F + x_M \sigma_M^* \quad , \quad x_F > x_{F_{min}} \, , \tag{2-4}$$

where

$$x_{F_{min}} = \frac{\sigma_M - \sigma_M^*}{\sigma_F + \sigma_M - \sigma_M^*} \, ,$$

$$E_{V\,cont} = x_F E_F + x_M \left(\frac{d\sigma_M}{d\varepsilon_M}\right) \tag{2-5}$$

and

$$E_{V\,disc} = E_{V\,cont} \, , \quad l > l_{crit} \tag{2-6}$$

x_F, x_M = fractions, by volume, of fiber and matrix

$x_{F_{min}}$ = minimum fraction of fiber, by volume, which must be exceeded if the composite is to exhibit a higher tensile strength than the matrix without fiber

σ_F, σ_M = tensile strengths of fiber and matrix

σ_M^* = tensile stress in matrix at fiber fracture point

$\bar{\sigma}_F$ = mean tensile strength in fiber which results from the stress profile along the fiber

E_F = fiber modulus of elasticity

$d\sigma_M/d\varepsilon_M$ = slope of matrix stress/strain curve at fiber fracture point /11

l, l_{crit} = length and critical length of fiber

Equations (2-3) through (2-6) apply to an elastically deforming fiber in an elastic or plastic matrix, but only under

the condition that the load be applied in the fiber direction. If the load is applied at an angle to the fiber direction, the mechanical behavior of the composite changes. The composite tensile strength σ_V predicted by equations (2-3) and (2-4) decreases at an $\phi = 0$ —angle $\phi \geq \phi_{crit}$. The relationship for the reduced tensile strength is [41]:

$$\sigma_{V_{\phi>\phi_{crit}}} = \frac{1.5\,\tau_M}{\sin\phi\,\cos\phi} \qquad (2\text{-}7)$$

where

$$\phi_{crit} = tg^{-1}\frac{1.5\,\tau_M}{\sigma_{V_{\phi=0}}}$$

and;

τ_M = shear strength of matrix

ϕ = angle between fiber direction and direction of applied load

ϕ_{crit} = critical angle beyond which composite strength is impaired.

2.3. Measurement of mechanical properties

A knowledge of the mechanical properties of fiber-reinforced composites is a condition for their use as construction materials. Due to the anisotropic nature of the materials, many problems arise in the determination of their strength behavior which do not occur in the testing of conventional materials. /12

The same testing methods generally used for isotropic materials are sometimes applied to fiber-reinforced composites. In addition, test methods are applied which are tailored to the problems associated with composites, e.g., the measurement of interlaminar shear strength (see Section 2.31).

Test methods which are based on the destruction of a specimen and nondestructive test methods are both employed. Due to the anisotropy of fiber-reinforced composites, data concerning the directional dependence of the properties are absolutely necessary.

The standardization of specimens and test conditions is still in its initial stages. Even standards which already exist for fiber-reinforced composites frequently prove to be inadequate [42].

2.31. Survey of test methods

For certain applications, it is sufficient to know the behavior of fiber-reinforced composites under static loads. If these materials are to be widely applied, moreover, it is also necessary to know their behavior under dynamic loads. The most important tests presently applied as standard methods for fiber-reinforced composites are discussed in the following.

a) Tensile test (static test)

It has already been indicated in Section 2.1 that for composites with discontinuous fiber reinforcement, external forces must be transmitted to the fibers via the matrix. Measuring /13
tensile strength thus tells something about the state of bonding between matrix and fibers.

In the case of composites with continuous fiber reinforcement, this information is lost, since the external load is taken up and transmitted by the fibers. The tensile test is still very important, however, in that it provides information as to whether the fibers have been damaged during incorporation into the matrix or whether the matrix itself has caused fiber damage.

Shouldered specimen bars such as those used for testing isotropic materials have proven unusable for testing composites with continuous fiber reinforcement. Due to the high ratio of longitudinal strength to interlaminar shear strength in these materials, necking causes premature failure of the specimens [43]. NOL rings complying with ASTM Standard D 2290-64 T and unnecked flat bars, reinforced at the ends by cementing on metal strips (tabs), have proven themselves.

b) Bending test (static test)

The bending test has the advantages, over the tensile test, that all clamping problems are dispensed with and simple specimen shapes can be used. In addition, the bending test ensures an unequivocal uniaxial state of stress, whereas in the tensile test, the specimen is frequently subjected to multiaxial loads as the result of a certain amount of bearing friction in the specimen mount. Premature failure occurs in such cases, particularly when brittle materials are involved.

When the bending test is performed on continuously reinforced composites, the external load must be transmitted from the matrix to the fiber, so the measurement of bending strength primarily yields information on the structural integrity of the composites. We know from the literature that excessively low strength values /14
are generally determined if ratios of support width to specimen thickness are too small, due to shear deformation on the neutral

axis. In order to measure true values, shear deformation must be reduced to the point that pure tensile or compressive failure occurs. In general, l/d ratios between 40 and 60 are required for this [44].

c) Shear test (static test)

Fiber-reinforced composites are frequently subjected to a shear load, in addition to tensile and compressive loads. Due to the layered structure of these materials, the shear component is very important, since the individual layers can be separated by shear stress. This separation process (delamination) is primarily a function of the state of matrix/fiber bonding.

A quantitative measure of the state of bonding is interlaminar shear strength. Four test methods are known for determining its [45]:

1. tensile shear test (in accordance with ASTM D 2345-65 T)

2. bending shear test (in accordance with ASTM D 2344-65 T)

3. transverse tensile test

4. cutting shear test.

Of the test methods listed, the bending shear test (short beam test) is the simplest to perform and is therefore generally used. The problem associated with this test method is that pure shear failure of the specimen on the neutral axis (delamination) only occurs with a narrowly limited l/d ratio (in general, l/d = 4 to 6). If this range is exceeded, tensile or compressive fracture occurs. With too small an l/d ratio, on the other hand, puncture fracture occurs. Thus, the l/d ratio must always be /15 specified along with bending shear strength. In addition, the fracture pattern must also be considered. If the specimen does not tear on the neutral axis, but puncture, tensile or compressive fracture occurs, the calculated shear strength (see Eq. (2-9), Section 2.32) provides only a minimum value, at which no delamination yet occurs.

d) Impact test (dynamic test)

In contrast to the above static test methods, material fracture with highly reduced deformation occurs in impact tests, due to the high rate of load application [46]. The impact energy consumed in specimen separation, divided by the broken-through specimen cross section, is defined as impact toughness.

The impact toughness of composites is generally tested by the Charpy or Izod method with a pendulum impact machine. The specimens subjected to bending here are usually notched in order

to reduce deformation and thus the absorption of work. Both specimen dimensions and notch dimensions greatly influence the absorption of work. When impact toughness is specified, it should therefore be given with an exact description of the specimen shape used.

Under the action of impact loads, composites generally exhibit a complex fracture behavior. If the fibers are imbedded in the matrix without defects and if adhesion between the two components is good, brittle fracture occurs. In this case, the impact energy consumed in specimen separation is low. If the state of bonding between fiber and matrix is poor, delamination processes occur in the specimen and the fibers are also pulled out of the matrix (pull-out effect); this is connected with a high consumption of impact energy [47].

e) Fatigue test (dynamic test) /16

The test methods covered so far are limited to a study of the behavior of composites under a single load. The fatigue test, on the other hand, is used to study the behavior of materials under alternating dynamic loads. Production effects are manifested primarily under alternating dynamic loads, so the results of fatigue tests simultaneously provide information on the quality of the production method.

It is known from studies on carbon-fiber-reinforced plastics that the tolerable alternating torsional or bending load is still about 50% of the static fracture load after 10^6 load cycles [48]. Fiber-reinforced composites thus likewise prove to be high-performance materials with regard to their dynamic properties.

f) Ultrasonic test (dynamic test)

Of the conventional nondestructive materials tests, ultrasonic testing has primarily been adopted for fiber-reinforced composites. The following methods of ultrasonic testing are used [49]:

1. resonance method (in accordance with ASTM E 113 - 55T)

2. pulse reflection method (in accordance with ASTM E 114 - 63 and ASTM E 214 - 63T)

3. transmission method

All three methods prove to be usable for determining defects in specimens. Cracks, cavities and bonding defects can be localized very precisely with their aid.

The determination of dynamic elastic constants of composites by means of ultrasonic methods has so far proved to be

problematical. The geometric structure of these materials and their fiber and air-bubble content affect sonic velocity considerably, so the data obtained exhibit high dispersion [47]. /17

2.32. Measurement methods used in this work.

Of the test methods listed in Section 2.31, the tensile and bending tests and the bending shear tests were used to evaluate the strength behavior of unidirectionally reinforced composites. A tensile test was the only method used in the case of matrix materials. All measurements were performed at room temperature.

a) Tensile test

The tensile strength and moduli of elasticity of the composites and of the matrix materials were determined from graphs of force versus change in length, taken with a type TM-ML electronic tensile testing machine by Instron, England. Length change was measured with a type G-51-11 M strain pickup by Instron, with a resolution of 1:1000. The rate of load application was 0.1 cm/min. The gauge length of the specimen bars was 70 mm; grip length was between 25 and 50 mm.

In order to avoid a high surface pressure on the specimens in the gripping device as the result of poor frictional linkage and thus to prevent clamping fractures, frictional linkage was improved by lining the metal clamps with Pegulan (soft PVC) and by cementing the specimens to the gripping faces with medium-fine emery paper and UHU-Plus.

b) Bending test /18

The bending tests (three-point bending) were performed on a type Z 423 bending test machine by Zwick, Einsingen. A span to specimen thickness ratio of 40:1 was chosen. Test speed was 0.16 cm/min; the bending ram used had a radius of curvature of 4 mm. Composite bending strength was calculated with the expression:

$$\sigma_B = \frac{3}{2} \frac{P_{max} \cdot L_s}{b\, d^2} \left[kp/mm^2\right], \qquad (2\text{-}8)$$

where:

P_{max} = maximum load force on specimen [kp]

L_s = span [mm]

b = width of specimen bar [mm]

d = thickness of specimen bar [mm]

kp = kilogram force

c) Bending shear test

Interlaminar shear strength was measured in a bending test (three-point bending) with a shortened support distance. The span to specimen thickness ratio was 5:1. The small spans were compensated for with a specially constructed ram with a radius of curvature of 1.5 mm. The test speed selected was 0.16 cm/min. The interlaminar bending shear strength of the composites was calculated with the expression [45]

$$\tau_B = 0.75 \frac{P_{max}}{b\,d} \left[kp/mm^2\right] \qquad (2\text{-}9)$$

where:

P_{max} = maximum load force on specimen [kp]

b = width of specimen bar [mm]

d = thickness of specimen bar [mm]

Dispersion of data /19

The values given for the mechanical properties of composites and matrix materials represent means from ten individual measurements in each case. Maximum mean error in the mean is ± 5%.

3. Characterization of the starting materials used /20

3.1. Matrix materials

3.11. Survey of the thermal stability and mechanical properties of polymeric materials

Polymers can be divided into two classes, corresponding to their behavior in heat. We thus distinguish between thermoplastics and thermosets. Thermoplastics consist of linear or branched macromolecules which are held together by intermolecular forces but not by chemical bonds. The chain-like molecules can shift relative to one another; the mobility of the chains can be increased by raising the temperature. When heated sufficiently, the thermoplastics soften until plastic flow occurs. Upon cooling, they return to their original state, provided chemical degradation has not occurred as the result of excessive temperatures [50, 51].

The dimensional stability of thermoplastics when heated is determined by the mobility of the chain molecules. In addition to temperature values determined by conventional test methods, "glass temperature" can be used as a measure of high-temperature dimensional stability. It possesses the advantage that it represents a quantity which is unequivocally defined physically as a phase-transition temperature [52].

Thermosets consist of chain-like macromolecules which possessed chemically active points on the chains. During curing, cross-linking has occurred, i.e., molecular chains have become bonded to one another at the chemically active sites by bridging members to form a three-dimensional network. Displacement of the molecules as in the case of thermoplastics is no longer possible. The cross-linked thermosets can no longer soften even if heated [50, 51].

In addition to the question of a polymer's high-temperature dimensional stability, its chemical stability at high temperature is of great importance. We know that both thermoplastics and thermosets decompose when heated; not only the temperature but also the time decisively affects decomposition. While the thermosets can be subjected to brief thermal loads considerably above their decomposition temperatures, their sustained-use temperatures are far below the decomposition temperatures. In the case of thermoplastics, the maximum utilization temperatures are on the order of their softening temperatures, even under brief thermal loads. /21

Table 1 provides a survey of the thermal and mechanical properties of conventional plastics. Due to their low sustained-temperature stability, these products are subject to narrow limits in their use as construction materials. Intense efforts to increase heat-resistant polymers have led to the development of a series of new high-temperature-resistant plastics.

These new developments are primarily semiconductor polymers with heterocyclic building blocks. In general, they are non-cross-linked and thus belong in the thermoplastics category [53]. Due to the highly polar groups in the polymer chains, interactions between the chains are so strong, however, that the glass temperatures of these polymers are above their decomposition temperatures. Known representatives of these new heat-resistant materials include the polysulfones, polyimides and polybenzimidazoles listed in Table 2, which are already being employed in industry. Their sustained-use temperatures lie between 200 and 300°C. Like all polymers, these new types are sensitive to oxidation, and it is necessary to distinguish between maximum application temperatures in air and in inert gas.

3.12. Resins used /25

Conventional and new, high-temperature-resistant plastics were sought for this work. Of the conventional plastics, epoxy resins, phenolic resins and furfuryl alcohol resins were used from the thermosetting class. The reasons for choosing these resins have already been given in Section 1.2.

Of the epoxy resin group, a mixture of the two technical epoxy resins Epikote 828 and 1031 by Shell Chemie, Hamburg, 1:1,

TABLE 1. PROPERTIES OF CONVENTIONAL PLASTICS

Class	Group	Sustained-use temperature [°C]	Dimensional stability (Martens) [°C]	Density [g/cm³]	Tensile strength at RT [kp/mm²]	Modulus of elasticity at RT [kp/mm²]	Elongation at fracture, at RT [%]
Thermoplastics	Polyvinyl chloride and copolymers [54]	50- 60	40- 70	1.19-1.40	1.4-6.0	0.5-300	20- 400
	Polystyrene and copolymers [54]	63- 85	63- 77	1.05-1.08	3.0-7.5	330+	3- 30
	Polyethylenes [54]	80- 95	40++	0.92-0.97	1.0-3.3	20-140	200-1000
	Polymethyl methacrylates and copolymers [54]	75-100	80-105	1.17-1.18	7.0-9.0	320-480	3- 60
	Polyimides [54]	80-100	50+++	1.06-1.15	3.0-7.0	150-240	60- 250
	Polycarbonates [54]	135-140	115-127	1.20	6.2-6.7	220-250	80

\+ Standard types
++ High-pressure polyethylenes with densities of 0.92 - 0.93 g/cm³
+++ 6-polyimide (Perlon)

TABLE 1, continued

Class	Group	Sustained-use temperature	Dimensional stability (Martens)	Density	Tensile strength at RT	Modulus of elasticity at RT	Elongation at fracture, at RT
Thermosets	Phenolic resins [55]	70-100	> 40	1.21-1.30	2 - 8	100-900	0.5-6.0
	Melamine resins [55]	100	>125	1.48	1 - 10	ca. 900	0.5-1.0
	Epoxy resins [55]	100 (80-130) (6)	105-125	1.20-1.30	4 - 8	350-450	1 - 2
	Unsaturated polyester resins [55]	90-150 (80-120) (6)	40- 85	1.20-1.40	2 - 6	200-550	1.5-2.5
	Furan resins [56]	180++++	-	-	-	-	-
	Silicone resins [57]	230-260 (140-200) (6)	-	1.6 -1.9	2.8-3.5	-	-

++++ Distortion temperature in accordance with ASTM 648-45T

TABLE 2. PROPERTIES OF NEW PLASTICS STABLE AT ELEVATED TEMPERATURES

Category	Group	Commercial name	Manufacturer	Sustained use temperature [°C]	Dimensional stability (Martens) [°C]	Density [g/cm³]	Tensile strength at RT [kp/mm²]	Modulus of elasticity at RT [kp/mm²]	Elongation at fracture, at RT [%]
Single-coordination polyaromatics	Polysulfones	Polymer 360 [53]	Minnesota Mining	200-250	-	1.36	9.1	260	10
Heterocyclic polyaromatics	Polyimides	P 13 N [58]	Ciba-Geigy	250	-	1.33	7.7	390	2.5
		Kapton [53]	Du Pont	240-260	340 (ASTM D 648)	1.42	9.5	270	90
		Vespel SP-1 [59]	Du Pont	260	250 (ASTM D 648)	1.43	7.4	-	5-6
	Polybenzimidazoles [53]	-	-	250-300	-	-	12	280	-

was used. Epikote 828 is a liquid resin based on epichlorohydrin and diphenylolpropane. Its epoxy value (moles epoxy per 100 g resin) is 0.51 to 0.55. Epikote 1031 is a solid resin, melting at about 80°C, based on epichlorohydrin and tetraphenylolethane, with an epoxy value of 0.42 to 0.48. While the required mechanical properties are obtained with Epikote 828, Epikote 1031 improves heat resistance. Acid anhydrides are preferably used as curers for the Epikote resins, since they promise optimum cross-linkage and thus good mechanical properties.

Of the phenolic resin group, a commercial resole was used: solid Phenodur PR 373 (formerly Phenodur 373 U) by Reichhold-Albert-Chemie, Wiesbaden. The resin melts about 80°C and is thermally curable, only. In the uncured state it is soluble in alcohol, esters, ketones and glycol ethers.

Of the furfuryl alcohol resin group, a commercial furfuryl alcohol resin, Furesan by Hüttenes, Düsseldorf-Heerdt, and a furfuryl alcohol / formaldehyde resin developed at the Institute (molar ratio of furfuryl alcohol to formaldehyde, 3:2) [34] were used. Both are liquid resins which are cured with acid catalysts.

Of the new high-temperature-resistant plastics, non-cross- /26
linked polyimides were sought from the heterocyclic aromatic group. Only incomplete data are available on the chemical nature of the polyimides. Basically, they are condensates of aromatic diamines and tetracarboxylic acid anhydrides [53] which are used in the form of their prepolymers in solution. The amide carboxylic acid formed as an intermediate is not cyclized until the curing step.

DuPont's first products are built up from pyromellitic dianhydride and 4,4'-diaminodiphenylmethane or 4,4'-diaminodiphenyl ether:

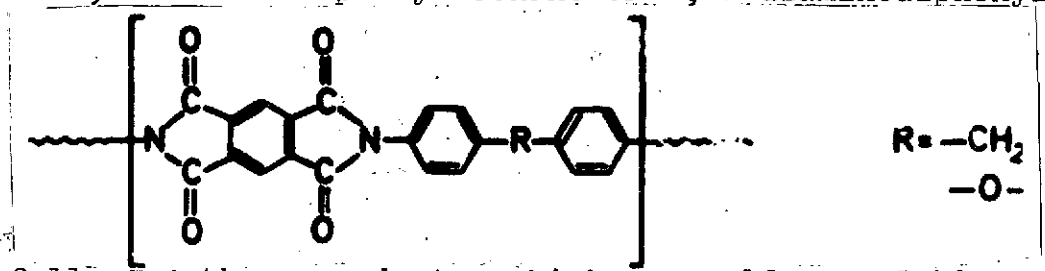

The following three products, which are sold as soluble prepolymers, were used in this work:

1. Polimide P 13 N by CIBA-Geigy, Basel, available in a ca. 40% dimethylformamide (DMF) solution. The polymer is synthesized from nadic anhydride, methylenedianiline and benzophenonetetracarboxylic dianhydride:

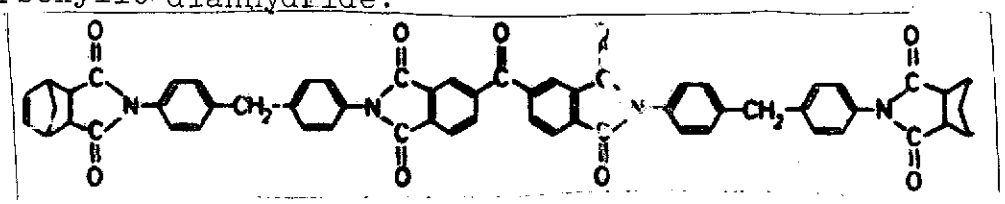

Curing takes place via the reactive end groups.

2. Kerimid 601 polyimide by Rhône-Poulenc, Paris. This resin is available as a fine powder and is very soluble in polar solvents, e.g., N-methyl-2-pyrrolidone (NMP). This polyimide is a poly-bis-maleimide of the following formula: /27

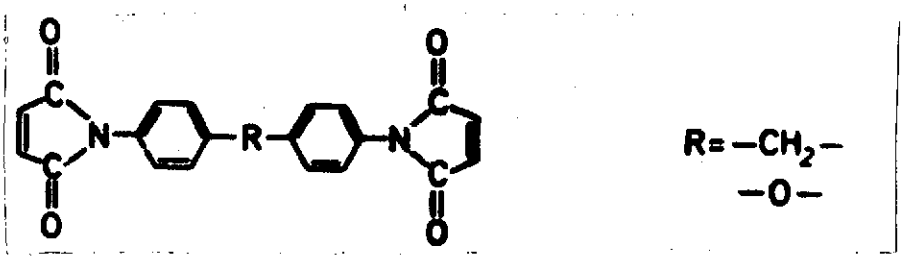

It is cured in an addition reaction without the formation of volatile components.

3. Polyimide QX-13 by Imperial Chemical Industries (ICI), England, a powder. Suitable solvents include acetone and ethyl methyl ketone. As a variant, the prepolymer can contain an acetylated amine, causing the elimination of acetic acid during curing.

3.2. Carbon fibers

3.21. Survey of technology and properties

Carbon fibers are produced by the controlled thermal degradation of synthetic organic fibers. Suitable starting materials include only those fibers which do not melt during pyrolysis and which ensure a high carbon yield. Regenerated cellulose (rayon), polyacrylonitrile and, very recently, pitch are the starting materials used to produce commercially available carbon fibers.

Carbon fibers are generally produced in three steps [60]: /28

Step I : Pretreatment (up to about 300°C)
Step II : Coking (up to about 1200°C)
Step III : Graphitization (up to about 2800°C)

The first step includes stretching and cross-linking the textile fibers. Thermal decomposition of the fiber materials has already begun in this step.

In the second step, the pretreated fibers are decomposed thermally in a vacuum or in an inert gas atmosphere to produce "carbon fibers." Their carbon content is 91 - 98% [2].

During the third step, the carbon fibers are converted into so-called "graphite fibers." The carbon content of the graphite fibers is more than 98% [2]. According to Roland [61], the graphite fiber is made of wavy bundles of parallel-packed, ribbon-like planes of carbon hexagons which extend over a length of several thousands of Angstroms in the direction of the fiber. Subjecting the fibers to a stretching treatment in the carbon's plastic temperature range can be used to enhance the orientation of the wavy ribbons in the fiber's longitudinal direction, thereby increasing the modulus of elasticity and tensile strength of the fiber [60].

Today, carbon fibers are largely manufactured by continuous methods and are available commercially as yarns and rovings with 1440 to 10000 individual fibers. The properties of various commercially available carbon fibers can be seen from Table 3. The products exhibit different characteristics, depending on the degree of carbonization and stretching. The effect of the starting material on the mechanical properties of carbon fibers is of lesser importance. Regardless of the raw materials used, approximately equivalent maximum values for tensile strength and modulus of elasticity can be obtained. Density is merely higher in carbon fibers of polyacrylonitrile.

The geometric profiles of carbon fibers correspond to /31
those of their starting fibers, since a fiber shape is retained during thermal decomposition. Carbon fibers of dry-spun polyacrylonitrile exhibit a kidney-shaped cross section. Carbon fibers of wet-spun polyacrylonitrile and carbonized pitch fibers possess a circular cross section. The surface of pitch fibers is smooth, whereas polyacrylonitrile fibers are slightly wavy in the radial direction. Pyrolized rayon fibers have a square to round cross section, and their surface is covered with deep fluting in the axial direction.

The high sensitivity of carbon fibers to abrasion forces the manufacturers to cover almost all of their products with a thin protective film. A coating of polyvinyl alcohol is common. The PVA film can be rinsed off in boiling water or evaporated by heating.

In addition to the standard types, fiber producers frequently offer a type of fiber in their line which is characterized by a special surface treatment. Adhesion between fiber and polymer matrix is considerably increased by this additional production step, without the other properties of the fiber being thereby impaired. While the fiber manufacturers do not provide any information regarding the type of surface treatment, various measures for improving adhesion are described in the literature. Possibilities include partial oxidation and the whiskering of fibers [63]. Covering the fiber surface with reactive groups such as carboxyl groups likewise proves to be a useful method [64].

TABLE 3. PROPERTIES OF CARBON FIBERS AT ROOM TEMPERATURE

Manufacturer	Starting material	Type	Fiber diameter [μ]	Density [g/cm³]	Carbon content [wt. %]	Specific surface area [m²/g]	Tensile strength [kp/mm²]	E Modulus · 10^{-3} [kp/mm²]	Elongation at fracture [%]
Union Carbide Corp. (USA)	Regenerated cellulose	VYB+	9.5	1.53	90.0	130	84	4.2	2.0
		WYB++	8.9	1.32	98.8	<4	63	4.2	1.5
		Thornel 25++	7.4	1.40-1.45	99.1	4	126	17.5	0.7
		Thornel 50++	6.6	1.63	99.9	1	200	35.0	0.6
		Thornel 75++	5.8	1.86	99.9	1	263	52.5	0.5
Sigri GmbH (Germany)	Polyacrylonitrile	Sigrafil+	8.2	1.70	-	-	165	17.5	0.9
Morganite Modmor Ltd. (England)	Polyacrylonitrile	I+	7.0-8.0	1.90	-	-	140-210	39.0-46.0	-
		II+	7.0-8.0	1.70	-	-	250-320	25.0-32.0	-
Courtaulds Ltd. (England)	Polyacrylonitrile	Grafil A+	9.2	1.75	-	-	175-210	17.5-22.5	-
		Grafil HM+	8.2	1.95	-	-	175-245	35.0-42.0	-
		Grafil HT+	8.9	1.80	-	-	210-280	22.5-28.0	-

\+ Designated "carbon fiber" by manufacturer
++ Designated "graphite fiber" by the manufacturer

TABLE 3 continued

Manufacturer	Starting material	Type	Fiber diameter [μ]	Density [g/cm³]	Carbon content [wt.%]	Specific surface area [m²/g]	Tensile strength [kp/mm²]	E Modulus 10^{-3} [kp/mm²]	Elongation at fracture [%]
Kureha Chemical Industry Co., (Japan)	Pitch	**Kureha carbon fibre**+	**7.5**	**1.61**	**99.5**	-	**112**	**7.0**	**1.8**
Universität von Britisch Columbia (Vancouver, Canada) [62]	Pitch	Experimental product ++	**8.0-25.0**	**1.77**	-	-	**260**	**63.0**	-

\+ Designated "carbon fiber" by manufacturer
++ Designated "graphite figer" by the manufacturer

3.22. Fibers used

Carbon fibers based on cellulose, produced by Union Carbide Corp., and carbon fibers made from polyacrylonitrile, produced by Courtaulds, Ltd., England, were used in this work. /32 Characteristics of the carbon yarns employed are summarized in Table 4. The properties of the individual fibers can be obtained from Table 3 (see Section 3.21).

All carbon fibers were used as supplied. A special cleaning treatment for the Thornel fibers coated with polyvinyl alcohol proved to be unnecessary, since the yarns were permeated well by the matrix materials.

4. Curing and thermal degradation of matrix materials /34

Specimens free of cracks and pores are an important condition for the clean characterization of matrix material properties in various stages of curing and pyrolysis. The conditions for preparing satisfactory molded pieces of the thermosets and polyimides characterized in Section 3.12 were therefore first determined in preliminary tests.

With the exception of Furesan technical furfuryl alcohol resin, it was possible to determine a suitable curing schedule for each of the resins with which defect-free molded pieces with wall thicknesses between 2 and 6 mm could be prepared. Furesan was consequently left out of further experiments.

4.1. Thermosets

4.11. Preparation of molded specimens

Molded specimens were prepared by casting the resins in molds and then curing them at elevated temperatures. It was found desirable to remove the castings of the resins studied from their molds prior to complete curing and to machine them with cutting tools while still in the partially cured stage. The fully cured resins exhibited high brittleness and tended to spall and break during machining.

The Epikote resin mixture was cured by adding pyromellitic dianhydride, which, due to its high melting point of 285°C, could only be used in dissolved form. A 1:1 mixture of ethanol and ethyl acetate was used for the solvent. The following composition proved to be usable: /35

50 g Epikote 828
50 g Epikote 1031
16.6 g pyromellitic dianhydride in 120g solvent mixture

TABLE 4. ROOM TEMPERATURE PROPERTIES OF THE CARBON YARNS USED

Type of yarn	VYP 105-1/5 (UCC)	WYB 125-1/5 (UCC)	Thornel 25 WYD 115-1/2 (UCC)	Thornel 50 WYG 130-1/2 (UCC)	Grafil HM* (Courtaulds Ltd.)	Grafil HT* (Courtaulds Ltd.)
Degree of treatment	coked	graphi-tized	stretch-graphi-tized	stretch-graphi-tized	coked	coked
Finish	-	-	PVA	PVA	-	-
Yarn diameter [mm]	1.02	1.02	0.46-0.56	0.38	n.a.	n.a.
Fiber count	2400	2400	1440	1440	10 000	10 000
Ultimate strength [kp]	8.6	4.5	3.6	2.9	n.a.	n.a.
Elongation [%]	3.2	1.4	0.7	0.53	n.a.	n.a.

* Unspun roving

The resin mixture, combined with hardener solution, was cast into molds and initially placed under a water-aspirator vacuum at 80°C for 1/2 h in a vacuum drybox in order to remove a large portion of the solvent. It was then initially cured in air with the following temperature program:

2 days at 80°C
3 days at 90°C
4 days at 100°C
6 days at 110°C
1 day at 120°C
4 days at 140°C

Full curing of the resin castings was carried out in four temperature stages:

Stage I: 3 days at 180°C (in air)
Stage II: 3 days at 220°C (in air)
Stage III: 3 days at 250°C (in nitrogen)
Stage IV: 2.5 days at 300°C (in nitrogen)

Solid Phenodur PR 373 was cured thermally, only, i.e., without catalysts. Since the fusion process and curing reaction overlap for this resin, it had to be made into castings in the dissolved state. A 60 wt.% solution of the resin in n-butyl alcohol, just barely castable at room temperature, proved to be satisfactory.

The resin solution, cast in molds, first had a portion of the solvent removed from it in the vacuum drybox at 100°C under water-aspirator vacuum for 1/2 h and was then partially cured in air for 24 h at 100°C and 90 h at 110°C. The resin specimens were fully cured to 800°C in an ultrapure nitrogen atmosphere /36 at a heating rate of 12°C/h.

Furfuryl alcohol / formaldehyde resin was cured catalytically with 0.1 wt.% p-toluenesulfonic acid, added in the form of a 10% solution in methanol. After the cast resin/hardener/system was degassed for 1/2 h at 70°C in the vacuum drybox under aspirator vacuum, the following initial curing schedule was applied in air:

3 days at 70°C
1 day at 80°C
2.5 days at 90°C

The resin specimens were fully cured to 210°C in an ultrapure nitrogen atmosphere at a heating rate of 12°C/h.

4.12. Properties of the cured castings

Rough bar-shaped specimens were sawed out of the partially cured resin castings (plates measuring 315 X 185 X 5 mm) for

TABLE 5. PROPERTIES OF THE THERMOSETS STUDIED, AS FUNCTIONS OF CURING TEMPERATURE (MEASURED AT ROOM TEMPERATURE)

Resin/hardener system	Abbreviated designation	Curing temperature [°C]	Weight loss [%]	Linear shrinkage [%]	Tensile strength [kp/mm²]	Modulus of elasticity [kp/mm²]
Epoxy resin mixture of Epikote types 828 and 1031 (1:1 by weight) / pyromellitic dianhydride	EO	140	0	0	5.3	260
		220	9.3	4.4	7.3	325
		300	30.2	8.9	5.3	365
Phenodur PR 373 (formerly Phenodur 373 U) phenolic resin / self-curing	PH	110	0	0	2.8	135
		210	8.6	4.9	6.7	340
		300	21.9	10.1	10.8	510
Furfuryl alcohol formaldehyde resin (3:2 molar ratio) / p-toluenesulfonic acid	PA	90	0	0	7.3	365
		210	3.8	0.8	7.0	390

determining weight loss and shrinkage and for measuring mechanical properties. The rough specimens were then surface-milled with hard metal cutting tools to produce smooth specimen surfaces. The final dimensions of the specimen bars were 150 X 10 X 2 mm.

The thermoset properties studied are compiled in Table 5 for various curing temperatures. In determining weight loss, it appeared desirable not to start with the liquid resins but from the initially cured resins, since with the exception of furfuryl alcohol / formaldehyde resin, they had been prepared in dissolved form. Thus the weight loss of the resins during initial curing was not taken into consideration.

Due to their volatile reaction products, the partially cured thermosets experience increasing weight loss as curing progresses, particularly high for the phenolic resin and the epoxy resin mixture. Solvent remaining in the partially cured resin castings and evaporating during curing contributes to the high weight loss. /38

The extremely high weight loss of 30% in the case of fully cured epoxy resin mixture has the following explanation: damage to the highly cross-linked resin structure is already occurring during long-term curing at 300°C, producing an increase in weight loss.

Longitudinal contraction of the resins during initial curing is less than 0.1% and can therefore be neglected. Much as in the case of weight loss, linear shrinkage increases with curing temperature. The phenolic resin and the epoxy resin mixture are likewise considerably above the furfuryl alcohol / formaldehyde resin with regard to longitudinal contraction. The epoxy resin mixture exhibits less shrinkage than the phenolic resin, in spite of its higher weight loss.

The effect of curing temperature on the tensile strength and the moduli of elasticity of the thermosets varies considerably. In the case of phenolic resins, full curing at elevated temperatures produces a considerable increase in tensile strength. For the epoxy resin mixture, a rise in strength can likewise initially be detected, but it is lost again during the last curing step at 300°C. This drop in strength can be interpreted as the first indication of damage to the highly cross-linked resin structure as the result of long-term curing. The tensile strength of furfuryl alcohol / formaldehyde resin does not change appreciably during the curing stages studied, in contrast to the thermosets discussed above.

While no uniform trend is observed for tensile strength, the modulus of elasticity increases with curing temperature as the result of progressive cross-linkage. Approximately the same tensile strength and the same modulus of elasticity are obtained for resin/hardener systems studied after curing at 210 to 220°C. /39

4.13. Chemical decomposition of castings to vitreous carbon

4.131. Survey of the thermal decomposition of polymers to vitreous carbon

Vitreous carbon represents a new form of elementary carbon, the development of which began at the end of the 1950s. In searching for a carbon impervious to gas in 1962, a Japanese research group [65] and, at about the same time, Davidson [66] succeeded in preparing castings of vitreous carbon which exhibited not only extremely low permeability but also a series of other remarkable properties, such as low density, high strength and good resistance to oxidation. While Davidson produced his vitreous carbon from cellulose by thermal decomposition, the Japanese used another starting material, about which they provided no detailed information, however.

The intense interest which has been shown for vitreous carbon on the part of research and industry since it became known is manifest in numerous patents and publications. Yamada [67] and Chekanova and Fialkov [68] provide a comprehensive survey of the level of knowledge in the field of vitreous carbon at those times. According to them, the production of vitreous carbon is principally based on a controlled solid-state pyrolysis of certain organic polymers. In addition to cellulose, three-dimensionally cross-linked thermosets such as phenolic and furan resins are given in the literature as starting materials.

One paper which covers the thermal decomposition of thermo- /41
sets to vitreous carbon in detail is Schäfer's dissertation [34]. The content of this work is the characterization of the thermoset pyrolysis mechanism and a study of the effect of the starting resin and pyrolysis on the ultimate properties of the vitreous carbon. Of the thermosets studied by Schäfer, two have been used in the present work, namely Phenodur PR 373 phenolic resin (formerly Phenodur 373 U) and furfuryl alcohol / formaldehyde resin (3:2 molar ratio of furfuryl alcohol to formaldehyde). The above dissertation thus serves as a guide for performing the thermal decomposition of resins cured as described in Section 4.11 and also for interpretation of the results of the present study.

Castings of vitreous carbon are presently being produced in limited amounts by several firms. The most important physical properties of such industrial products are summarized in Table 6. Although vitreous carbon is produced from various types of raw materials and by various methods, the carbonized end products always exhibit properties typical of them. It belongs to the category of so-called paracrystalline carbons and exhibits completely isotropic behavior.

TABLE 6. PHYSICAL PROPERTIES OF INDUSTRIAL VITREOUS CARBONS AT ROOM TEMPERATURE

Designation	Glassy Carbon [69]			Cellulose Carbon [70]	Vitreous Carbon [71]	Sigradur [72]	LMSC Glass-Like Carbon [73]	
	GC-10	GC-20	GC 30				2000	3000
Treatment temp. [°C]	1300	2000	3000	1700	-	-	2000	3000
Density [g/cm³]	1.48-1,51	1.47-1,50	1.44-1.47	1.55	1.47	1.5	1.43-1.50	1.36-1.42
Porosity [%]	0.2-0.4	1 - 3	3 - 5	-	<0.05	-	-	-
Gas permeability [cm²/s]	10^{-11}-10^{-12}	10^{-10}-10^{-12}	10^{-7}-10^{-9}	10^{-12}	$<2{,}5\cdot10^{-11}$	10^{-11}	10^{-10}-10^{-12}	10^{-7}-10^{-9}
Tensile strength [kp/mm²]	-	4.5	4.2	-	-	-	12 - 20	11 - 20
Young's modulus · 10^{-3} [kp/mm²]	3.0 - 3.3	3.0 - 3.3	2.5-2.5	2.8	2.1-2.8	2.6	2.8	2.4
Bending strength [kp/mm²]	9 - 10	10 - 12	5 - 6	18	7 - 21	7	13 - 16	9 - 11
Shore hardness	110-120	100-110	70-80	95	-	120	-	-
Thermal conductivity [kcal/mh°C]	3 - 4	7 - 8	13 - 15	3.6	3.6-7.2	3	3.6	4.3
Electrical resistivity · 10^4 [Ωcm]	45 - 50	40 - 45	35-40	40	30 - 80	50	168	18

TABLE 7. WEIGHT LOSS AND LINEAR SHRINKAGE OF EO, PH, AND FA THERMOSETS DURING PYROLYSIS TO 1200°C, REFERRED TO FULLY CURED STATE

	Epoxy resin mixture of types 828 and 1031 Epikote EO		Phenodur PR 373 phenolic resin PH		Furfuryl alcohol / formaldehyde resin (3:2 molar ratio) FA	
Treatment temperature [°C]	Weight loss [%]	Linear shrinkage [%]	Weight loss [%]	Linear shrinkage [%]	Weight loss [%]	Linear shrinkage [%]
210					0	0
250					4.5	0.9
300	0	0	0	0	7.4	1.6
400	4.6	0,7	9.9	3.0	22.4	6.4
450	8.9	0.8	12.3	3.3	27.3	8.4
515	-	-	31.1	11.8	39.5	14.3
630	24.8	5.6	30.0	11.0	40.7	15.3
700	-	-	33.2	15.4	42.3	18.5
780	28.4	11.1	33.0	16.1	43.2	20.1
910	-	-	33.9	18.1	43.4	21.2
1060	29.5	13.1	33.9	17.9	43.3	21.7
1190	29.5	13.0	35.2	18.8	43.9	22.0

4.132. Pyrolysis procedure

The fully cured thermoset castings were decomposed thermally in an ultrapure nitrogen atmosphere in a tube furnace (inside diameter of tube D_I = 75 mm, heated tube length L_H = 500 mm). Heating rate was controlled with an Elnik program regulator, type REP 31 e 1 Z (R) by Joens, Düsseldorf, and was 12°C/h. Pyrolysis was performed until various final temperatures were reached, maximum treatment temperature being 1200°C. After the particular final temperature had been reached, the specimens were cooled immediately and the partially or totally pyrolyzed specimen /42 material was removed from the furnace at a temperature of 150 to 200°C. Cooling times between 2 and 8 h were obtained for the various furnace charges, as a function of the heat capacity of the furnace and the various treatment temperatures. In order to prevent warpage of the specimens during thermal decomposition, they were pyrolyzed in specimen holders of graphite (see Fig. 1).

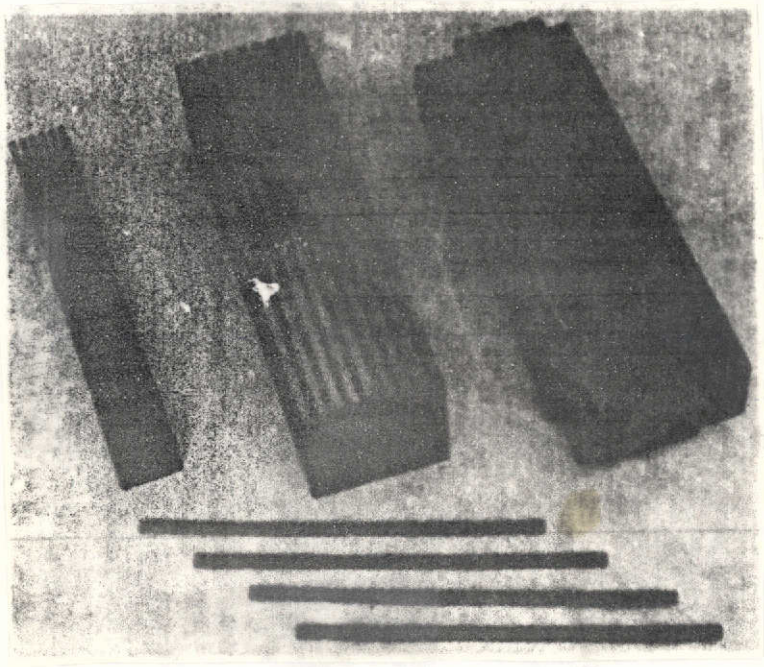

Fig. 1. Various specimen holders of graphite

4.133. Properties of the castings

The weight losses and the linear shrinkage, as well as the tensile strength and moduli of elasticity of the thermosets were studied in various stages of decomposition.

The increase in /43 weight loss and in linear shrinkage of the resins relative to the fully cured state can be seen from Table 7. Weight loss and linear shrinkage are plotted in Fig. 2 as functions of final treatment temperature. In contrast to Table 7, however, these values are referred to the partially cured state, only.

As the results show, the fully cured resins continually lose weight during their thermal decomposition to vitreous carbon. They experience the greatest weight loss in the temperature range between 300 and 500°C. Above 550°C, only small quantities of volatile decomposition products are still produced, so only a

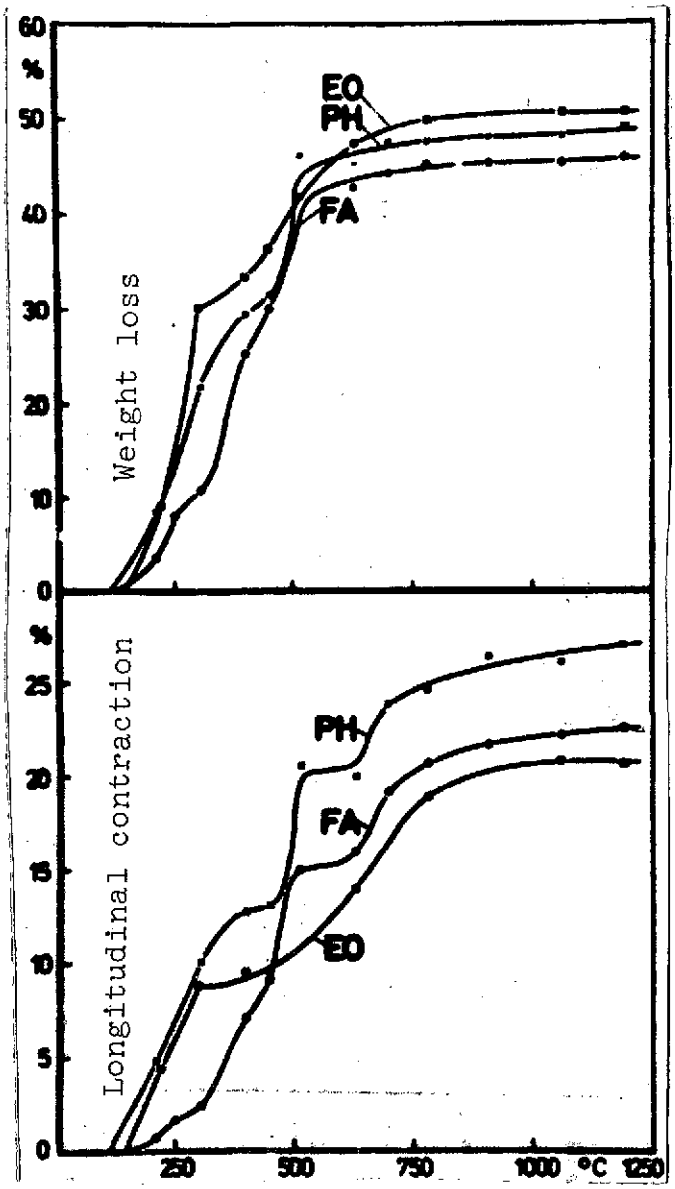

Fig. 2. Weight loss and longitudinal contraction of EO, PH and FA thermosets as functions of treatment temperature.

small weight decrease is recorded in the temperature interval between 550 and 1200°C for all resins.

If we start with resins already fully cured, the furfuryl alcohol / formaldehyde resin exhibits the greatest weight loss at the end of pyrolysis (1200°C), with a value of 44%. In contrast, the epoxy resin mixture and the phenolic resin are considerably more favorable, with weight losses of 30 and 35 wt.%, respectively. If we take the weight losses of the resins during their full curing, approximately equal residues are obtained for the completely pyrolyzed thermosets, lying in the 46 - 51 wt.% range.

The weight loss and linear shrinkage of the resins during pyrolysis to 1200°C cannot be correlated with one another. The greatest shrinkage occurs in the temperature range between 300 and 800°C, while weight loss is largely complete at just 550°C. Different longitudinal shrinkages are sometimes obtained for the partially cured resins following their coking to 1200°C. The smallest longitudinal contraction is experienced by the epoxy resin mixture, at 21%, although it exhibits the greatest weight loss (51%). The furfuryl alcohol / formaldehyde resin, with the lowest weight loss (46%) shrinks by 23%, on the other hand. The greatest linear shrinkage occurs with the phenolic resin. It amounts to 27%, with a weight loss of 49%.

The change in the tensile strength and the moduli of /46
elasticity of the fully cured thermosets as pyrolysis temperature rises to 1200°C can be seen from Table 8. These properties are plotted in Fig. 3 as functions of treatment temperature; the

TABLE 8. CHANGE IN THE TENSILE STRENGTH AND YOUNG'S MODULI OF FULLY CURED EO, PH AND FA THERMOSETS WITH INCREASING PYROLYSIS TEMPERATURE (DETERMINED AT ROOM TEMPERATURE)

Treatment temperature	Epoxy resin mixture of types 828 and 1031 Epikote		Phenodur PR 373 phenolic resin		Furfuryl alcohol / formaldehyde resin (3:2 molar ratio)	
	Tensile strength	Young's modulus	Tensile strength	Young's modulus	Tensile strength	Young's modulus
[°C]	[kp/mm^2]	[kp/mm^2]	[kp/mm^2]	[kp/mm^2]	[kp/mm^2]	[kp/mm^2]
210					7.0	390
250					6.1	400
300	5.3	365	10.8	510	4.6	335
400	4.9	365	7.5	435	4.1	360
515	—	—	3.7	575	3.3	645
630	6.0	740	4.1	835	4.4	820
700	—	—	6.8	1390	6.0	1340
780	5.9	1820	7.8	1880	6.3	1770
910	—	—	11.3	2530	10.6	2490
1060	10.2	2980	12.2	3040	12.3	2960
1190	10.8	3190	12.2	2970	10.3	3100

results for thermosets in various stages of curing are included (see Section 4.12).

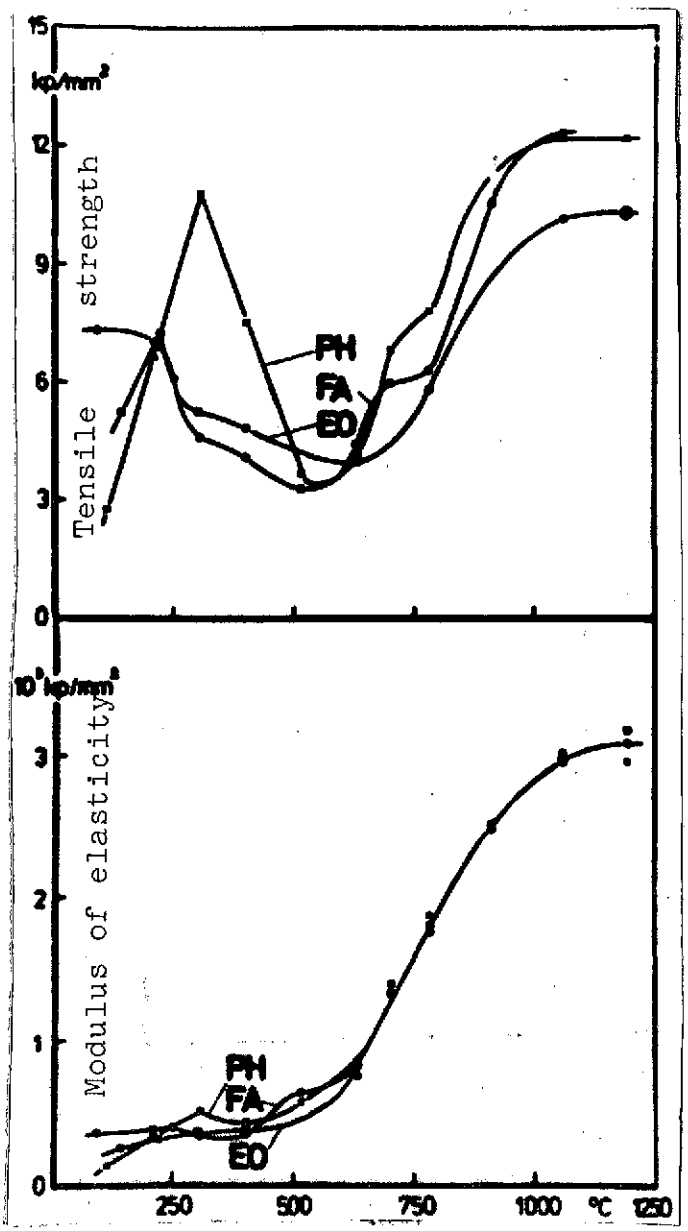

Fig. 3. Tensile strength and moduli of elasticity of the EO, PH and FA thermosets as functions of treatment temperature (determined at room temperature).

The strength of thermosets already completely cured initially decreases with increasing pyrolysis temperature. Between 500 and 650°C, the resins pass through a minimum in strength, with a value of 3 - 4 kp/mm². Above 500 to 650°C, a pronounced strengthening occurs, which reaches its maximum of 10 to 12 kp/mm² at 1100 to 1200°C. An explanation of the decrease in strength is that increasing damage to the highly cross-linked resin structure commences above the curing temperature as the result of heat treatment, without the resultant rupture fragments being able to reorganize into a new structure at first. The reorganization of fragments, which are stabilized with the formation of aromatic structures, commences only above 500 to 650°C [34], i.e., at temperatures at which the major portion of volatile cleavage products has already been formed and weight loss has largely been completed.

The modulus of elasticity of fully cured thermosets exhibits a similar curve to that of tensile strength with increasing treatment temperature. A pronounced minimum in the temperature range between 500 and 650°C does not occur, however. Above this temperature range, it begins to rise sharply and reaches a maximum of 3000 to 3200 kp/mm² at 1100 to 1200°C.

As can be seen from these studies, no appreciable differences are observed between various thermosets with regard to their

strength and moduli of elasticity at given pyrolysis temperatures. To the extent that a comparison between the vitreous carbon produced here and the industrial products (see Section 4.131) is at all permissible, on the basis of the different treatment temperatures, the tensile strength and modulus of elasticity values of the products prepared here (σ = 10 to 12 kp/mm^2, E = 3.0 to 3.2 · 10^3 kp/mm^2, T = 1100 to 1200°C) lie in the same range as the values for industrial products (σ = 4 to 20 kp/mm^2, E = 2.1 to 3.3 · 10^3 kp/mm^2, T = 1300 to 3000°C). /49

4.134. Model studies on shrinkage behavior of matrix materials

Even more detailed information on the shrinkage behavior of these resins during thermal aftertreatment is necessary for using the thermosets as a matrix for carbon-fiber-reinforced composites, particularly for their use as matrix raw material for carbon-fiber-reinforced carbon objects. Such studies were carried out using Phenodur PR 373 phenolic resin as an example. /50

In order to determine the effects of specimen geometry, the studies were made with model specimens of different geometric shape. Fig. 4 shows the various model specimens of phenolic resin before and after coking. Measuring the specimens accurately (measurement precision ± 0,005 mm) after initial curing at 110°C (see Fig. 4, top) and after thermal decomposition to 1150°C (see Fig. 4 bottom) shows that the thermosets shrink isotropically, regardless of specimen geometry.

4.135. Plasticity of matrix materials

It was shown in Section 4.134 that in the absence of external stresses, the phenolic resin studied shrinks quite isotropically. On the other hand, a pronounced difference between the extents of shrinkage parallel and perpendicular to the orientation of fibers is observed upon the thermal aftertreatment of the composites. This indicates that the direction of shrinkage can be affected by an internal as well as external stresses; this requires a certain plasticity on the part of the matrix during thermal aftertreatment.

In order to determine the extent of plastic deformability, resin platelets of various degrees of curing and pyrolysis with dimensions of 10 X 10 X 2 mm were decomposed thermally up to 600°C under loads, with a hardened steel ball of diameter 6 mm pressing on the specimen with a force of 1000 p [gram force]. The spherical depressions forced into the platelets after pyrolysis to 600°C were measured microscopically. The base diameters of the spherical impressions and the load per unit area resulting from the surface of the depression are shown in Table 9 and Fig. 5 as functions of pretreatment temperature for the various thermosets. /51

TABLE 9. PLASTIC DEFORMABILITY OF EO, PH AND FA THERMOSETS DURING THERMAL TREATMENT TO 600°C AS FUNCTIONS OF PRETREATMENT TEMPERATURE

	Epoxy resin mixture of types 828 and 1031 Epikote		Phenodur PR 373 phenolic resin		Furfuryl alcohol / formaldehyde resin (3:2 molar ratio)	
	EO		PH		FA	
Pretreatment temperature [°C]	Diam. of ball impression [mm]	Load per unit area [kp/mm²]	Diam. of ball impression [mm]	Load per unit area [kp/mm²]	Diam. of ball impression [mm]	Load per unit area [kp/mm²]
90	-	-	-	-	1.71	0.42
110	-	-	3.09	0.12	-	-
300	2.67	0.17	2.93	0.14	-	-
360	-	-	2.67	0.17	1.49	0.56
400	-	-	1.87	0.35	-	-
450	1.81	0.38	1.71	0.42	0.96	1.33
515	0.75	2.12	0	∞	0.52	4.83

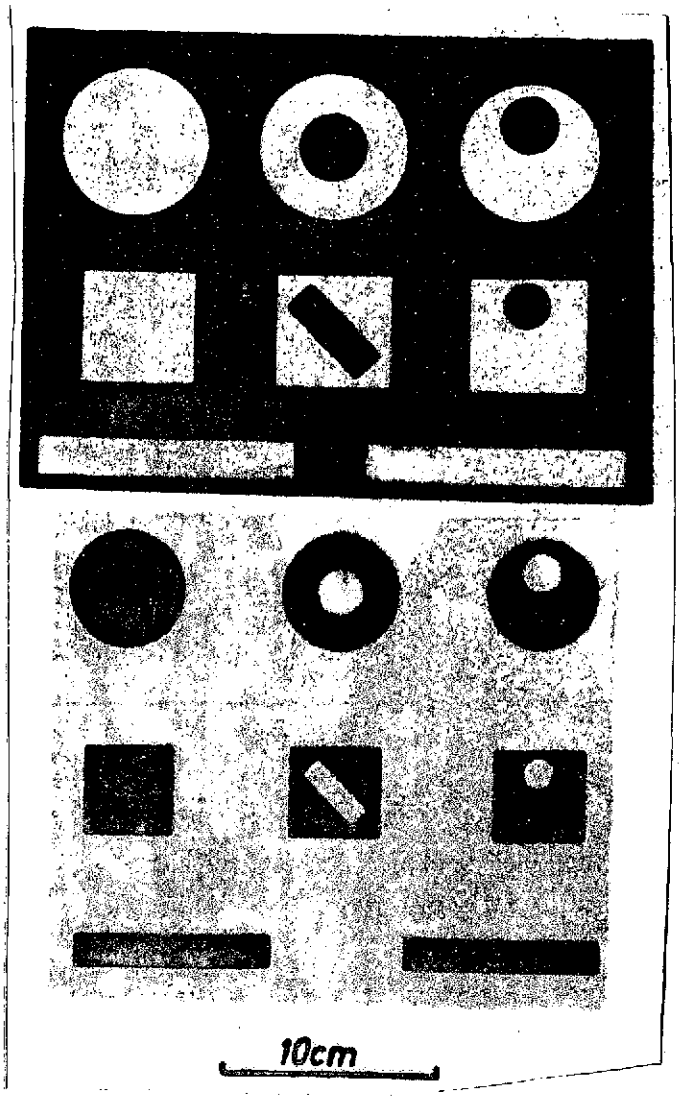

Fig. 4. Model specimens of Phenodur PR 373 phenolic resin after initial curing at 110°C (top) and after thermal decomposition to 1150°C (bottom)

As the results show, the thermosets can still be deformed plastically during high temperature treatment to 600°C even if the pretreatment temperature was above their complete curing temperature. To be sure, the plastic deformabilities of the resins did decrease sharply with increasing pretreatment temperature in all cases. The phenolic resin and the epoxy resin mixture, both of which possess conspicuously greater plasticity than the furfuryl alcohol / formaldehyde resin up to 300°C, approach the latter more and more here. Above 500 to 550°C, the thermosets already exhibit such great embrittlement that plastic deformation could no longer be achieved with any of the resins under the given test conditions.

The example of furfuryl alcohol / formaldehyde resin was used to study how the application of mechanical pressure during pyrolysis affects the isotropic shrinkage of this matrix material. A tablet-shaped specimen of the resin, partially cured to 110°C, was studied; it was decomposed thermally in a closed pressure mold under a pressure of 30 kp/mm^2 to 600°C (heating rate 15°C/h).

Measurement of the specimen indicated that isotropic shrinkage of the resin matrix had been reduced to unidimensional shrinkage by the mechanical pressure, because of its plasticity. The pyrolyzed specimen exhibited no shrinkage perpendicular to the direction of compression, whereas it had shrunk about 55% in /53 the direction of compression. Another consequence of the high pressure was an increase in volumetric shrinkage from 40 to 55%.

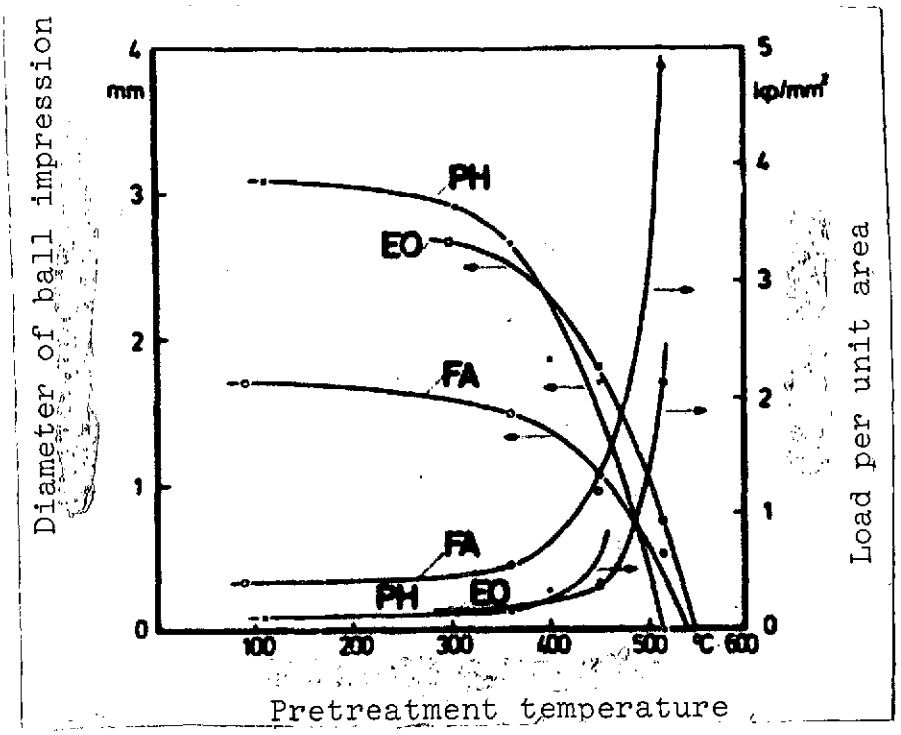

Fig. 5. Plastic deformability of EO, PH and FA thermosets during thermal treatment to 600°C as function of pretreatment temperature.

4.2. Polyimides

/54

To date, compact objects of vitreous carbon have been prepared by the thermal decomposition of three-dimensionally cross-linked polymers, particularly thermosets based on phenol. It is characteristic of such polymers that they are neither soluble or fusible and that they decompose thermally in the solid phase. As was shown in Section 4.135, the partially decomposed thermosets do exhibit a limited plasticity on into the 500°C range, but this plasticity is not sufficient to alleviate the shrinkage stresses which occur during the thermal decomposition of fiber-reinforced thermosets (see Section 7.2).

While the infusibility of thermosets is caused by three-dimensional cross-linkage via principal valence bonds, other polymers exist whose infusibility is caused merely by interactions between highly polar groups on neighboring chains. Increased plasticity should be expected of these polymers upon thermal decomposition. It must be taken into consideration here, however, that three-dimensional cross-linkage via principal valence bonds

likewise occurs during thermal decomposition, reducing plasticity.

The amount of linear shrinkage following the onset of cross-linkage will be decisive for the usability of such polymers as matrix raw material for carbon-fiber-reinforced carbon composites. Preliminary studies with the various polymers have shown that this shrinkage is considerably less in the case of the primarily linear-structured polyimides than for the thermosets, so the polyimides appear to be at least potentially suitable as matrix raw material [74].

4.21. Preparation of molded specimens /55

Molded specimens of the polyimide resins described in Section 3.12 were produced by casting, pressing or a combination of the two techniques and by high-temperature curing. The two polyimide resins P 13 N and Kerimid 601 were cast in the form of solutions (40 wt.% P 13 N in dimethylformamide, 50 wt.% Kerimid 601 in N-methyl-2-pyrrolidone); QX-13 polyimide was pressed without solvent. The curing conditions which proved to be usable for preparing nonporous resin specimens can be seen from Table 10.

Processing QX-13 polyimide resin to produce dense solids involves serious problems due to the large quantities of volatile components liberated during curing. Tablet-shaped specimens with a diameter of 20 mm could be cured with absolutely no porosity only up to a thickness of about 2 mm.

For unknown reasons, ICI has since ceased to produce QX-13. The same resin is now manufactured under the name "polyimide 212" by Yorkshire Chemicals Ltd., England, however [75].

4.22. Thermal aftertreatment

4.221. Thermogravimetric study

A thermogravimetric study of the polyimide resins, which provides an indication of their pyrolysis behavior, was performed with a Thermoanalyzer No. 113 thermobalance by Mettler, Zürich. The resin specimens were decomposed thermally in argon at two different heating rates (0.5 and 25°C/min) to 1000 and 1200°C, respectively. The weight losses of polyimides cured as described in Section 4.21 are shown in Table 11 and Fig. 6 as a function /57 of treatment temperature.

The three polyimide resins studied exhibit appreciable differences with regard to their thermal stability and coke yield. Kerimid 601 cured to 160°C, like the thermosets (see Fig. 2, Section 4.133), already begins to decompose spontaneously above 200 to 250°C and experiences a weight loss of 68% up to

TABLE 10. CURING CONDITIONS FOR P 13 N, KERIMID 601 AND QX-13 POLIMIDE RESINS

Resin type	P 13 N (40 wt.% solution in DMF)	Kerimid 601 50 wt.% solution in NMP)	QX-13 (no solvent)
Curing conditions	1. Removal of solvent and initial curing of resin without pressure in drybox: 15 h at 80°C 20 h at 140°C (Heating rate to 140°C: 10°C/h)	1. Removal of solvent and initial curing of resin without pressure in drybox: 75 min at 120°C 40 min at 130°C 20 min at 140°C 15 min at 150°C	1. Degassing and initial curing of resin without pressure in drybox: 7 h at 200°C 15 min at 300°C
	2. Pressure curing of partially cured resin in a heatable pressure mold: 1 h at 300°C, pressure: 3 kp/mm^2	2. Further curing of resin without pressure in drybox: 15 h at 160°C	2. Pressure curing of partially cured resin in a heatable pressure mold: 30 min at 300°C, pressure: 6 kp/mm^2
	3. Aftercuring of pressure-cured resin without pressure in drybox: 5 h at 300°C		3. Aftercuring of pressure-cured resin without pressure in drybox: 5 h at 300°C

TABLE 11. WEIGHT LOSSES OF P 13 N, KERIMID 601 AND QX-13 POLYIMIDE RESINS DURING THERMAL DECOMPOSITION

Temperature [°C]	Weight loss [%]			
	P 13 N Curing temperature 140°C		P 13 N Curing temperature 300°C	
	Heating rate [°C/min] 0.5	25	0.5	25
200	0	0		
250	0.5	0.7		
300	3.0	2.7	0	0
350	4.5	5.2	0.5	1.0
400	7.0	7.0	4.0	3.5
450	11.0	10.2	6.5	6.0
500	16.8	16.7	12.0	11.0
550	28.5	28.0	21.7	19.3
600	39.8	39.7	32.5	30.0
650	44.2	43.5	38.5	36.2
700	46.0	45.5	41.0	38.7
750	47.0	46.5	42.2	40.2
800	47.7	47.0	42.7	41.0
900	49.3	47.5	44.5	41.5
1000	53.0(53.8)*	48.0	48.5(49.5)*	42.2
1100		48.5		43.0
1200		49.2(50.2)*		43.1(*

* Weight loss after one-hour holding time

TABLE 11 continued

Temperature [°C]	Weight loss [%]			
	KERIMID 601 Curing temperature 160°C		OX - 13 Curing temperature 300°C	
	Heating rate [°C/min]		Heating rate [°C/min]	
	0.5	25	0,5	25
50	0			
100	2.1	0		
150	5.3	1.5		
200	9.2	3.3		
250	13.0	7.5		
300	17.7	10.2		0
350	26.3	25.0		1.2
400	40.0	38.5	0	3.2
450	45.0	51.0	4.3	6.3
500	50.7	55.7	8.5	11.0
550	53.8	60.5	16.5	18.5
600	55.3	63.5	29.0	29.0
650	56.0	64.5	35.0	34.3
700	7.0	65.3	38.0	36.5
750	57.2	65.8	39.0	37.5
800	57.5	66.0	39.5	38.3
900	58.2	66.5	40.5	39.5
1000	59.7(60,3)*	67.0	43.0(44.0)*	40.0
1100		67.5		40.5
1200		68.2(69,0)*		40.7(42.0)*

* Weight loss after one-hour holding time

1200°C (heating rate 25°C/min). Under the same experimental conditions, P 13 N cured only to 140°C exhibits a similarly spontaneous decomposition, but only above 400°C and of less magnitude. Weight loss reaches a value of 49% at 1200°C. P 13 N and QX-13 polyimides cured to 300°C exhibit the highest thermal stability. A pronounced weight loss occurs only above 450°C. Up to the completion of pyrolysis (1200°C), P 13 N loses 43% of its initial weight; the QX-13 weight loss is 41%.

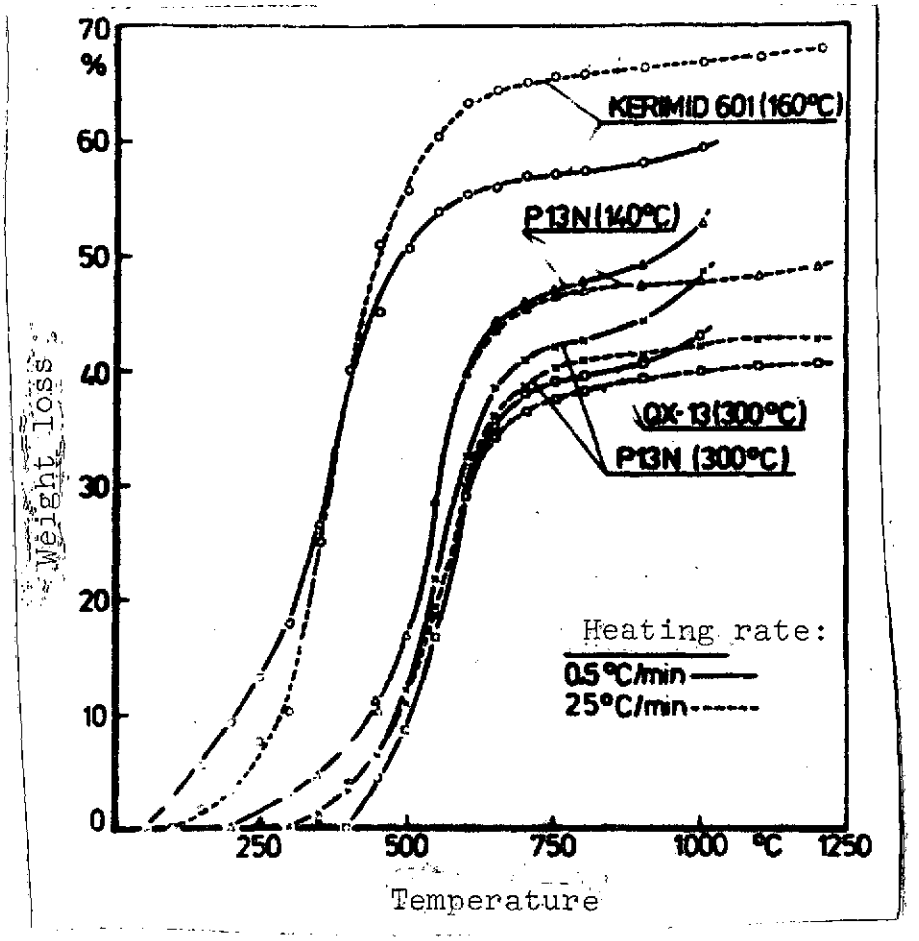

Fig. 6. Thermograms for P 13 N, Kerimid 601 and QX-13 polyimide resins.

Reducing the heating rate from 25 to 0.5°C/min causes an increased weight loss for P 13 N and QX-13 during the advanced pyrolysis stage. At 1000°C, slow coking produces 3 to 6% greater weight losses than rapid pyrolysis. In the case of Kerimid 601, however, a 7% lower weight loss is obtained.

If we compare the pyrolysis behavior of the polyimides (heating rate 0.5°C/min) with that of the thermosets (heating rate 0.2°C/min), we find that the polyimides, with the exception of Kerimid 601, are not only of higher thermal stability but also produce the highest coke residue. The maximum is 57% and is obtained with QX-13 polyimide.

4.222. Thermal decomposition of molded polyimide specimens /60

The studies on the thermal decomposition of molded polyimide specimens cured as described in Section 4.21 are limited to an investigation of the question as to whether these resins can be decomposed to yield crack-free pieces of carbon and as to the weight losses and longitudinal contraction which they experience in the process. The molded specimens were pyrolyzed under the /61 same conditions as the thermoset matrices (heating rate 12°C/h, ultrapure nitrogen).

Pyrolysis trials with the molded polyimide specimens indicated that P 13 N and QX-13 polyimide resins can be decomposed thermally to produce defect-free pieces of carbon. In the case of Kerimid 601 polyimide, on the other hand, the carbon product was no longer true to form and exhibited cracks and bubbles.

The weight losses and longitudinal contraction experienced by the thermally decomposed specimens are compiled in Table 12. Of the three polyimide resins, Kerimid 601 pyrolyzed to 1000°C shows the poorest decomposition behavior, with a weight loss of 63% and a longitudinal contraction of about 27%. The two polyimides P 13 N and QX-13 are largely equivalent in their behavior during thermal decomposition. At the end of pyrolysis, in the temperature range of 1000 to 1100°C, the weight losses of these resins lie between 43 and 49%, longitudinal contraction between 18 and 19%. QX-13 experiences the smallest weight loss (43%) and the smallest longitudinal contraction (18%).

TABLE 12. WEIGHT LOSSES AND LONGITUDINAL CONTRACTION OF POLYIMIDE SPECIMENS DURING THERMAL DECOMPOSITION

Type of resin		P 13 N	Kerimid 601	QX-13	
Decomposition temperature	[°C]	1000	1000	550	1100
Weight loss	[%]	49.1	63.1	24.2	42.6
Longitudinal contraction	[%]	18.7*	ca.27	9.4	17.5

* Pyrolyzed to 1150°C

Comparison of the weight losses of molded specimens (heating rate 0.2°C/min) with the results of the thermogravimetric study (see Fig. 6, Section 4.221, heating rate 0.5°C/min) shows that although very different specimen sizes were used, the two experimental methods yielded data that agree well.

5. Wetting behavior of matrix materials with respect to carbon fibers /62

5.1. Basic principles

Wetting of the reinforcing material by the liquid matrix is very important in the production of fiber-reinforced composites. A solid matrix that represents an effective bond between reinforcing elements can be expected only from a polymer which wets the fiber. Complete contact between the two components, i.e., liquid resin and carbon fiber, thus permits the formation of an effective interface which transmits forces from the matrix to the fiber, thereby giving strength to the composite system.

The wetting of a fiber by a liquid is given by the angle of contact θ which forms on the fiber when it is dipped into the liquid medium (see Fig. 7). Complete wetting of the solid surface occurs if the angle of contact becomes 0°. If the angle is 180°, the liquid is not wetting the solid. The magnitude of the angle of contact is determined by basic interfacial-energy parameters of the media in contact with one another. The relationship between angle of contact θ, solid surface tension σ_{13} (solid-gas), liquid surface tension σ_{23} (liquid-gas) and interfacial tension σ_{12} (solid-liquid) is given by Young's equation: /63

$$\sigma_{13} - \sigma_{12} = \sigma_{23} \cos\theta \, . \qquad (5\text{-}1)$$

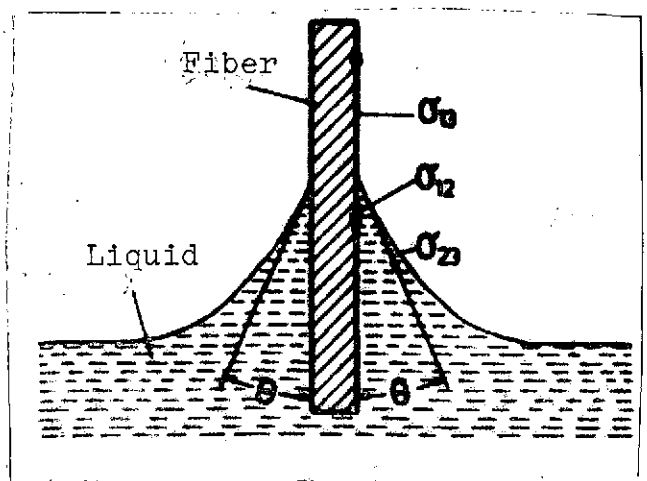

Fig. 7. Liquid miniscus on a fiber (schematic)

Angles of contact on fibers are generally determined by indirect methods, since direct measurement with an optical goniometer or by photographic methods is not feasible for small fiber diameters and angles of contact due to the very poor accuracy. A usable procedure described in the literature is the weight method [76, 77, 78], which is based on dipping the fiber, suspended on a highly sensitive balance system, perpendicularly into the test liquid and determining the quantity of liquid raised above the surface plane of the liquid by capillary action by weighing. From the equilibrium of forces on the fiber and from Young's equation, we obtain the relationship we seek for the angle of contact which develops [1]:

$$\cos\theta = \Delta G \cdot g/(U_F \cdot \sigma_{23}) \qquad (5\text{-}2)$$

where

ΔG = mass of liquid raised by capillary action [g]
g = earth's gravitational acceleration [dyn/g]
U_F = circumference of fiber [cm]
σ_{23} = liquid surface tension [dyn/cm]

It is possible to calculate the angle of contact from Eq. (5-2) if one knows the circumference of the fiber and the surface tension of the liquid.

5.2. Measurement of wetting angles /64

5.21. Indirect determination

The weight method described above was initially used to determine the wetting behavior of the polymers used in this work with respect to carbon fibers. The quantities of liquid drawn up by capillary action when the carbon fibers are dipped into the resins (see Table 13) were measured gravimetrically with a self-regulating electronic microbalance by Sartorius, Göttingen, at room temperature (23°C). The range of measurement was on the order of 0.2 mg.[1]

The resin surface tensions required for calculating angle of contact (see Table 13) were determined at 23°C with a Lauda Tensiometer, produced by the firm of Dr. R. Wobser KG., Lauda.[2] The principle by which measurements are made with this instrument

---

[1]The measurements were performed at the Institute of Plastics Processing of the Rhine/Westphalian Engineering College, Aachen. I would like to thank Prof. Dr. -Ing. G. Menges and his coworkers for their generous support.

[2]The measurements were performed at the Institute of Foodstuffs Processing Technology of Karlsruhe Engineering University. I would like to thank Prof. Dr. Dr. M. Loncin and his coworkers for their generous support.

TABLE 13. ANGLES OF CONTACT AND ADJUSTMENT TIMES FOR THERMOSETS WITH CARBON FIBERS AT 23°C, BY THE WEIGHT METHOD

Resin-hardener system	Abbreviation	Surface tension [dyn/cm]	Type of fiber	Fiber circumference (given by mfr.) [cm]	Amt. of liquid raised by cap. action, 10^3 [g]	Angle of contact [deg.]	Adjustment time [sec]
Epoxy resin mixture of Epikote 828 and 1031 (1:1 by wt.) /pyromellitic dianhydride	EO	35.7	VYB	0.00298	0.09011 ± 0.00165	33.8	5.3
			Thornel 25	0.00232	0.07424 ± 0.00213	28.5	5.2
			Thornel 40	0.00217	0.06397 ± 0.00154	35.9	5.0
			Grafil HM	0.00257	0.06488 ± 0.00056	46.1	4.9
			Grafil HT	0.00279	0.07524 ± 0.00133	42.2	5.4
Phenodur PR 373 phenolic resin / self-hardening	PH	40.8	VYB	0.00298	0.09568 ± 0.00083	39.5	5.3
			Thornel 25	0.00232	0.07832 ± 0.00224	35.7	7.4
			Thornel 40	0.00217	0.06112 ± 0.00039	47.3	5.1
			Grafil HM	0.00257	0.06230 ± 0.00249	54.3	5.3
			Grafil HT	0.00279	0.07981 ± 0.00252	46.5	5.9
Furfuryl alcohol-formaldehyde resin (3:2 molar ratio) / p-toluenesulfonic acid	FA	61.9	VYB	0.00298	0.13368 ± 0.00536	44.7	19.8
			Thornel 25	0.00232	0.11080 ± 0.00172	40.8	37.1
			Thornel 40	0.00217	0.09472 ± 0.00185	46.2	15.7
			Grafil HM	0.00257	0.08864 ± 0.00303	56.9	11.2
			Grafil HT	0.00279	0.09632 ± 0.00217	56.7	14.6

is based on the ring breakaway method, in which a horizontal ring of platinum is dipped into the liquid to be measured and pulled out again. As the ring is being pulled out, a lamina of liquid develops along its circumference which exerts a tensile force on it. After the maximum tensile force that occurs has been exceeded, proportional to the surface tension of the liquid, the lamelle breaks away from the ring. This process is amplified via an inductive force pickup connected to the ring and is plotted on a recorder. A reference measurement is made with a liquid of precisely known surface tension in order to calculate the recording instrument. Double-distilled ... was ... as a calibrating liquid ... [page missing from German document]

/66

5.22. Direct determination /67

In view of the inaccuracy which the weight method can involve because of the various measurement parameters, angles of contact on carbon fibers were also measured directly. Since the resolution of optical goniometers is generally not sufficient to exactly determine angles of contact on fibers of less than 10 µm diameter, a scanning electron microscope was used for this purpose, rather than conventional equipment. In order that the contact angle measurements would not be impaired by boiling of the liquid phase in the SEM vacuum chamber, the state of wetting was fixed beforehand by curing the resins.

Fig. 8 shows scanning electron micrographs of a type VYB carbon fiber produced from rayon which has been wetted by Phenodur PR 373 phenolic resin. Fig. 8, left, shows the overall profile of the resin miniscus close to the fiber, and Fig. 8, right, shows a detail of the tip of the profile, at which the resin /68 surface merges with that of the fiber. The angle between the tangent at the tip and the vertical margin of the fiber corresponds to the wetting angle being sought.

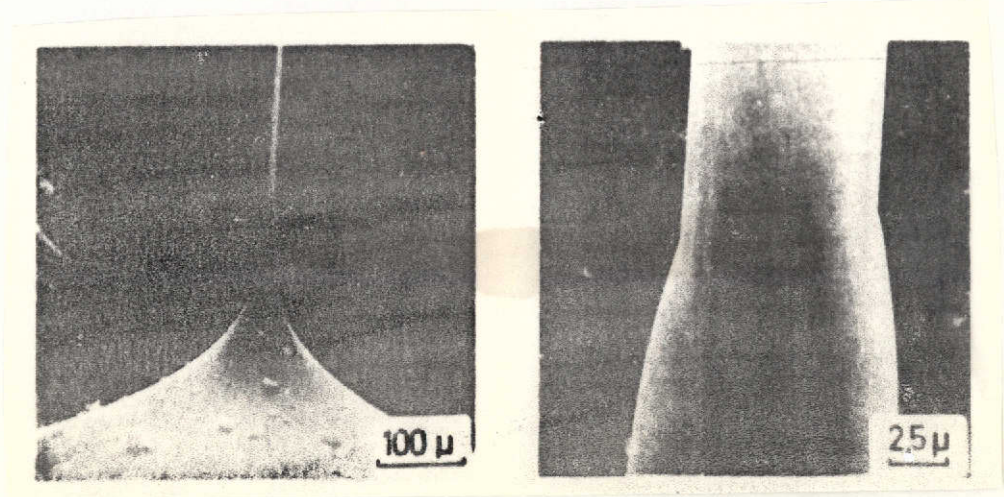

Fig. 8. Wetting of a carbon fiber (type VYB) by Phenodur 373 phenolic resin after curing at 110°C.

Angles of contact determined in this manner for Phenodur PR 373 phenolic resin and Kerimid 601 polyimide resin with various carbon fibers are compiled in Table 14. The 60 wt.% phenolic resin solution was fully cured to a temperature of 110°C, under the initial curing conditions in Section 4.11, but without previously removing the solvent from the resin under vacuum. The 50 wt.% polyimide resin solution was initially cured to 150°C under the curing conditions in Section 4.21. It can be seen from the data that it is not possible to categorize the carbon fibers on the basis of their wetting, independently of the [type of] resin, as in the case of the angles of contact determined indirectly (see Section 5.21).

5.23. Comparison of the two measurement methods

As the results of indirect contact angle measurements show, the carbon fibers produced from cellulose fibers, with very rough surfaces as compared to the relatively smooth-surface carbon fibers made from polyacrylonitrile are wetted better by the various thermosets. The different wettabilities of these two types of fibers agrees with the known fact that the wetting /69
of a solid by a liquid is not just a function of interfacial energy parameters such as surface and interfacial tensions, but is also affected by surface roughness.

TABLE 14. ANGLE OF CONTACT BETWEEN PHENODUR PR 373 PHENOLIC RESIN AND KERIMID 601 POLYIMIDE RESIN AND VARIOUS CARBON FIBERS AS DETERMINED BY THE DIRECT METHOD

Type of fiber — Angle of contact [degrees]

	Phenodur PR 373	KERIMID 601
VYB	14.0 ± 1.3	6.9 ± 0.2
Thornel 25	12.5 ± 1.4	16.3 ± 1.8
Thornel 50	20.5 ± 1.7	6.9 ± 1.3

Information regarding the angle of contact as a function of the surface roughness of a solid is provided by Wenzel's formula [79]:

$$\cos\theta' = r\cos\theta \quad \text{for } r \geq 1, \tag{5-3}$$

where:

θ' = angle of contact at a rough solid surface

θ = angle of contact at a smooth solid surface

r_r = surface roughness factor

According to Eq. (5-3), a smaller angle of contact forms on a rough surface than on a smooth surface if angle of contact θ is less than 90°. Since this condition applies for the resin/fiber systems studied, the better wettability of carbon fibers with the rougher surface proves to be correct.

If we compare the results of the two measurement methods for comparable wetting systems, we find that the direct method yields much lower angles of contact than the weight method. The better wetting behavior of phenolic resin relative to carbon fibers as indicated by the direct method is based on the fact that the wetting medium was initially cured thermally. Since we know that the surface tension of a liquid is a function of temperature -- elevated temperature reduces surface tension -- the smaller wetting angles from the direct method are quite justified in accordance with Eq. (5-2).

[line(s) missing from German document]
... the two measurement methods, the results of the weight /70
method cannot be evaluated by direct contact angle measurement with regard to its accuracy for given resin/fiber systems. Qualitatively, the results of the two measurement methods agree in indicating that the wetting behavior of phenolic resin relative to carbon fibers made from cellulose becomes poorer in the following sequence of fiber types: Thornel 25, VYB, Thornel 40[1] and Thornel 50.

The order of the types of stretch-graphitized Thornel fiber is that expected on the basis of information on crystalline alignment and the associated reduction in specific surface area (see Table 3, Section 3.21). The predictions of Eq. (5-3) are contradicted by the experimental finding that it yields a smaller angle of contact for stretch-graphitized fibers of the Thornel 25 type, with a low specific surface area of 4 m^2/g, than for the ungraphitized carbon fibers of the VYB type, with their large specific surface area of 130 m^2/g. This unexpected

---

[1] At the time at which contact angle measurements were being made by the weight method, Thornel 50 fibers were not yet commercially available. The Thornel 40 fibers were made available by the Institute of Plastics Processing of the Rhine/Westphalia Engineering College, Aachen.

behavior can probably be attributed to the sodium polyphosphate detected in the VYB fiber (see Section 7.221).

6. Production and properties of carbon-fiber-reinforced polymers /71

6.1. Literature

Thermosets are primarily used today as matrix materials for carbon-fiber-reinforced polymers, since these plastics have higher sustained-use temperatures than the thermoplastics. Semiconductor polymers such as the polyimides are commanding increasing interest because of their high sustained-temperature resistance (250 to 300°C).

Basically, the same methods can be considered for the production of carbon-fiber-reinforced polymers as are used for the production of fiberglass-reinforced plastics. The conventional fabrication methods are pressure molding, wet winding, and the lamination method.

In pressure molding [80], the polymer matrix with discontinuous reinforcing material is fully cured under pressure to form molded objects. The advantages of this method are low production costs, on the one hand, and on the other, the fact that complicated shapes can easily be produced. Its disadvantage is the random arrangement of the reinforcing component in the matrix, as a result of which only a portion of the imbedded fibers contribute to reinforcement and stiffening in a given direction of load application.

In the wet winding method [81], continuous reinforcing material is led through a resin bath and is wound on a winding core, after which the wound product is then cured. The advantage of this method is the possibility of precisely orienting the reinforcing component, so that all fibers come into play if a load is applied in the direction of this orientation.

Complicated shapes cannot be produced directly by this method, however. In such cases, use is made of the laminating technique, employing prepregs prefabricated by the wet winding /72
method. In the production of these prepregs, the matrix is initially cured just to the point at which it no longer adheres at room temperature. The prepregs are then tailored as a function of the required shape, glued together and fully cured under pressure to produce high-strength molded products [82].

Table 15 give literature data on the mechanical properties of carbon-fiber-reinforced polymers with unidirectionally oriented fibers. The strength behavior of such materials is determined by the mechanical properties of the components incorporated into their structure, as well as the fiber fraction by volume,

TABLE 15. MECHANICAL PROPERTIES OF CARBON-FIBER-REINFORCED POLYMERS WITH UNIDIRECTIONALLY ORIENTED FIBERS (DETERMINED IN FIBER DIRECTION AT ROOM TEMPERATURE)

Matrix material / Type of fiber	Fiber fraction [Vol.%]	Tensile strength [kp/mm^2]	Young's modulus [kp/mm^2]	Bending strength [kp/mm^2]	Bending modulus [kp/mm^2]	Interlaminar bending shear strength [kp/mm^2]
Polyester resin / HM (Morganite Modmor Ltd.) [83]	50	91	19600	84	14000	-
ERLA 2256 epoxy resin / Thornel 25 (Union Carbide Corp.) [84]	72	67	6300	48	10700	1.6
	-	-	-	-	-	2.5
ERLA 2256 epoxy resin / Thornel 25 (Union Carbide Corp.) [63]	-	-	-	-	-	5.1+
Epoxy resin / Thornel 25++ (Union Carbide Corp.) [63]	-	-	-	-	-	8.3
Epoxy resin / Thornel 50 (Union Carbide Corp.) [85]	-	75	16800	81	16200	2.5
Epoxy resin / Thornel 50 S+++ (Union Carbide Corp.) [86]	55	73	18000	75	16900	5.3
ERLA 2256 epoxy resin / Thornel 75 (Union Carbide Corp.) [87]	-	98	33500	66	27800	2.6
Epoxy resin / HT (Morganite Modmor Ltd.) [88]	59	123	14500	100-140	14100	4.4

Surface treated fibers:

+ partially oxidized (nitric acid)
++ whiskered (silicon carbide whiskers)
+++ unknown

TABLE 15 continued

Matrix material / Type of fiber	Fiber fraction [Vol.%]	Tensile strength [kp/mm²]	Young's modulus [kp/mm²]	Bending strength [kp/mm²]	Bending modulus [kp/mm²]	Interlaminar bending shear strength [kp/mm²]
EPN 1138 epoxy resin (Ciba) / HT (Morganite Modmor Ltd.) [89]	57	-	-	125	13100	3.6
EPN 1138 epoxy resin (Ciba) / HT +++ (Morganite Modmor Ltd.) [89]	62	-	-	167	13600	8.9
Epikote 828 epoxy resin / HT (Courtaulds Ltd.) [90]	40	98	11500	65	8400	6.4
SC-1008 phenolic resin (Monsanto Chemical Co.) / VYB (Union Carbide Corp.) [15]	62	46	2450	74	2350	3.0
QX-13 polyimide resin (ICI Ltd.) / HM+++ (Morganite Modmor Ltd.) [91]	52	-	-	84	15000	8.5
QX-13 polyimide resin (ICI Ltd.)/ HT+++ (Courtaulds Ltd.) [92]	50	-	-	132	11200	9.1
P 13 N polyimide resin (Ciba-Geigy) / C Fiber based on PAN [93]	57	-	-	159	19600	66

Surface treated fibers:
+++ unknown

the state of fiber/matrix bonding, and the absence of cracks and pores in the composite structure. A suitable surface treatment of the carbon fibers, such as partial oxidation, whiskering or the application of an adhesive, can be used to considerably improve the state of fiber/matrix bonding and thus improve bending strength and interlaminar shear strength.

6.2. Author's studies on the carbon-fiber reinforcement of thermosets /75

6.21. Selection of composite systems studied

Of the large number of possible composite systems which result from combining the various thermosets and carbon fibers, four systems (see Table 16) were selected on the basis of special considerations, and their mechanical properties in particular were studied.

TABLE 16. COMBINATIONS OF MATERIALS IN THE COMPOSITE SYSTEMS STUDIED

Abbreviated designation*	Matrix	Reinforcing component
I (PH-VYB)	Phenodur PR 373 phenolic resin	C Fiber VYB (105 - 1/5)
II (EO-VYB)	Epoxy resin mixture of Epikote types 828 and 1031	C Fiber VYB (105 - 1/5)
III (PH-Thornel 25)	Phenodur PR 373 phenolic resin	C Fiber: Thornel 25 (WYD 115 - 1/2)
IV (PH-Thornel 50)	Phenodur PR 373 phenolic resin	C Fiber: Thornel 50 (WYG 130 - 1/2)

*These abbreviated designations are used throughout the following text.

Among the three thermosets studied, Phenodur PR 373 phenolic resin was primarily used in addition to the epoxy resin mixture of Epikote 828 and 1031 as matrix material for carbon fibers. The main reasons for this are the relatively short curing times for this resin, its good machineability and its excellent strength in the fully cured state.

The thermoset matrices were reinforced and stiffened exclusively with carbon fibers based on rayon, since only these types were available in the form of endless fibers at the /76

beginning of this work. As could be seen from the studies on wetting behavior (see Section 5.2), carbon fibers based on PAN are more poorly wetted by these resins.

6.22. Preparation and curing of composites

Continuously reinforced specimens with unidirectional orientation of the carbon fibers were prepared by the wet winding method (see Section 6.1) for evaluation of the selected composite systems.

Fig. 9 shows a schematic diagram of the design and operation of the wet winding apparatus, set up in a horizontal mode, and Fig. 10 shows an overall view of this equipment. The reinforcing component, wound on a spool, is unwound via a self-braking filament delivery device, by a driven transport roller of continuously adjustable speed and is passed through a thermostated impregnation setup, where it is impregnated with liquid matrix (see Fig. 11). A pierced plate which immediately follows the impregnating bath and through which the matrix-covered reinforcing component passes serves as a wiper for excess matrix material. The impregnated string of fiber is led via a system of guide rollers to a traversing mechanism which lays it on a rotating panel-shaped winding core, oriented unidirectionally under constant tension (see Fig. 12).

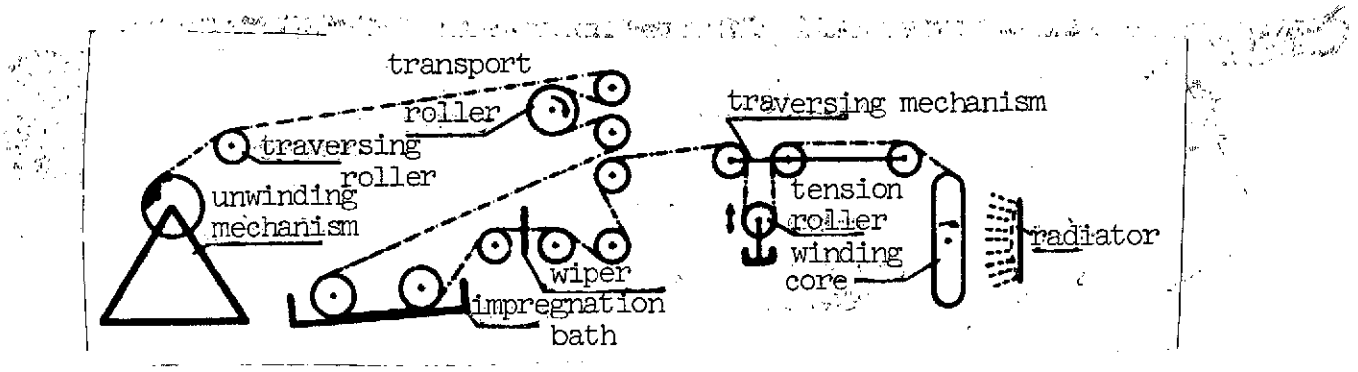

Fig. 9. Diagram of the wet winding apparatus

A tension roller which can be loaded with weights and /77
which can move freely between two guide rollers on the traversing arm maintains constant fiber tension and thus can also compensate for different unwinding and winding speeds. A TW 30 automatic wire reel winding machine by Thonke, Aldingen, was used as the winding unit; it was modified only as needed to reduce winding shaft rpm.

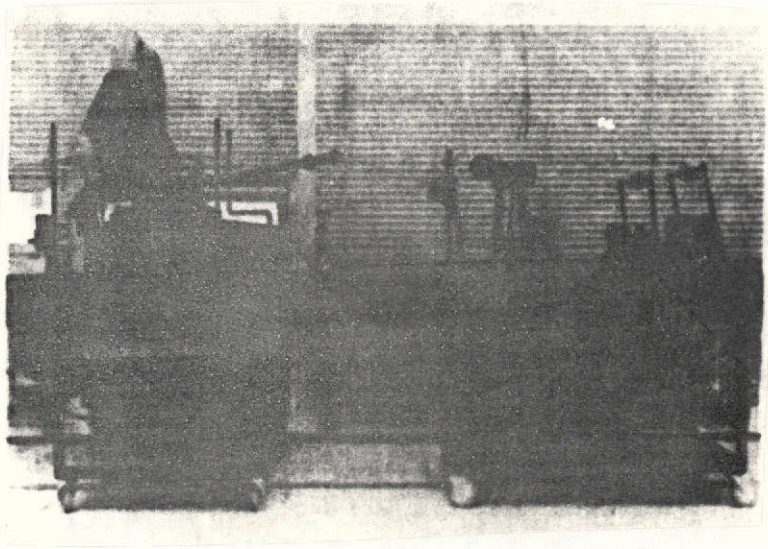

Fig. 10. Overall view of wet winding apparatus

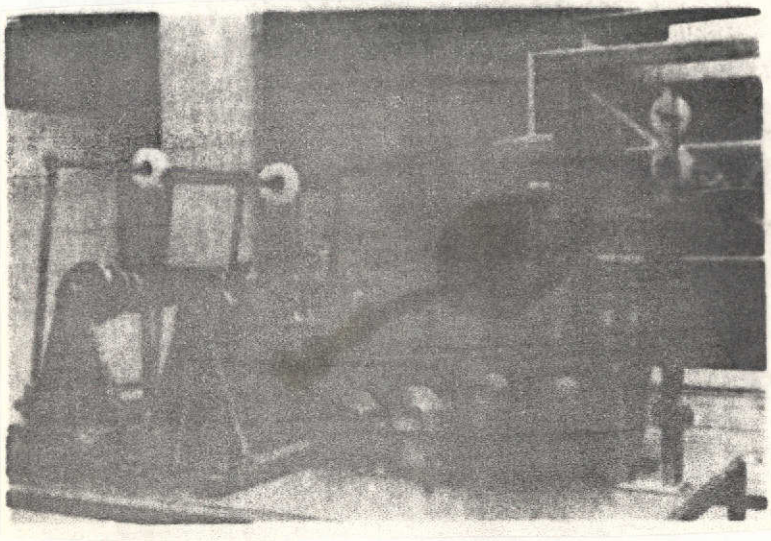

Fig. 11. Partial view of wet winding apparatus: unwinding and impregnating mechanisms

To produce specimen bars of composite systems I through IV (see Section 6.21, Table 16), the carbon yarns impregnated with resin solutions were first wound in several layers, with a filament tension of 250 p, on the demountable panel-shaped winding core of aluminum, with nominal dimensions of 400 X 175 mm. The winding parameters for composite types I through IV can be seen from Table 17. The Thornel fibers were wound with a slower fiber speed, since there was a danger of fiber breakage because of the low filament strength (see Table 4, Section 3.22) and high shearing sensitivity of these fibers.

Even while the laminates were being wound, much of the solvent was being removed from the resin matrix by infrared radiation. The temperature of the laminate was 60 - 80°C here. After the winding process, the laminates were initially /80 cured on the winding core in the drybox (curing step I) and then pressed between two hot plates (see Fig. 13) (curing step II).

Hot-pressing the wound products proved to be absolutely necessary to achieve smooth composite surfaces and low porosity. In addition, a desired fiber or resin content in the laminates could be adjusted to simply by using suitable pressures.

After pressure curing, the initially cured laminate shell was taken off the winding core by hand, after the wedge-shaped center piece of the winding core had been pushed out about halfway, following removal of the side portions. An inserted

Teflon sheet prevented the resin matrices from adhering fast to metal surfaces of the winding core and the heating plates.

The laminates cured under pressure (see Fig. 14) were then /81 sawed up into small, flat, parallel-sided bars with a precision wet-saw in such a manner that the carbon yarns lay parallel to the longitudinal axis of the bars. The length of the bars was 170 to 175 mm, the width was 6 mm (composites I and II) and 5 mm (composites III and IV). Bar thickness was 0.80 to 1.55 mm. A winding produced about 100 such specimen barlets.

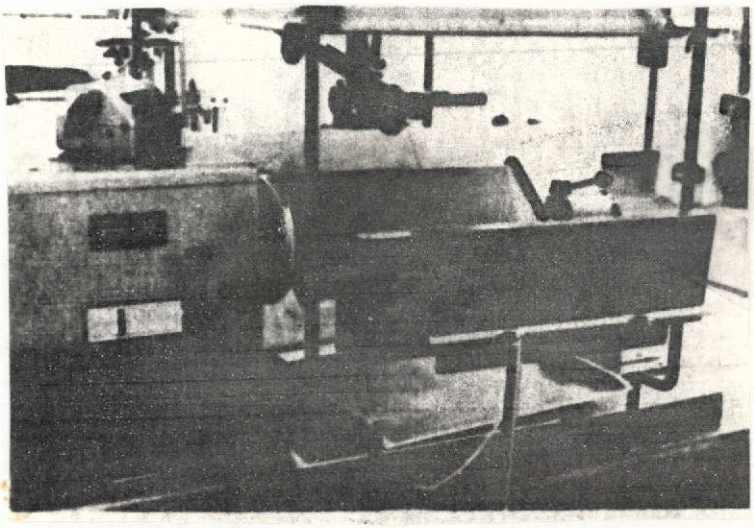

Fig. 12. Partial view of wet winding apparatus: winding machinery with winding core and infrared radiator

The further initial curing and full curing of the sawed specimens was done in curing stage III. Curing conditions for the three-step composite curing program are compiled in Table 18. Due to the thinness of the specimens, the curing times for the carbon-fiber-reinforced resin moldings (see Section 4.11) were shortened in some cases.

The fiber fraction by volume necessary for predicting composite strength was determined by means of the fiber weight employed and the dimensions of the wound product. The following relationships were used here:

$$x_{F_o} = \frac{G_F}{\rho_F \, s_W \, l_W \, (u_K + \pi s_W)} \, 100 \quad [\%] \qquad (6\text{-}1) \; /83$$

and

$$x_F = \frac{V_o}{V} \, x_{F_o} \quad [\%] \, , \qquad (6\text{-}2)$$

where:

x_{F_o} = fiber fraction by volume in initially cured composite [%]

TABLE 17. WINDING PARAMETERS FOR COMPOSITE TYPES I - IV

Type of composite	I (PH-VYB)	II (EO-VYB)	III (PH-Thor-nel 25)	IV (PH-Thor-nel 50)
Fiber advance per turn of winding core [mm]	1.00	1.00	0.60	0.65
Winding core speed [rpm]	17	17	12	12
Fiber speed [m/min]	7.3	7.3	5.2	5.2
Fiber dwell time in bath [sec]	1.8	1.8	2.6	2.6
Number of winding layers	4	4	5	5
Length of winding process [h]	1.6	1.6	4.6	4.3

G_F = quantity of fiber in a wound piece [g]

ρ_F = fiber density [g/cm^3]

s_W = thickness of initially cured spool [cm]

l_W = length of initially cured spool or winding core (40.00 cm)

u_K = circumference of winding core (43.35 cm)

x_F = Fiber fraction by volume in composite, the treatment temperature for which is above the initial curing temperature of the matrix [%]

V_o = volume of initially cured composite [cm^3]

V = volume of composite, the treatment temperature of which is above the initial curing temperature of the matrix [cm^3]

6.23. Properties of the cured composites

The strength behavior, weight loss and shrinkage of the carbon-fiber-reinforced thermoset matrices were studied as functions

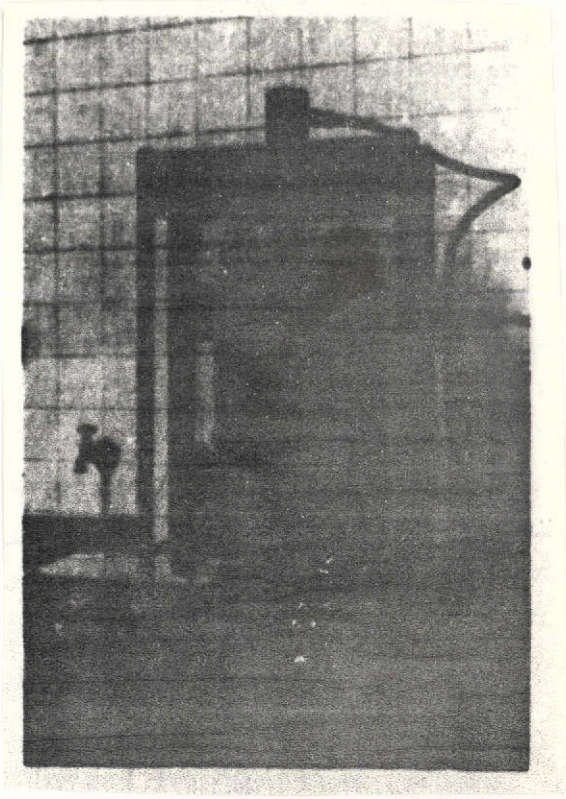

[Fig. 13]

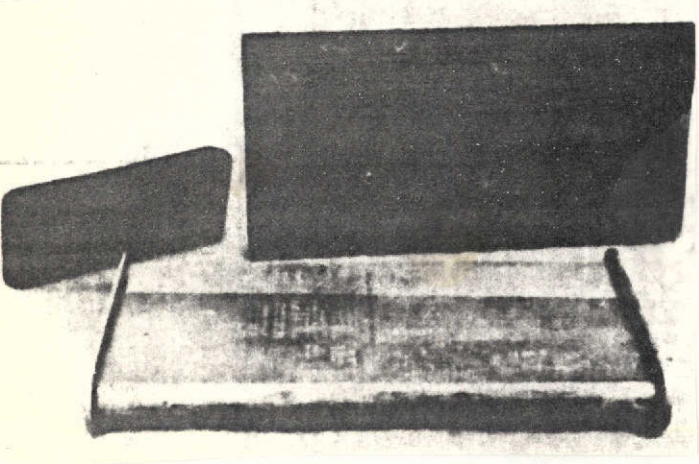

Fig. 14. Winding core and pressure-cured windings

of curing temperature. The mechanical properties of composites I - IV are shown in Table 19. The tensile strength and moduli of elasticity calculated by alligation (Eqs. (2-3) and (2-5); see Section 2.2) are included for comparison. It was assumed in the calculation of bending strengths that the composites experience purely elastic deformation to the point of fracture and that bending fracture is initiated by a tensile failure. The calculated tensile and bending strengths are therefore identical.

The predicted values apply to optimum conditions. It was assumed /85 here, both for the reinforcing component and for the matrix component, that their properties are fully exploited in a composite. In the case of the reinforcing component, the characteristic data for the filaments, rather than the yarns, were used for calculating composite properties. The σ_M^* values and $d\sigma_M/d\varepsilon_M$ values for the matrix materials were replaced by their tensile strength and modulus of elasticity values (see Section 4.12) in the equations.

The measured tensile strengths and moduli of elasticity of the four types of composites reach maxima in the temperature range between 200 and 220°C. The initial improvement in these two mechanical properties during the curing process can be attributed to hardening, but also to embrittlement of the thermoset matrices with increasing curing temperature and increasing cross-linkage. Full curing of the composites at 300°C causes a reduction in their tensile strengths and their moduli of elasticity. The reason for this is damage to the composite structure, caused by matrix shrinkage (see Section 6.24).

TABLE 18. CURING CONDITIONS FOR COMPOSITE TYPES I - IV

Type of composite	Curing step I	Curing step II	Curing step III
I (PH-VYB)	18 h at 70°C	2 h at 100°C, pressure: 0.03 kp/cm² 27 h at 100°C, pressure: 5 kp/cm²	45 h at 110°C 110 - 130°C Heating rate: 12°C/h in N_2 atmosphere
II (EO-VYB)	15 h at 70°C	3 h at 100°C, pressure: 0.03 kp/cm² 20 h at 100°C 70 h at 130°C pressure: 5 70 h at 140°C kp/cm²	72 h at 180°C 72 h at 220°C in air 75 h at 250°C 60 h at 300°C in N_2 atmosphere
III (PH-Thornel 25)	15 h at 70°C	2 h at 100°C, pressure: 0.03 kp/cm² 27 h at 100°C, pressure: 5 kp/cm²	45 h at 110°C 110 - 300°C Heating rate: 12°C/h in N_2 atmosphere
IV (PH-Thornel 50)	15 h at 60°C	2 h at 100°C, pressure: 0.03 kp/cm² 24 h at 100°C, pressure: 5 kp/cm²	45 h at 110°C 110 - 300°C Heating rate: 12°C/h in N_2 atmosphere

TABLE 19. MECHANICAL PROPERTIES OF COMPOSITE TYPES I - IV AS A FUNCTION OF CURING TEMPERATURE (DETERMINED IN FIBER DIRECTION AT ROOM TEMPERATURE)

Type of composite	Curing temperature [°C]	Fiber content by vol. [%]	Tensile strength [kp/mm²]			Young's modulus [kp/mm²]			Bending strength [kp/mm²]			Interlaminar bending shear strength [kp/mm²]
			measured	calculated	achieved [%]	measured	calculated	achieved [%]	measured	calculated	achieved [%]	
I (PH-VYA)	110	47.5	38.8	41	94	1860	2070	90	32.1	41	78	4.30+
	205	47.5	39.8	43	92	1920	2160	89	29.8	43	69	4.62+
	305	49.2	33.4	47	71	1950	2330	84	-	-	-	3.29+
II (EO-VYB)	140	60.7	39.4	53	74	2150	2650	81	27.9	53	53	2.47
	220	60.0	45.6	53	86	2150	2650	81	29.8	53	56	4.24
	300	56.5	32.3	58	56	1960	2820	70	25.7	58	44	2.17
III (PH-Thor-nel 25)	110	43.6	53.1	57	94	6940	7710	90	43.8	57	77	2.04+
	200	47.7	56.1	63	89	7570	8520	90	31.5	63	50	1.74+
	305	46.8	47.2	65	73	6980	8460	83	21.7	65	33	0.98
IV (PH-Thor-nel 50)	110	42.8	72.2	87	83	17080	15060	113	35.0	87	40	2.30+
	210	43.9	75.6	92	83	17720	15560	114	31.5	92	34	2.48+
	300	43.9	62.7	94	67	17330	15650	111	18.8	94	20	1.13+

The values calculated by alligation for the tensile strengths of composite types I - IV are achieved 85 - 95% with the experimentally determined values at the optimal curing temperatures. Composites with Phenodur PR 373 phenolic resin as the matrix component (composites I and III) yield the best utilization of the fiber and matrix strengths employed. The measured values for moduli of elasticity reach 80 to 115% of the calculated values with optimum curing. In this case, too, the best utilization of the fiber and matrix moduli employed is obtained for the composites with matrices of phenolic resin (composites I, III and IV).

The bending strength of initially cured composites decreases with progressive curing. A strength maximum in the temperature range between 200 and 220°C, as occurs in the tensile strength of the composites as the result of hardening of the matrix, is exhibited only by composite II (EO-VYB). /86

Although the bending test yields higher strength values than the tensile test under some conditions for brittle materials (see Section 2.31) and in general for plastically deformable materials, the measured values for bending strengths of the initially cured composites reach only 50 - 80% of the measured tensile strength values. Since the load acting from outside on the fiber-reinforced composite must be transmitted to the fibers by the matrix in the bending test, a poor state of fiber/matrix bonding can be concluded from the low bending strength data (see Section 6.24). In such a case, it is no longer possible to achieve complete utilization of the strength properties of the fibers.

The ratio of bending strength to tensile strength remains approximately constant over the entire curing range for composites I and II, with ungraphitized type VYB carbon fiber of high specific surface area. For composites III and IV, with stretch-graphitized Thornel 25 and 50 fibers of low specific surface area, the ratio decreases with increasing curing temperature, so the utilization of fiber strength is even poorer. This fact can be attributed to curing shrinkage of the matrix, on the one hand, and poorer adhesion between the smooth surface of the Thornel fiber types and the resin binder, on the other. Increased separation of the matrix from the filaments occurs, as a result of which the bonding of the reinforcing component in the resin matrix and thus bending strength as compared to the tensile strength of the composite deteriorate further.

The measured values for the bending strengths of composites I - IV reach only 40 - 80% of the predicted values in the optimum curing stage. Composites of Phenodur PR 373 phenolic resin reinforced with VYB and Thornel 25 fibers (composites I and III) yield the best utilization of the fiber and matrix strengths

employed, as in the case of tensile strength.

The accuracy of the composite values calculated from the /87
mechanical properties of the pure components should not be overestimated, since the carbon fibers used are industrial products subject to fluctuations in quality. Let us refer to composite IV as an example, whose measured modulus of elasticity is about 15% above the calculated value in the optimum curing stage. Similar cases are also known from the literature [20, 90, 94].

The bending shear strengths of composites is primarily a function of curing temperature and the type of fiber used. Much as in the case of tensile strength, the bending shear strengths of type III reach maxima in the temperature range between 200 and 220°C. Thus hardening of the resin matrices as curing progresses contributes not only to an improvement in tensile strength but also to a rise in the bending shear strength of composites. Full curing at 300°C is accompanied by a drop in shear strength, as is the case with tensile and bending strengths, due to damage to the composites as a result of matrix shrinkage (see Section 6.24). As expected, higher strength values are obtained from the composites with nongraphitized carbon fibers of the VYB type, with high specific surface area (composites I and II), in all stages of curing. In the case of composites III and IV, with stretch-graphitized carbon fibers of the Thornel 25 and 50 types, such good adhesion does not occur between fiber and matrix, as the result of the low specific surface area of these fibers, so these systems fail under relatively small loads per unit area.

Delamination of the composites (see Fig. 15) did not always occur with the selected support to specimen thickness ratio of 5:1. The specimens then failed without any sign of delamination due to premature fracture on the side subjected either to tension or to compression. In this case, the bending shear strength values obtained (specially labeled in the table) represent a minimum at which no delamination yet occurs. /88

Weight loss and longitudinal contraction in the fiber direction can be seen for composites I - IV as functions of curing temperature. The resin/fiber systems, like the unreinforced thermoset matrices, experience increasing weight loss as curing progresses. The extent to which the experimentally determined weight loss of composites agrees with the weight loss which can be calculated from their pure components is indicated in Table 20 with the calculated data that are presented. These values were calculated with the following formula:

$$G_L = G_M \; y_{M_0} \quad [8] \qquad (6\text{-}3)$$

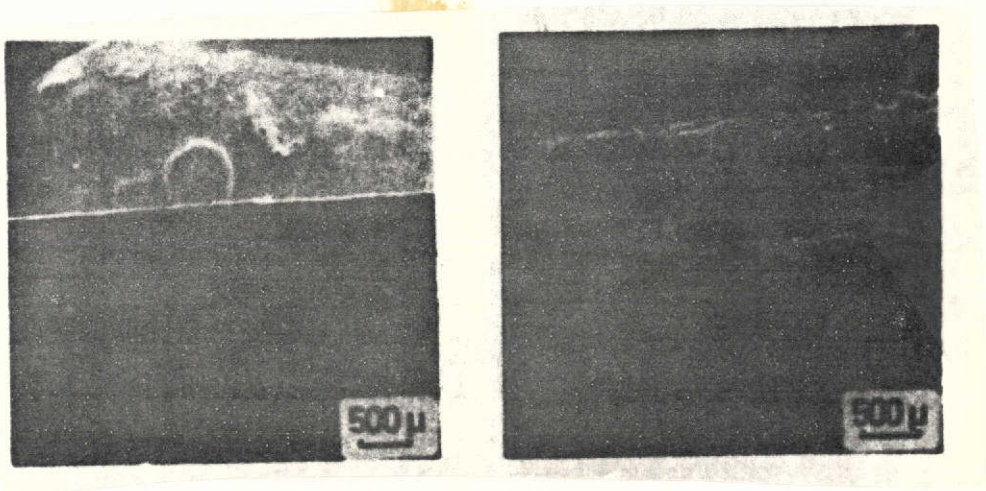

Fig. 15. Scanning electron micrographs of a delaminated laminate of composite II (E)-VYP), treatment temperature 300°C

where

$$y_{M_o} = \frac{1}{1 + \frac{\rho_F \, x_{F_o}}{\rho_{M_o} (1 - x_{F_o})}} \quad [1]$$

and:

G_L = weight loss of fiber-reinforced composite [%]

G_M = weight loss of thermoset matrix without fiber reinforcement [%]

Y_{M_o} = matrix component by weight in initially cured composite [1]

ρ_F = fiber density [g/cm³]

ρ_{M_o} = density of matrix in cured state [g/cm³]

(ρ_{PH} = 1.18 g/cm³, ρ_{EO} = 1.25 g/cm³)

x_{F_o} = fiber content by volume of initially cured composite [1]

Eq. (6-3) covers only the weight loss of the matrix component. It was assumed that the reinforcing component experiences no weight loss (G_F = 0%).

The measured composite weight losses exhibit a more or less pronounced positive or negative deviation from the calculated values. For composites III and IV, with /90

TABLE 20. WEIGHT LOSS AND LONGITUDINAL CONTRACTION IN FIBER DIRECTION OF COMPOSITES I - IV DURING CURING (ROOM TEMPERATURE DATA)

Type of composite	Curing temperature [°C]	Weight loss [%] measured	Weight loss [%] calculated	Longitudinal contraction in fiber direction [%]
I (PH-VYB)	110	0	0	0
	205	3,4	3,7	0,06
	305	9,2	10,1	0,24
II (EO-VYB)	140	0	0	0
	220	7,8	3,2	0,17
	300	22,1	10,4	0,35
III (PH-Thornel 25)	110	0	0	0
	200	3,5	3,9	0
	305	5,5	11,3	0
IV (PH-Thornel 50)	110	0	0	0
	210	2,5	4,2	-0,06
	300	4,8	10,5	0,03

stretch-graphitized Thornel 25 and 50 carbon fibers, cured at 300°C, twice as high a weight loss is calculated as measured. This finding indicates that the loss of weight and thus curing of the thermosets is delayed by imbedded carbon fibers. In the case of composite II, with ungraphitized VYB fiber, the weight loss figures calculated were only 40 - 50% of the measured data.

A weight loss on the part of the imbedded reinforcing component can thus no longer be ruled out, according to the above results. Studies in this regard have confirmed that, in contrast to Thornel fibers, VYB fibers lose weight if they are subjected to heating for a prolonged period in an atmosphere containing oxygen. A 300-hour heat treatment applied to this type of fiber in air at 300°C caused a 63% weight loss. The weight loss experienced by VYB fiber is also reflected in the results obtained from composite I. Due to the shorter curing times for this resin/fiber system, however, the weight loss of the imbedded VYB fibers is smaller, so the measured weight losses do not exceed the calculated values, as in the case of composite II, but only approach them.

Linear curing shrinkage in the fiber direction of composites is largely prevented by the low compressibility of the carbon fibers. In the case of composites I and II, with low modulus VYB fibers, it is more than an order of magnitude less than longitudinal contraction in the unreinforced thermosets. Composites III and IV, with high modulus Thornel 25 and 50 fibers, exhibit no shrinkage in the fiber direction, or only an amount lying within the limits of measurement error.

6.24. Structure of the cured composites /91

In order to characterize the structure of the cured composites, use is made of light microscopy and, due to its depth of field, scanning electron microscopy. The primary intention was to determine the causes for the drop in composite strength with increasing curing temperature. Conditions at the interface between fiber and matrix and damage to the composite as the result of matrix shrinkage were mainly studied.

The photomicrographs of sections of composites I, II and III in various stages of curing are shown in Figs. 16 - 19; Type III (PH Thornel 25) is structurally identical to Type IV (PH Thornel 50), which is not shown.

Fig. 16 shows the structure of composite I (PH-VYB) after initial curing at 110°C, representative of the other composites in the same curing stage. We see the irregular distribution of the reinforcing component in the matrix, which is characteristic of low fiber contents and twined fiber bundles. The good penetration of the carbon yarn with matrix material, i.e., the extensive isolation of monofilaments by the resin component, can also be seen. These conditions agree with the results of the wetting studies (see Section 5.2), according to which the thermosets wet the carbon fibers made from cellulose well. Microcracks, which primarily run along the fiber/matrix interface (see Fig. 16, top right), can be attributed to mechanical stressing of the specimen during grinding and polishing and indicate poor bonding between fiber and matrix. Pores occur only very occasionally.

During the course of full curing, the composites experience increasing damage which can be attributed exclusively to matrix shrinkage. Figs. 17 - 19 show the extent and nature of damage which the composites exhibit after full curing at 300°C. In /93 composite I (PH-VYB), the curing shrinkage in a matrix which occurs perpendicular to the fiber direction causes separation of the matrix from the fiber, on the one hand, and, on the other, causes the matrix to tear open in the fiber direction (see Fig. 17, top). The separation phenomena occur exclusively in the area of high fiber concentrations, i.e., within the fiber bundles. Damage to the matrix by cracks in the fiber direction, on the other hand, occurs only in relatively large fiber-free areas of matrix between the individual fiber bundles. In the area of the fiber

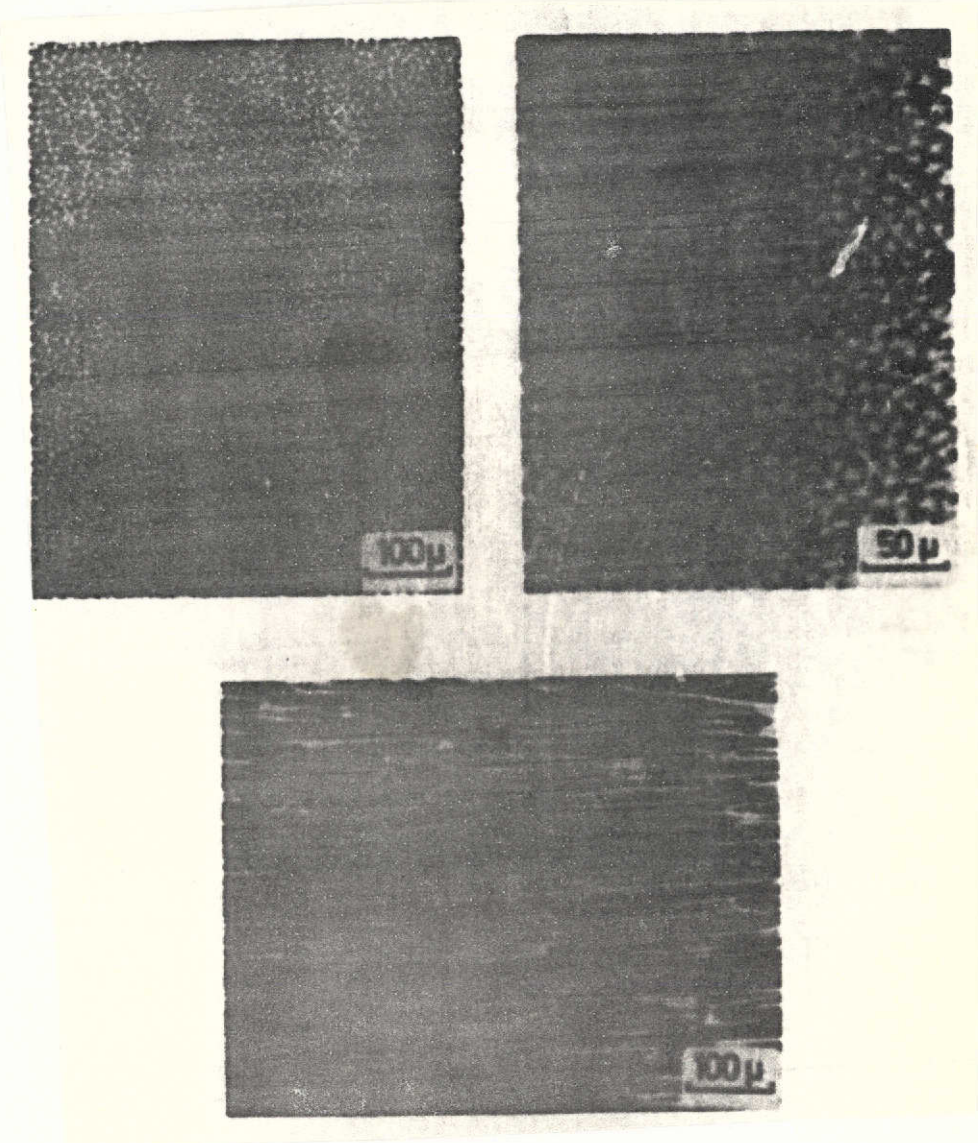

Fig. 16. Photomicrographs of a laminate of composite type I (PH-VYB), treatment temperature 110°C; top: cross section; bottom: longitudinal section

bundle margins, adequate bonding is insured between the two composite components. Within the fiber bundles, imperfect wetting of the individual fibers by matrix material must have occurred at various points, allowing the matrix to shrink away from the fiber unhindered at such locations. Separation of adhering parts of the matrix can also occur under more favorable conditions at such defects.

There is no damage to the composite from cracks running perpendicular to the fiber direction in the matrix (see Fig. 17, bottom), although linear shrinkage of the composite is less than 0.5% in the fiber direction. The matrix shrinkage in the

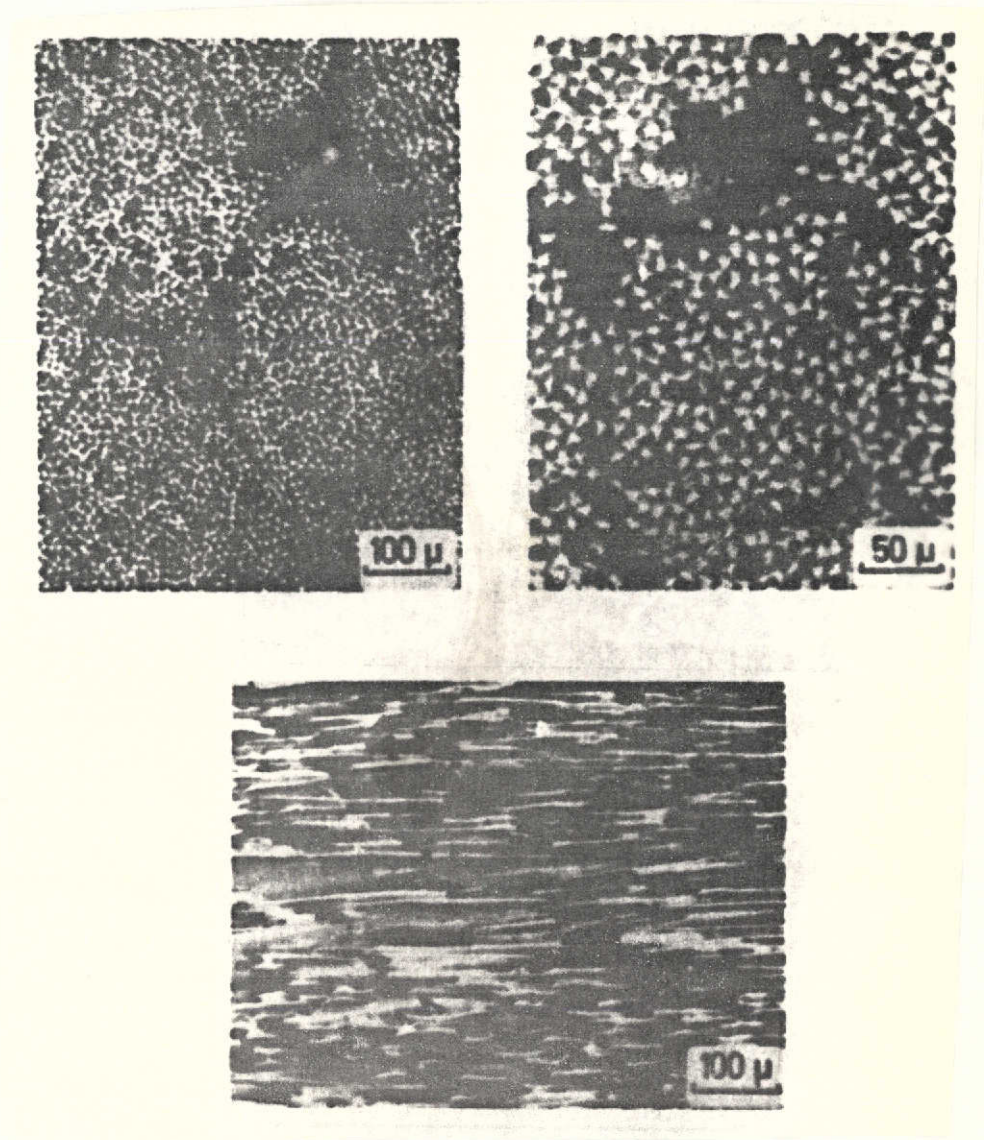

Fig. 17. Photomicrographs of a laminate of composite type I (PH-VYB), treatment temperature 305°C; top: cross section; bottom: longitudinal section.

fiber direction prevented during full curing is compensated for by a corresponding transverse contraction due to the plastic deformability of the matrix (see Section 4.135).

Composite II (EO-VYB) likewise exhibits longitudinal cracks in the areas of matrix delimited by carbon yarns. Within the fiber bundles, spherical pores can be observed in the matrix as the result of curing shrinkage, instead of the separation phenomena of the type occurring in composite I (see Fig. 18). This indicates that curing of the epoxy resin commences at the fiber surface.

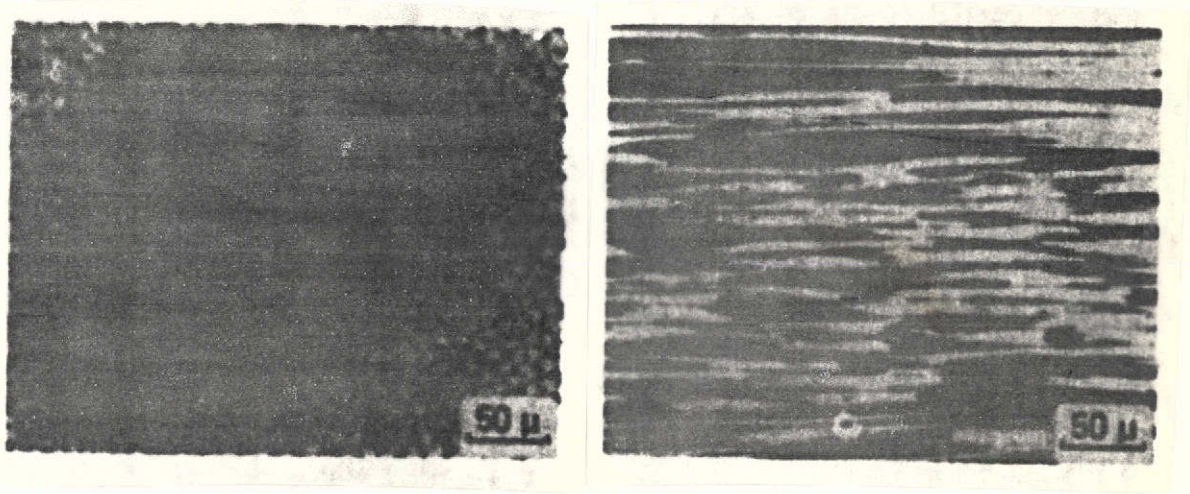

Fig. 18. Photomicrographs of a laminate of composite II (EO-VYB), treatment temperature 300°C; left: cross section; right: longitudinal section

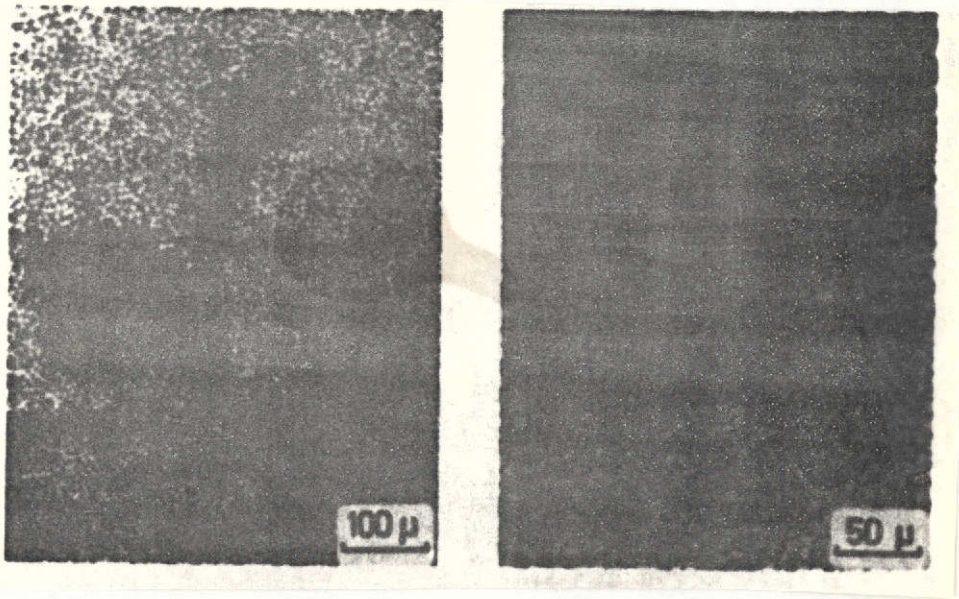

Fig. 19. Photomicrographs of a laminate of composite III (PH-Thornel 25), treatment temperature 305°C; cross section.

In composites III (PH-Thornel 25) and IV (PH-Thornel 50), no cracks form in the areas of matrix containing no fiber. In addition to separation phenomena, however, longitudinal cracks always occur in the fiber bundles, too, (see Fig. 19). The different form of cracking in these two composites as compared /95

to composite I can be attributed to the fact that the phenolic resin matrix adheres to the Thornel fibers, with a small specific surface area, more poorly than to the VYB fiber, with its large specific surface area. In the case of the Thornel fibers, adhesion is so poor that it is unable to inhibit crack formation along the fiber/matrix interface. Defects which develop from improper wetting of the monofilaments within the fiber bundles /96 form the starting points for longitudinal cracks here. Damage to the composite structure by cracks perpendicular to the fibers occurs just as infrequently in the composites reinforced with Thornel fibers as in composite I.

Figs. 20 - 23 show scanning electron micrographs of fracture surfaces of composites I and III from tensile tests at various stages of curing. The fracture behavior of composite II corresponds to that of type I, and that of IV corresponds to that of type III.

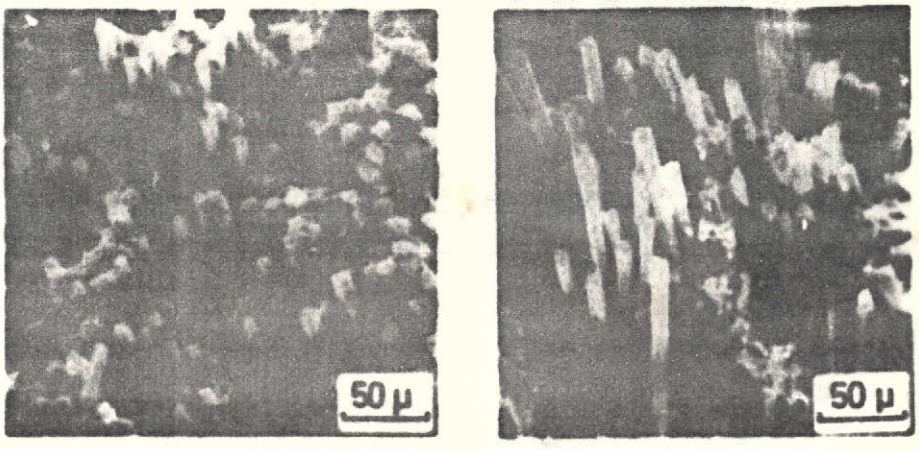

Fig. 20. Scanning electron micrographs of fracture surfaces of composite I (PH-VYB) from tensile test; left: after initial curing at 110°C; right: after full curing at 305°C.

The overview micrographs (see Figs. 20 and 21) show fiber ends projecting from the matrix surface. Their length represents a measure of the state of bonding between fiber and matrix, i.e., the shorter the fiber length, the better the bonding. It is better in the composites with nongraphitized VYB carbon fiber, /98 of high specific surface area, than in the composites with stretch-graphitized Thornel 25 and 50 carbon fibers, of low specific surface area. Fiber/matrix bonding in the composites is impaired by curing shrinkage in the matrix. This can be seen from the fact that the fiber ends project farther from the surface of the matrix after full curing at 300°C than in the initial curing stage.

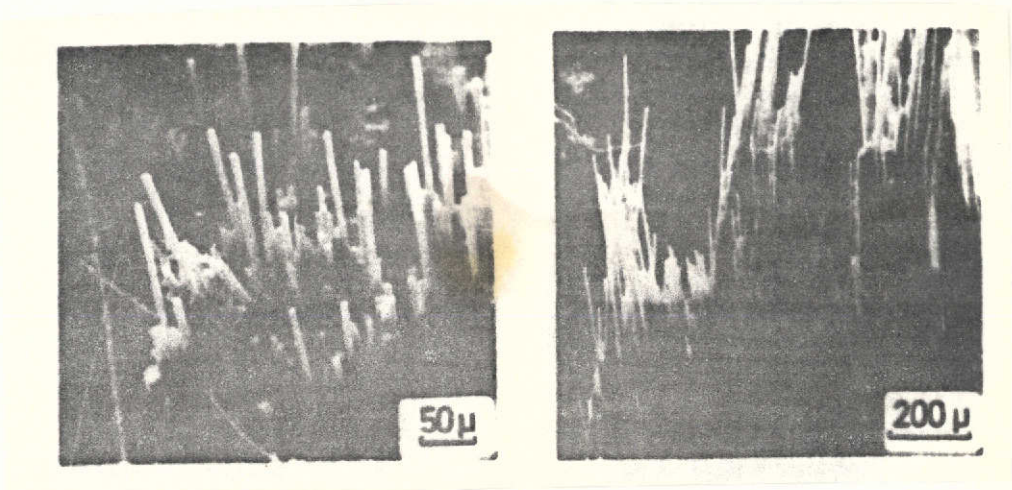

Fig. 21. Scanning electron micrographs of fracture surfaces of composite III (PH-Thornel 25) from tensile test: left: after initial curing at 110°C; right: after full curing at 305°C.

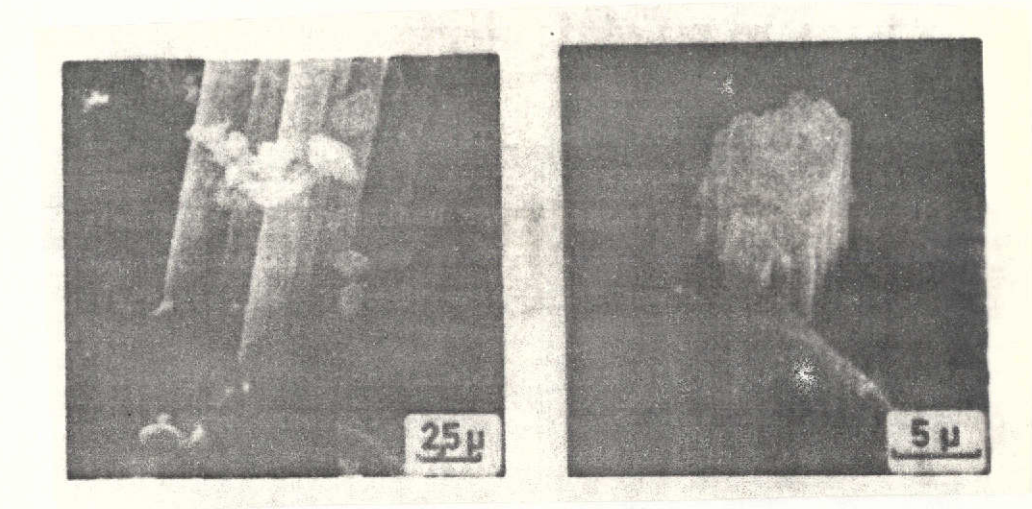

Fig. 22. Defective imbedding of carbon fibers in thermoset matrices after initial curing at 110°C; left: composite I (PH-VYB); right: composite III (PH-Thornel 25)

The closeups (see Figs. 22 and 23) show symptoms of damage to the composite structures. Fig. 22 indicates the imperfect wetting of monofilaments in the initially cured resin matrix as the result of imperfect wetting. Separation of the matrix from the fibers as the result of curing shrinkage can be seen from Fig. 23. The information which can be obtained from the microscopic studies agrees with the results of the strength

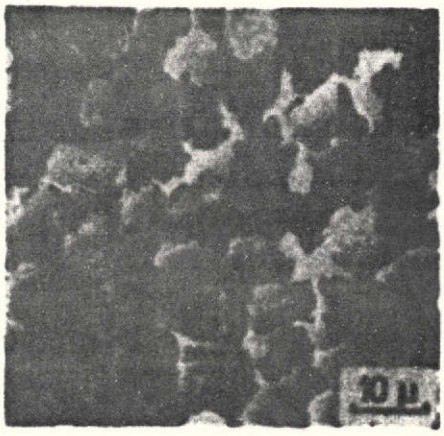

Fig. 23. Separation of resin matrix from carbon fiber; composite III (PH-Thornel 25) after full curing at 305°C.

studies (see Section 6.23), according to which increasing damage to the composites occurs as curing progresses, and a better state of bonding is achieved with the VYB fiber than with the Thornel types.

6.3. Author's studies on the carbon-fiber reinforcement of polyimides /99

6.31. Selection of composite systems studied

Only the composite systems made up of Kerimid 601 and QX-13 with Thornel 50 fiber were studied with the polyimide resins that were available. As already shown in Section 4.21, Kerimid 601 could be worked with easier than QX-13, whereas QX-13 exhibited both better thermal stability and greater coke residue. Only a few composites were prepared with P 13 N polyimide for preliminary pyrolysis experiments.

6.32. Preparation and curing of composites /100

It was possible to apply the technique used to prepare carbon-fiber-reinforced thermosets to the preparation of unidirectionally reinforced composites based on Kerimid 601 polyimide resin and Thornel 50 carbon fiber (wet winding followed by pressure curing of the wound product). The carbon fibers were impregnated with a 50 wt.% solution of Kerimid 601 in n-methyl-2-pyrrolidone (NMP). The data for preparation of the composites are compiled in Table 21.

Composites of QX-13 polyimide resin unidirectionally reinforced with Thornel 50 fibers could not be produced without defects with the technique used previously, due to the pronounced foaming of the matrix material. A method which has proven itself is to wind a layer of Thornel 50 yarn dry on a stretching frame (fiber advance / turn: 2.5 mm) and then impregnate the fibers with a 20 wt.% solution of QX-13 in acetone. In order to achieve complete sheathing of the fibers with resin, impregnation was done 12 times. Each impregnation was followed by ten minutes of heat treatment of the fiber cords in the drybox at 100°C in order to evaporate solvent and fix the resin to the fibers. After the last impregnation, the resin-coated carbon fibers were partially cured at 100°C for one hour and 200°C for seven hours.

TABLE 21. DATA ON THE PREPARATION OF UNIDIRECTIONALLY REINFORCED COMPOSITES BASED ON KERIMID 601 POLYIMIDE RESIN / THORNEL 50 FIBER

Fiber tension [p]	250
Fiber advance / winding turn [mm]	0.56
Number of winding layers	5
Curing conditions in air	2 h at 80°C 75 min at 120°C 40 min at 130°C 20 min at 140°C 15 min at 150°C (Pressure 1.5 kp/cm²) 1 h at 120°C 1 h at 140°C 15 h at 160°C 30 h at 200°C 20 h at 250°C 15 h at 300°C
Composite thickness [mm] (after curing at 160°C)	0.80
Fiber content by volume [%] (after curing at 160°C)	40.0

The precured fiber cords were made into specimen bars with dimensions of 200 X 5 X 1.5 mm in a die heated to 325°C under a pressure of 2.1 kp/mm². Curing time under these conditions was 30 min. The specimen bars were aftercured without pressure and exposed to air at 300°C for 15 h. The fiber content was varied by changing the number of impregnated fiber cords per specimen bar and by pressing the bars to equal thickness.

The same method with the following modified curing schedule was applied to the P 13 N polyimide resin / Thornel 50 fiber composites prepared for performing a preliminary pyrolysis /101 experiment:

1. Resin-impregnated fiber cords dried in vacuum drybox under water-aspirator vacuum:

1 h at 80°C
1 h at 100°C
3 h at 120°C

2. Dried fiber bundles, covered with additional pulverized P 13 N, pressure-cured (maximum curing temperature 140°C) in a

TABLE 22. PROPERTIES OF CURED CARBON-FIBER-REINFORCED POLYIMIDES (DETERMINED IN FIBER DIRECTION AT ROOM TEMPERATURE)

Type of composite	Curing temperature [°C]	Fiber content by vol. [%]	Tensile strength [kp/mm²] measured	Tensile strength [kp/mm²] calculated+	Tensile strength [kp/mm²] achieved [%]	Young's modulus [kp/mm²] 10-3 measured	Young's modulus [kp/mm²] 10-3 calculated+	Young's modulus [kp/mm²] 10-3 achieved [%]	Bending strength [kp/mm²] measured	Bending strength [kp/mm²] calculated+	Bending strength [kp/mm²] achieved [%]	Interlam. bending shear strength [kp/mm²]	Weight loss [%]	Longitudinal contraction [%]
KERIMID 601/Thornel 50	160	40.0	80.8	80	101	15.9	14.0	114	38.4	80	48	1.73	0	0
	200	41.3	79.3	83	96	16.7	14.5	115	35.9	83	43	1.42	3.9	0
	250	41.6	80.6	83	97	17.2	14.6	118	35.7	83	43	1.37	4.3	0
	300	43.1	76.1	86	89	16.7	15.1	111	31.4	86	37	1.15	5.8	0
QX-13/ Thornel 50	300	30.4	37.7	61	62	10.1	10.6	95	21.1	61	35	2.51++	-	-
	300	46.3	68.3	93	74	15.1	16.2	93	39.9	93	43	2.64	-	-
P13N/Morganite Modmor II-S	310	60	-	-	-	15.8+++	15.0-19.2	105-82	107.5	150-192	72-56	4.56	-	-

\+ Matrix component was neglected

++ 50% of specimens did not delaminate

+++ Bending modulus

die open at the ends:

30 min at 300°C; pressure: 0.75 kp/mm^2

3. Composites aftercured without pressure in air: /102

20 h at 150°C
15 h at 200°C
15 h at 250°C
10 h at 300°C

6.33. Properties and structure of the cured composites

The measurements were performed on the fiber-reinforced polyimide resins under the same test conditions as those on which the studies of fiber-reinforced thermosets were based. The data obtained on the composite properties are compiled in Table 22. Composites of P 13 N with surface-treated carbon fibers by Morganite Modmor Ltd. were prepared and tested by a colleague at the same time as the author's experiments. The properties of these composites are included in Table 22.

The composite based on Kerimid 601 / Thornel 50 fiber studied in various stages of curing exhibits approximately constant tensile strength and modulus of elasticity values over the entire curing range. If the unknown characteristic matrix data are neglected, allegation (Eqs. (2-3) and (2-5); see Section 2.2) indicates 95% utilization of fiber strength and 115% utilization of fiber modulus of elasticity, averaged over the curing range.

The bending strength and interlaminar bending shear strength of the composite decrease with progressive hardening, indicating increasing damage to the composite structure as the result of curing shrinkage of the polyimide matrix. About 50% of the predicted composite bending strength is achieved in the initial hardening stage. After full curing at 300°C, utilization of the fiber strength used amounts to only about 35%. A comparison of the mechanical properties of composites /104 of Kerimid 601 polyimide resin / Thornel 50 fiber and Phenodur PR 373 phenolic resin / Thornel 50 fiber cured at 300°C (see Section 6.23) shows that the polyimide resin is superior to the thermoset as matrix material for heat-resistant composites.

Scanning electron micrographs of fracture surfaces of the carbon-fiber / polyimide laminate from tensile testing (see Fig. 24) provide an impression of the composite structure and the state of fiber/matrix bonding. The fiber tips projecting far from the matrix surface indicate poor adhesion of the matrix to the fibers. Imperfect imbedding of the fibers in the polymer matrix because of poor wetting can be ruled out, since angle of contact measurements made by the direct method with the scanning

electron microscope (see Section 5.22) showed excellent wetting behavior.

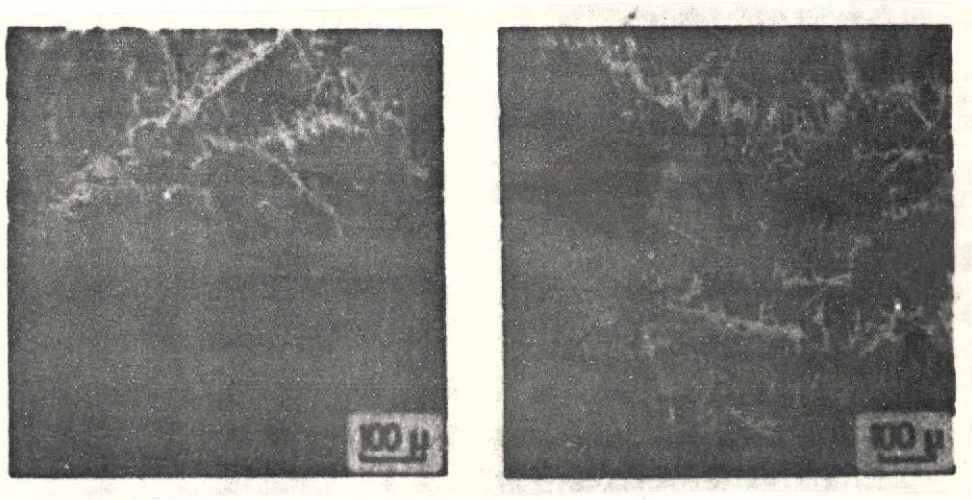

Fig. 24. Scanning electron micrographs of fracture surfaces of the Kerimid 601 polyimide / Thornel 50 fiber composite from tensile test: left: aftercuring at 160°C; right: after full curing at 300°C.

The composite material of QX-13 polyimide resin reinforced with Thornel 50 fiber and cured at 300°C does not provide the full extent of composite strength properties to be expected on the basis of alligation. The measured tensile strength for the composites of low fiber content (30.4 vol.%) is 62% and that for the composites of high fiber content (46.3 vol.%) is 74% of the calculated value, neglecting matrix strength. While 93% (x_F = 46.3 vol.%) and 95% (x_F = 30.4 vol.%) of the calculated composite modulus of elasticity is achieved, it is somewhat lower than the value achieved by the Kerimid 601 (115%) or Phenodur PR 373 (111%) reinforced with Thornel 50 fibers. In the case of bending strength, only 35 to 43% of fiber strength is utilized. /105

The cause of reduced utilization of the strength of Thornel fibers in the QX-13 matrix rests in the technique for preparing this composite. The high pressure necessary for compacting the composite impairs unidirectional fiber orientation and causes damage to the fibers. The relatively high interlaminar bending shear strength of the composite, hardly affected by the above, indicates good adhesion of the matrix to the fiber.

Photomicrographs and scanning electron micrographs of specimen bars (see Figs. 25 and 26) show the structural characteristics of the polyimide resin reinforced with 30 vol.%

carbon fibers. In spite of the high pressure used for pressing, it was not possible to produce a composite which was completely compact in the interior. Defect-free imbedding of the fiber in the matrix can be observed in areas containing no pores. Fracture behavior is similar to that of thermosets reinforced with VYB fibers after their partial curing. The tensile test produced fracture surfaces with short fiber tips projecting from the matrix surface, characteristic of good-fiber/matrix bonding, on the one hand, and on the other hand, supportive of information obtained from the bending shear test.

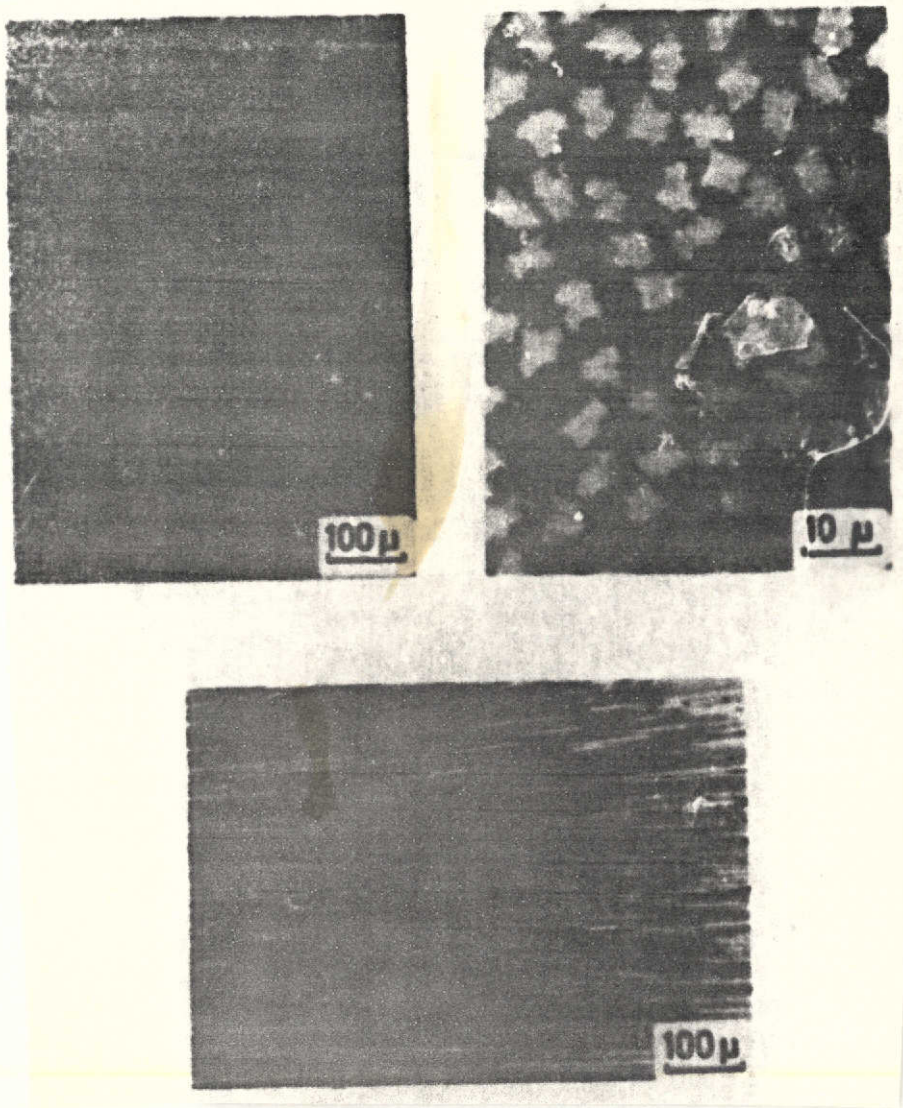

Fig. 25. Photomicrographs of composites of QX-13 polyimide resin and Thornel 50 fibers after curing at 300°C, fiber content 30.4 vol.%; top: cross section; bottom: longitudinal section.

In contrast to the composites discussed above, those of P 13 N polyimide resin with surface-treated Morganite Modmor fibers are characterized both by high interlaminar bending shear strength and, in the case of bending strength, by better utilization of the strength of the fibers used. These facts agree with predictions based on a knowledge of the strength behavior of polymers which are reinforced with surface-treated fibers. /106 /107

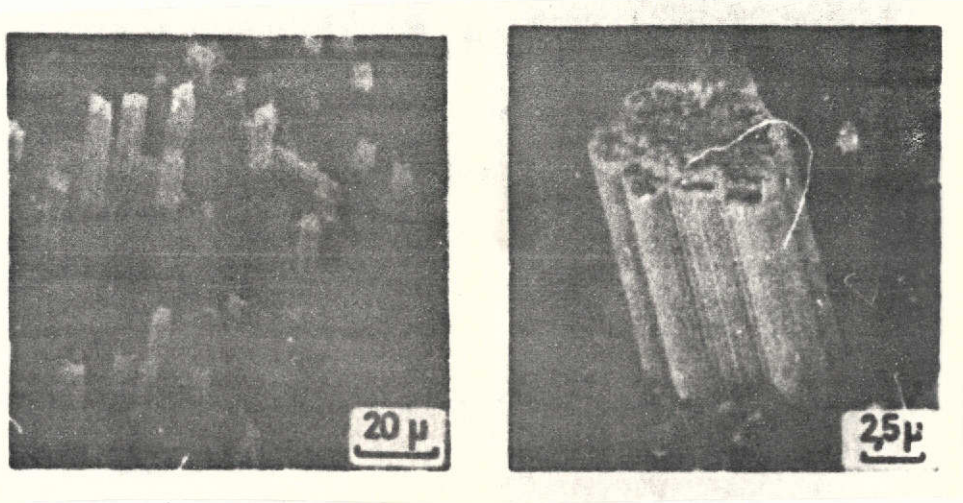

Fig. 26. Scanning electron micrographs of fracture surfaces of QX-13 polyimide / Thornel 50 fiber composite from tensile test, curing temperature 300°C, fiber component 30.4 vol.%.

6.4. Aging behavior of carbon-fiber-reinforced thermosets and polyimides

Curable carbon-fiber-reinforced polymers are known to resist high thermal loads for brief periods in air. Under prolonged thermal loads above their sustained-use temperature, however, they experience shrinkage, primarily as the result of oxidative decomposition, causing the impairment of mechanical properties. In an inert gas atmosphere, on the other hand, thermal decomposition of the polymer matrices contributes considerably to a change in composite properties.

Table 23 shows the properties of fully cured carbon-fiber-reinforced thermosets and polyimides after hot aging at 300 - 400°C in air and at 400°C in a nitrogen atmosphere. The ratio, in percentage, between the strength values for hot-aged and fully cured composite systems are included in parentheses. /110

The results of the thermal aging tests show that the carbon-fiber-reinforced thermosets are destroyed in air even at 300°C.

TABLE 23. PROPERTIES OF HOT-AGED CARBON-FIBER-REINFORCED THERMOSETS AND POLYIMIDES, CURED AT 300°C (DETERMINED IN FIBER DIRECTION AT ROOM TEMPERATURE)

Resin/fiber system	Fiber content by volume after curing at 300°C [%]	Aging conditions	Tensile strength [kp/mm²]	Bending strength [kp/mm²]	Interlaminar bending shear strength [kp/mm²]	Weight loss [%]
Phenodur PR 373/ VYB	49.2	300 h at 300°C in air	0.78 (2%)	<0.01 (<0.04%)	<0.01 (<0.03%)	76.5
		150 h at 400°C in nitrogen	-	18.5 (68 %) 24.4+	1.18++ (36%)	10.8
Phenodur PR 373/ Thornel 25	46.8	300 h at 300°C in air	23.8 (50%)	<0.01 (0.05%)	<0.01 (<1%)	38.1
		150 h at 400°C in nitrogen	-	3.6 (17%) 13.1+	0.32 (33%)	6.2
KERIMID 601/ Thornel 50	43.1	300 h at 300°C in air	-	<0.01 (<3%)	<0.05 (<5%)	33.9
		300 h at 400°C in air	-	<0.01 (<0.03%)	<0.05 (<5%)	36.4
		300 h at 400°C in nitrogen	-	10.7 (34%) 17.5+	0.45 (39%)	20.1

+ determined at 300°C; support/thickness ratio 25:1
++ specimens did not delaminate

TABLE 23 continued

Resin/fiber system	Fiber content by volume after curing at 300°C [%]	Aging conditions	Tensile strength	Bending strength	Interlaminar bending shear strength	Weight loss
QX-13/Thornel 50	30.4	300 h at 300°C in air	-	39.9 (189%) 35.5+	2.30 (92%)	9.0
		300 h at 400°C in air	-	0 (0%)	0 (0%)	99.9
		300 h at 400°C in nitrogen	-	36.2 (172%) 32.5+	2.32++ (92%)	6.5
	46.3	300 h att 300°C in air	-	35.4 (89%) 29.3+	1.72++ (65%)	9.0
		300 h at 400°C in air	-	0 (0%)	0 (0%)	90.6
		300 h at 400°C in nitrogen	-	32.6 (82%) 28.8+	1.73 (66%)	5.6

* + determined at 300°C; support/thickness ration 25:1
++ specimens did not delaminate

It can be seen from the high weight loss and the 26% longitudinal contraction of phenolic resin reinforced with VYB fibers that oxidative attack is not limited to just the resin matrix but also affects the reinforcing component. Aging tests performed under equivalent conditions with the types of resin-free carbon fiber yield a weight loss of 63.3% and a longitudinal shrinkage of 22.3% for the nongraphitized VYB fiber. For the stretch-graphitized Thornel 25 and 50 fibers, the weight loss amounts to between 0.5 and 1%. Shrinkage in the fiber's longitudinal direction is not observed.

The resistance of both Kerimid 601 and QX-13 fiber-reinforced polyimides to aging in air at 300°C differs considerably. While the ability of the matrix to hold the fibers together is lost to a large extent in the composite made with Kerimid 601 polyimide, the composites with QX-13 matrices exhibit 89 to 189% of their original bending strength and 65 to 92% of their interlaminar bending shear strength.

Hot aging at 400°C in air causes complete destruction of the fiber-reinforced polyimides. Under these aging conditions, the Thornel 50 fibers are completely oxidized in the presence of the QX-13 matrix in the case of low fiber content by volume, whereas for higher fiber content, the fiber is only partially oxidized. On the other hand, Kerimid 601 does not affect oxidation of the fiber.

The heat resistance of Phenodur PR 373 and Kerimid 601 fiber-reinforced resins in ultrapure nitrogen at 400°C is considerably better than that in air at 300°C. When subjected to purely thermal loads, the materials retain 17 to 68% of their initial bending strength and 33 to 39% of their initial interlaminar shear strength. The composites with a QX-13 polyimide resin matrix exhibit almost just as good strength behavior after heating as 400°C in an inert gas atmosphere as after heat treatment at 300°C in air. /111

The hot bending strengths of heat aged composites determined at 300°C deviate considerably from the values taken at room temperature (see Table 23). Phenodur PR 373 phenolic resin and Kerimid 601 polyimide yield higher bending strength values at 300°C than at room temperature. Conditions are reversed for QX-13 polyimide.

In summary, it can be stated that composites made of Kerimid 601 and QX-13 polyimides withstand thermal loads at 300 to 400°C better than composites of Phenodur PR 373 phenolic resin, and their sensitivity to oxidation is also lower. Because of the very complex decomposition process, no final conclusion can be drawn from the small number of experiments regarding load limits.

7. Thermal decomposition of carbon-fiber-reinforced polymers to carbon-carbon composites /112

7.1. Literature

Two alternative methods are known for producing carbon-fiber-reinforced carbon composites, namely the precipitation of "pyrocarbon" from the gas phase (carbon vapor deposition) in carbon fiber structures and the thermal decomposition of carbon-fiber-reinforced composites with organic matrices [16, 19].

The CVD method involves serious technical problems but has so far yielded the best results (see Table 24). The technically simpler method of bonding agent pyrolysis is based on the controlled thermal decomposition of carbonizable material in which carbon fibers have been imbedded. Polymers, pitches, or combinations of these are used as starting material for the carbon matrix. Since, of the polymers, highly cross-linked thermosets are primarily capable of producing isotropic high-strength carbon without cracks and pores in controlled thermal decomposition, carbon-fiber-reinforced thermosets are primarily used as starting material for the carbon binder in carbon-carbon composites.

Due to the high volume shrinkage of the polymer and pitch matrices during carbonization, the carbon-carbon composites are porous and cracked. Their mechanical strengths are thus low (see Table 24). These materials can be considerably enhanced with regard to their strength behavior by suitable measures, however.

Table 25 provides a survey of present methods for producing solid carbon-carbon composites based on fiber-reinforced organic matrices and contains a compilation of the strengths which are achieved. Of / possibilities listed, the most impressive at /116 first glance are the two approaches given first: the cocoking of synthetic organic fibers in polymer matrices and the addition of solid or fusible fillers such as graphite powder or pitch. The cocoking of reinforcing fibers would offer the advantage that the fibers need not be carbonized first. The incorporation of fillers requires only a small amount of work. As can be seen from the literature data on the strength properties of carbon-carbon composites, however, only the addition of a solid lean material such as graphite powder has proven successful so far.

The method used most frequently at present to improve strength properties consists of impregnating the composites with an organic matrix after coking and then coking them a second time. This method, known and practiced as the impregnation method for decades in synthetic carbon technology, only proves to be desirable, however, if the fibers are not appreciably damaged by the first coking process. Since three to four

TABLE 24. LITERATURE DATA ON STRENGTH PROPERTIES OF CARBON-CARBON COMPOSITES AT ROOM TEMPERATURE

Method of production	Matrix precursor / Type of carbon fiber	Tensile strength [kp/mm²]	Bending strength [kp/mm²]	Interlaminar bending shear strength [kp/mm²]
Thermal decomposition of carbon-fiber-reinforced organic matrices (without reimpregnation)	R 10993 phenolic resin (Bakelite Ltd.) / HM carbon fiber (RAE, England) [20]	-	15	-
	Resin+ /C fabric+ (Union Carbide Corp.) [17]	-	10	1.4
	Furfuryl alcohol resin / C fiber+ [24]	-	21 - 23	2.2 - 2.7
	Pasing EP 77 pitch /VYB C fiber (Union Carbide Corp.) [25]	5	3	0.14
	Pasing EP 77 pitch /Thornel 50 C fiber (Union Carbide Corp.) [25]	>33	45	1.8
Precipitation of pyrocarbon in carbon fiber structures	Pyrocarbon / Thornel 50 C fiber (Union Carbide Corp.) [16]	72	77	2.8

+ no detailed information given

TABLE 25. MEASURES TAKEN TO PRODUCE SOLID CARBON-CARBON COMPOSITES BASED ON FIBER-REINFORCED ORGANIC MATRICES, AND STRENGTH PROPERTIES ACHIEVED

Measure	Components of uncoked composites	Strength properties of unidirectionally reinforced C-C composites (determined in fiber direction at room temperature)		
		Tensile strength [kp/mm^2]	Bending strength [kp/mm^2]	Interlaminar bending shear strength [kp/mm^2]
Cocoking of organic fibers in polymer matrices	Phenolic resin / partially pyrolyzed rayon fiber [14]	5	-	-
Incorporation of solid or fusible fillers into polymer matrices with carbon fiber reinforcement	Phenolic-epoxy resin mixture filled with graphite / HM C fiber (RAE, England) [20]	-	88	3.0
	438 epoxy resin (Dow Chemical Co.) modified with PR 275 pitch (3M Co.) / CY 5 C fiber (Carborundum Co.) [15]	12^{+}	29‡	2.1‡
Impregnation of carbonized carbon-fiber-reinforced polymers and pitches with new organic matrix, followed by recarbonization	98-638 phenolic resin (Reichhold Chemicals, Inc.) / CY-2 C fiber (Carborundum Co.) [15]	19^{+}	34^{+}	2.1^{+}
	Resin^{++++} / C fiber^{++++} [16]	-21^{+}	32^{+}	2.5^{+}
	Pasing EP 77 pitch / VYB C fiber (Union Carbide Corp.) [26]	1^{++}	4^{++}	0.35^{++}
	Pasing EP 77 pitch / Thornel 75 C fiber (Union Carbide Corp.) [26]	-	97^{+++}	3.2^{+++}

TABLE 25 continued

Measure	Components of uncoked composites	Strength properties of unidirectionally reinforced C-C composites (determined in fiber direction at room temperature)		
		Tensile strength [kp/mm²]	Bending strength [kp/mm²]	Interlaminar bending shear strength [kp/mm²]
Precipitation of pyrocarbon in thermally decomposed carbon-fiber-reinforced thermosets	Resin++++ / HM C-fiber (Morganite Modmor Ltd.) [18]	-	84 - 98	1.4 - 3.2
	Phenolic resin / Grafil HT C-fiber (Courtaulds Ltd.) [19]	-	105 - 124	-

\+ impregnated 3 x, recarbonized 3 x
++ impregnated 2 x, recarbonized 2 x
+++ impregnated 4 x, recarbonized 4 x
++++ no detailed information given

impregnation and recarbonization steps are generally necessary, this method consumes much effort and time. However, excellent strength data have been achieved recently in a concurrent study at this Institute [26].

The precipitation of pyrocarbon in thermally decomposed carbon-fiber-reinforced thermosets proved it to be the most successful method at the time this work was begun, according to the literature. The maximum bending strength achieved with such carbon-carbon composites is 124 kp/mm^2 [19].

7.2. Pyrolysis of carbon-fiber-reinforced thermosets /117

7.21. Model studies on shrinkage behavior

As can be seen from the strength and structural studies performed on the carbon-fiber-reinforced thermosets, even the curing shrinkage of the thermosets causes partial damage to the composites. Thus extensive destruction of the composite can be expected from shrinkage of the thermosets during pyrolysis.

In order to obtain information on the mechanism of damage to the composite structure, the shrinkage behavior of carbon-fiber-reinforced thermosets during curing and pyrolysis were studied with model specimens with particularly small fiber contents, by volume, in which an interaction between the individual monofilaments was ruled out. The studies were performed with Phenodur PR 373 phenolic resin and VYB and Thornel 25 carbon fibers, which exhibit very different specific surface areas (see Table 3, Section 3.21).

To prepare the model composites, a 15 mm long fiber bundle containing about 500 individual fibers was first mounted perpendicularly on the base of a glass cylinder and then covered completely with liquid matrix. Repeated spreading of the fiber bundle in the liquid matrix caused the filaments to be completely isolated from one another in the solid matrix. After initial curing of the composite blank at 110°C, a platelet with dimensions of 3 X 3 X 1 mm, as shown schematically in Fig. 27 a, was cut out of it, and its upper and lower surfaces polished. The platelet, serving as a model composite, was then subjected to a thermal treatment to 1000°C. After thermal decomposition, the specimens had different appearances, depending upon the type of fiber embedded, as shown schematically in Fig. 27 b.

Scanning electron microscopy studies of the thermally /118
decomposed model composites permit conclusions to be drawn regarding the processes which take place in the composites during curing and pyrolysis. Due to a poor state of fiber/matrix bonding in the initial curing stage, the phenolic resin matrix can shrink along the fiber in the initial stage of thermal treatment in both types of composite, as a result of which the

ends of the imbedded fibers are exposed. As treatment temperature rises, longitudinal shrinkage of the matrix becomes more and more difficult and finally is completely prevented.

The reason for the premature termination of longitudinal shrinkage can be sought in the shrinkage behavior of the matrix perpendicular to the fiber direction. This is a function of fiber concentration and can be shown using the model tests with a matrix without fiber reinforcement (see Section 4.134). At low fiber concentration, the matrix shrinks toward the fiber, whereas if fiber content is high, it shrinks away from the fiber, at least in the areas between fibers making contact with one another, as shown schematically in Fig. 28.

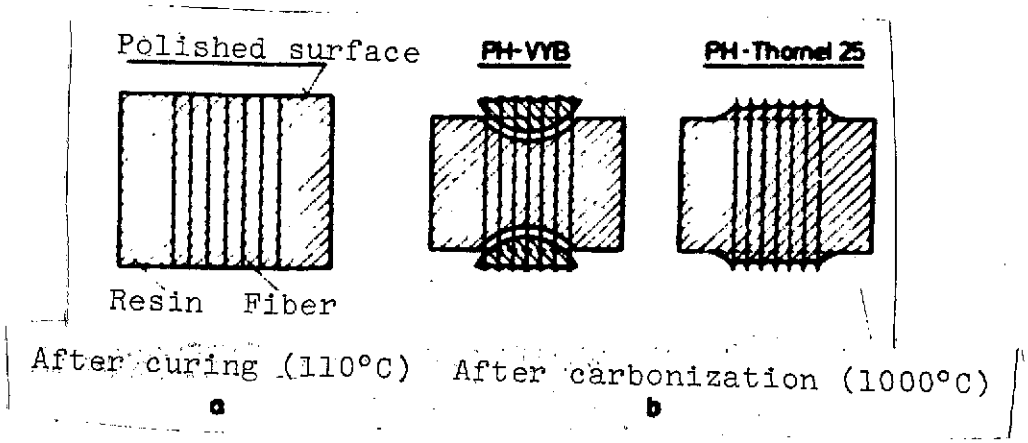

Fig. 27. Model composites (schematic)

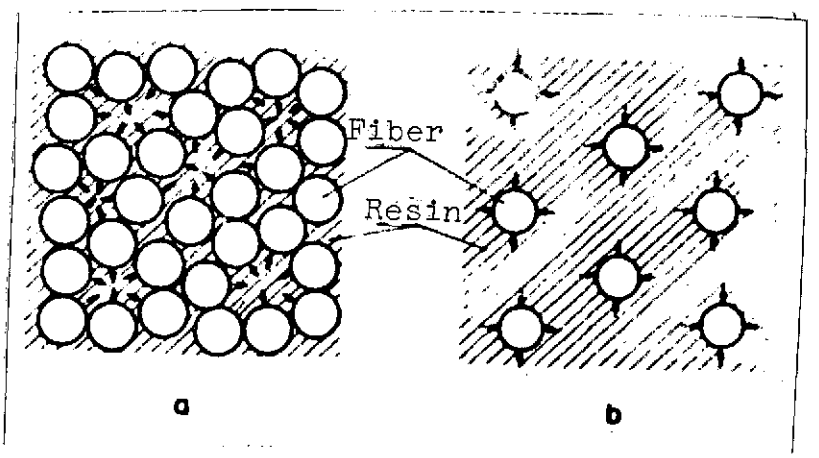

Fig. 28. Shrinkage mechanisms in thermoset matrices perpendicular to fiber direction (schematic); a) high fiber concentration, b) low fiber concentration

The former shrinkage mechanism applies to the model specimens, so the state of bonding between fiber and matrix is increasingly improved during the course of thermal treatment by /119
the process of shrinkage. To the same extent that adhesive forces between the two composite components are increased by the shrink "seat", shrinkage of the matrix along the fiber is hindered more and more and then completely prevented.

A certain delay in the development of a frictional bond which prevents longitudinal shrinkage is due to the initial plasticity of the matrix (see Section 4.135). Due to its plastic deformability, the matrix that has shrunk on the fiber is pushed away in the fiber's longitudinal direction, so the shrinkage stresses already existing are not increased, or only to the extent that the matrix loses plasticity. The extent to which the matrix flows away longitudinally with respect to the fiber can be seen from the folded structures which have formed on the matrix surface of the model specimens (see Fig. 29).

Fig. 29. Scanning electron micrographs of matrix surface topography (Phenodur PR 373 phenolic resin) after thermal decomposition to 1000°C; left, VYB carbon fiber; right: Thornel 25 carbon fiber.

The structural integrity of model composites pyrolyzed to 1000°C is determined primarily by the treatment temperature at which longitudinal shrinkage of the matrix is prevented. In /120
addition to the factors already listed, such as poor fiber/matrix bonding in the initial curing stage and plasticity of the matrix, primarily the surface character of the fiber has a decisive effect on this temperature. In the case of VYB fiber, which exhibits a higher specific surface area than Thornel 25 fiber, longitudinal shrinkage of the matrix is prevented in an earlier stage of thermal treatment. As a result, the model composite is

subject to such high stress during the further course of pyrolysis to 1000°C that it tears open perpendicular to the fiber (see Fig. 30). In the specimen with Thornel 25 fiber, the magnitude of stress is reduced because the matrix can slide along the fiber up to a higher treatment temperature. The shrinkage stresses obviously do not reach the ultimate strength of the matrix, since the composite decomposed thermally to 1000°C exhibits no damage due to crack formation (see Fig. 31).

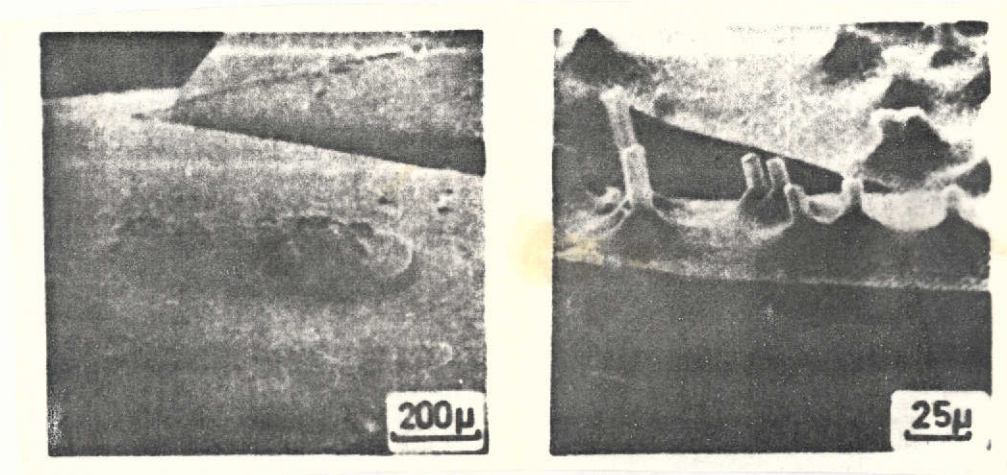

Fig. 30. Scanning electron micrographs of a model composite of Phenodur PR 373 phenolic resin and VYB carbon fiber, treatment temperature 1000°C, longitudinal dimension in the fiber direction: 1 mm.

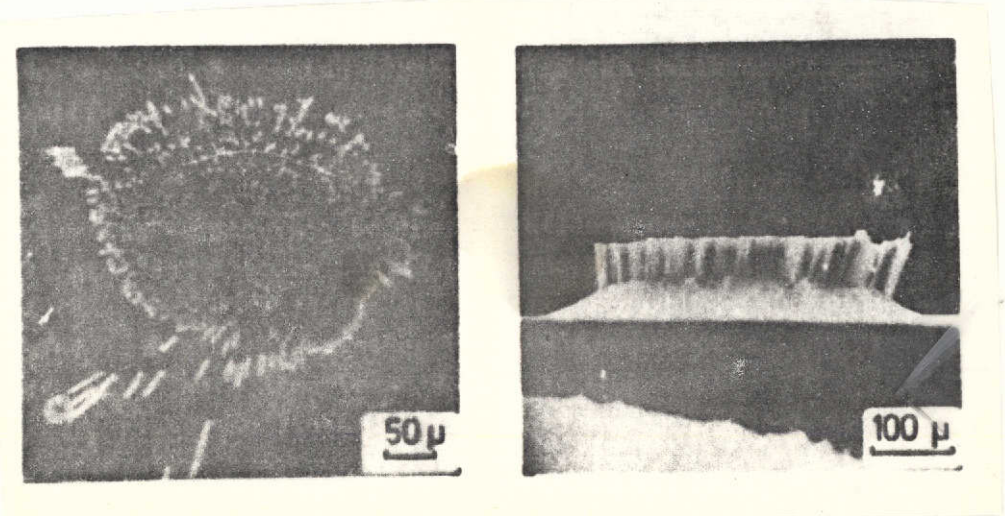

Fig. 31. Scanning electron micrographs of a model composite of Phenodur PR 373 phenolic resin and Thornel 25 carbon fiber, treatment temperature 1000°C, longitudinal dimension in the fiber direction: 1 mm.

But even in the case of Thornel 25 and 50 fiber, cracks occur if a model composite has a relatively large longitudinal dimension relative to the fiber. The coked specimens then have shrinkage cracks through them perpendicular to the fiber at intervals of about 1 mm (see Fig. 32, left). It is also found that the damage to the composites caused by shrinkage stresses is limited not only to the matrix but also includes the fibers (see Fig. 32, right). /122

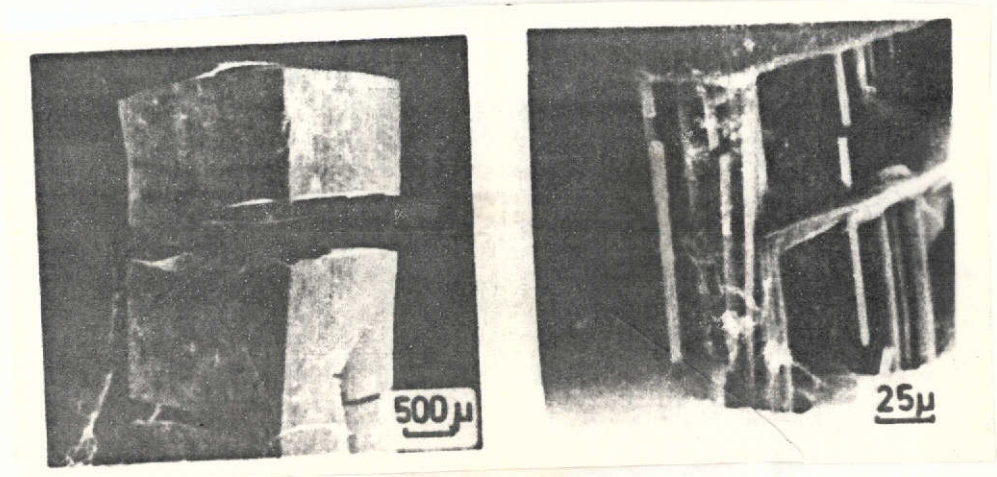

Fig. 32. Scanning electron micrographs of a model composite of Phenodur PR 373 phenolic resin and Thornel 50 carbon fiber, treatment temperature 1120°C, longitudinal dimension in the fiber direction: 5 mm.

7.22. Properties of thermally decomposed composites

It can be seen from the microscopic studies performed on the pyrolyzed model composites that pyrolysis shrinkage of the thermoset matrices causes extensive destruction of the composite structures. Strength studies on partially and fully pyrolyzed composites of specimen types I - IV were therefore aimed at quantitatively determining the damage in various stages of thermal decomposition. These composites were pyrolyzed under the same conditions as the unreinforced matrix materials (see Section 4.132).

The change in mechanical properties of the fully cured composites with increasing pyrolysis temperature to 1200°C can seen from Table 26. The fiber contents by volume determined from expressions (6-1) and (6-2) (see Section 6.22) and the tensile strength and modulus of elasticity values calculated for the four types of composites by alligation are also included. Mechanical properties are plotted in Figs. 33 - 35 as functions of treatment temperature; results for the composites in various stages of curing are included. /124

TABLE 26. MECHANICAL PROPERTIES OF COMPOSITES I - III IN VARIOUS STAGES OF PYROLYSIS (DETERMINED IN FIBER DIRECTION AT ROOM TEMPERATURE)

Type of composite	Pyrolysis temp. [°C]	Fiber content by vol. [%]	Tensile strength [kp/mm²]			Young's modulus [kp/mm²]			Bending strength [kp/mm²]			Interlam. bending shear strength [kp/mm²]
			measured	calculated	achieved [%]	measured	calculated	achieved [%]	measured	calculated	achieved [%]	
I (PH-VYB)	350	49.7	33.1	46	71	1950	2310	84	26.2	46	57	-
	400	50.4	31.2	46	68	1850	2330	79	-	-	-	2.29+
	460	50.9	-	-	-	-	-	-	12.1	46	26	-
	600	51.6	20.3	45	45	1850	2540	73	2.8	45	6	0.44+
	900	51.6	7.1	49	15	2690	3370	79	1.8	49	4	0.67+
	1190	50.7	5.9	49	12	2910	3590	81	≤0.7	49	≤1	0.35+
II (EO-VYB)	400	65.5	35.0	57	62	2140	2880	74	-	-	-	1.74
	500	67.7	28.0	58	48	2180	2940	73	12.6	58	22	1.19
	600	66.7	17.1	57	30	2150	3020	71	-	-	-	-
	700	67.7	11.5	58	20	2370	3260	73	3.4	58	6	0.40
	1190	68.7	5.7	61	9	2990	3880	77	≤1.0	61	≤2	0.18+
III (PH-Thornel 25)	460	46.8	-	-	-	-	-	-	≤1.1	62	≤2	-
	575	46.8	32.2	61	53	5260	8570	61	-	-	-	≤0.01
	700	47.7	31.0	64	49	6310	9070	70	≤1.1	64	≤2	≤0.01
	1120	47.7	28.9	67	44	6940	9950	70	≤1.1	67	≤2	≤0.01
IV (PH-Thornel 50)	460	45.1	54.8	93	59	16240	16050	101	7.5	93	8	0.32+
	690	46.4	48.9	96	51	16410	16900	97	2.9	96	3	0.03+
	1130	46.4	40.5	99	41	14820	17890	83	≤1.8	99	≤2	0.11+

* Specimens did not delaminate

7.221. Tensile strength and modulus of elasticity

The tensile strength of composites fully cured to 300°C and already structurally damaged continually decreases further with increasing treatment temperature, as Fig. 33 shows. In addition to the initial drop in the strength of fully cured thermoset matrices due to thermal decomposition to about 550°C (see Section 4.133), further damage to the composite structure due to pyrolysis shrinkage of the matrix materials (see Section 7.23) is the primary cause of the drop in composite strength. The greatest strength loss is found between 300 and 800°C. This exactly corresponds to the temperature range in which the thermoset matrices experience the greatest pyrolysis shrinkage (see Section 4.133).

Hardening of the matrices above 550 - 600°C is not reflected in the strength behavior of the composites. In the case of composites I and II, with nongraphitized VYB carbon fiber, the strength of the composite material instead drops below that of the unreinforced thermally decomposed thermosets after heat treatment above 850°C. In the case of composites III and IV, with stretch-graphitized Thornel 25 and 50 fibers, on the other hand, room temperature tensile strength fluctuates about a final value of about 30 kp/mm^2 (type III) and 40 kp/mm^2 (type IV) up to the termination of coking in the 1100 - 1200°C range. Thus strengthening by a factor of about 2.5 and 3.5 is obtained relative to unreinforced carbon matrix from thermally decomposed phenolic resin. /126

The composite strength values calculated by alligation (Eq. (2-3); see Section 2.2) increase with increasing pyrolysis temperature, since composite volume decreases because of matrix shrinkage, and the fiber content by volume consequently increases. As thermal decomposition progresses, the discrepancy between calculated and measured strength data likewise increases. After complete pyrolysis at 1100 - 1200°C, the actual tensile strength of composites reinforced with Thornel fibers is 40% of the calculated value. Only 10% of the calculated composite tensile strength is achieved with VYB fiber as the reinforcing component.

The extremely poor utilization of strength in the thermally decomposed composites with VYB fiber can only be explained if this type of fiber is damaged much more severely during the course of pyrolysis than the Thornel fibers. Since the VYB fibers are a pyrolyzed rather than graphitized carbon fiber with a carbon content of only 90 wt.%, this suggests, first of all, thermally induced fiber damage as the result of recoking of the fiber in the composite. In order to check this, VYB fibers were heated to 1000°C at 12°C/h in an inert gas atmosphere. Recoking caused a weight loss of 17.6% and fiber shrinkage of 0.6%. No effect on tensile strength and modulus of elasticity could be detected, however.

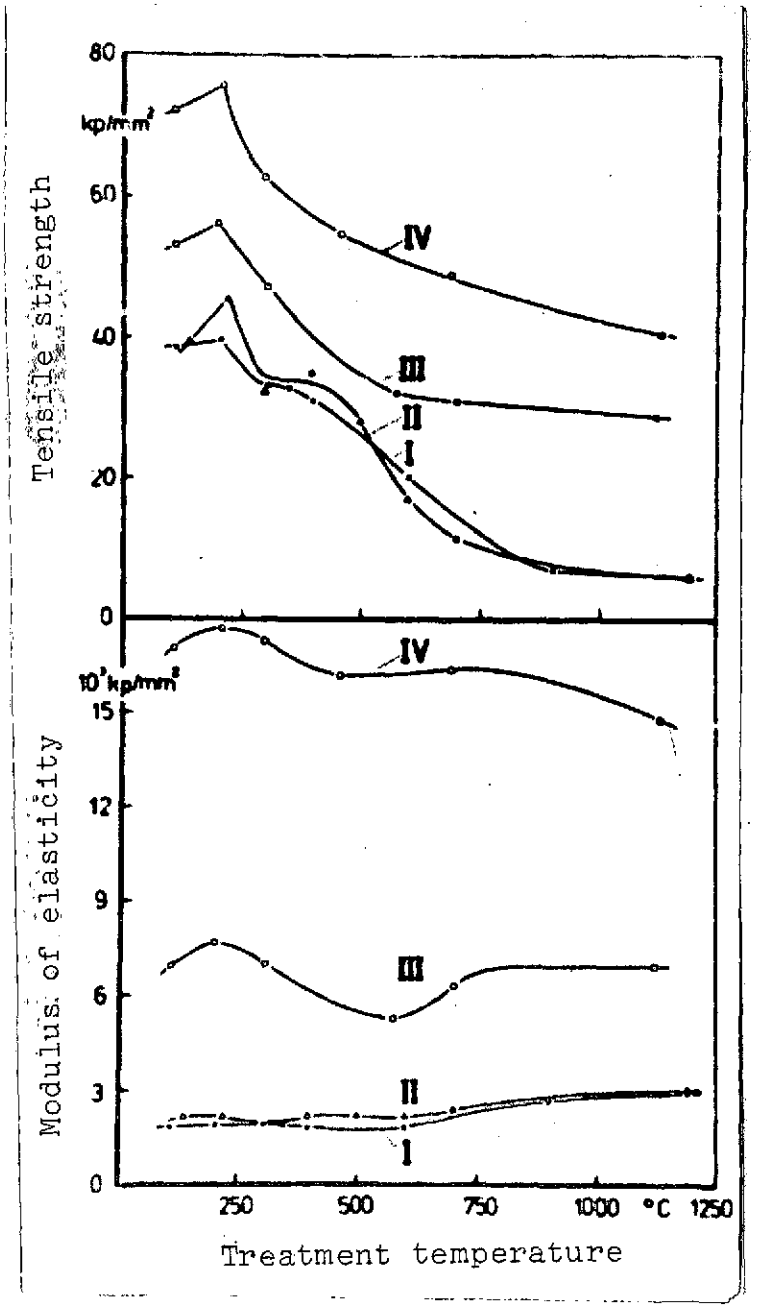

Fig. 33. Tensile strength and moduli of elasticity of composites I - IV as functions of treatment temperature (determined in fiber direction at room temperature)

Recrystallization of the fiber in the pyrolyzing resin matrix because of phosphorous-bearing additives in fiber production, as is postulated by MacKay [15], would be a conceivable cause of damage. Radiographic studies performed on powder samples of VYB fibers, on the one hand, and a

completely pyrolyzed composite material based on phenolic resins / VYB fiber (composite I, 1190°C), on the other hand, gave no indication of recrystallization, however, although the VYB fibers used in this work contained about 4 wt.% sodium polyphosphate [95]. /127

The severe damage to VYB fiber is therefore attributed to the high internal mechanical stress which accompanies the high degree of matrix/VYB fiber bonding and matrix shrinkage.

Strength studies performed on cured and pyrolyzed composites of Phenodur PR 373 phenolic resin reinforced with thermally aftertreated VYB fiber (see Section 7.254) have confirmed this assumption.

In contrast to tensile strength, the modulus of elasticity of the cured composites does not change significantly with progressive thermal decomposition. It experiences certain fluctuations in the temperature range between 300 and 1200°C. The rise in the modulus of elasticity of the matrix component during coking and the increase in fiber content by volume resulting from pyrolysis shrinkage of the matrix are counteracted by damage symptoms in the composite. After thermal decomposition to 1200°C, the measured composite modulus of elasticity data are 70 to 80% of the calculated values.

7.222. Bending strength

As Fig. 34 shows, the room temperature bending strength of composites fully cured to 300°C, determined in the fiber direction, decreases to a greater extent with progressive coking than does tensile strength (see Section 7.221). The greatest drop in strength occurs in the temperature range between 300 and 650°C. After partial pyrolysis to 650°C, the cohesiveness of the composite is so highly attenuated by shrinkage cracks and the separation of matrix from fiber (see Section 7.23) that bending strength is less than 5 kp/mm^2. Upon the completion of coking in the 1200°C range, the bending strength values are below 2 kp/mm^2, corresponding to less than 2% utilization of the strength of the fiber employed. /128

The higher tensile strength of the Thornel types of fiber does not contribute to any improvement in the composite bending strength values throughout the pyrolysis range. On the contrary, the weaker VYB fiber is superior to the Thornel fibers up to a treatment temperature of about 600°C, due to better adhesion of the matrix to the fiber.

7.223. Interlaminar bending shear strength /129

As Fig. 35 shows, curves similar to those for bending strength are obtained for the composite's interlaminar bending

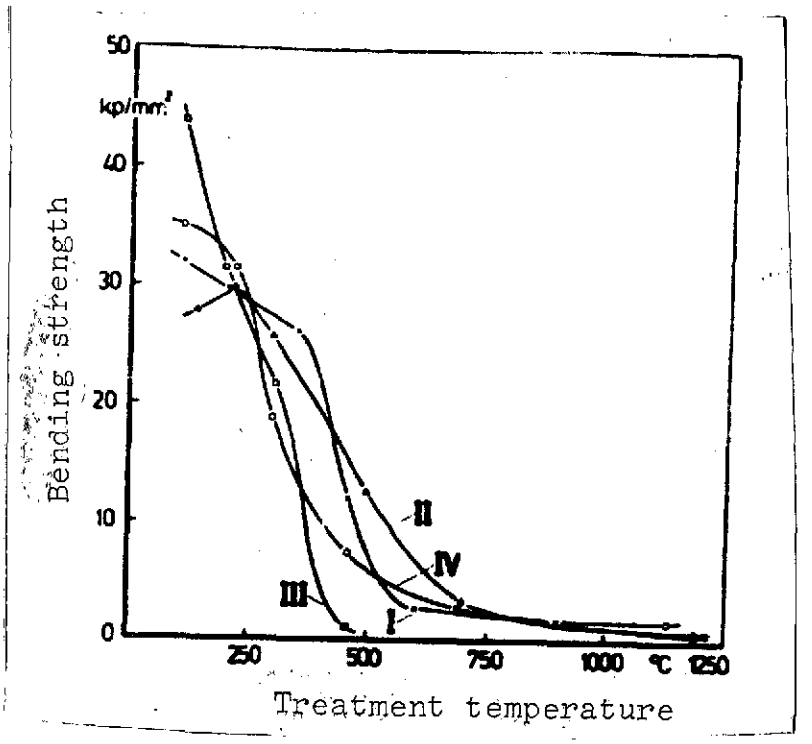

Fig. 34. Bending strength of composites I - IV as a function of treatment temperature (determined in fiber direction at room temperature)

shear strength. The greatest drop in strength occurs here in the temperature range between 300 and 650°C. Shear strength drops to values below 0.6 kp/mm^2, due to severe damage to the composite structure (see Section 7.23). After pyrolysis at 1100 - 1200°C, the values are below 0.4 kp/mm^2. Higher composite shear strengths are obtained with VYB fiber than with the Thornel types in all stages of decomposition. This fact agrees completely with the predictions derived from the large specific surface area of VYB fiber and a resultant good adhesion of the matrix to this fiber.

In spite of the severe damage to their structure, the composites frequently did not delaminate. While composite II failed to delaminate only in the highly decomposed state, this occurred to composites I and IV throughout the pyrolysis range, /130

7.224. Weight loss and shrinkage

In addition to the mechanical properties of the composites, their weight loss and longitudinal contraction in the fiber direction were also determined. The change in these properties,

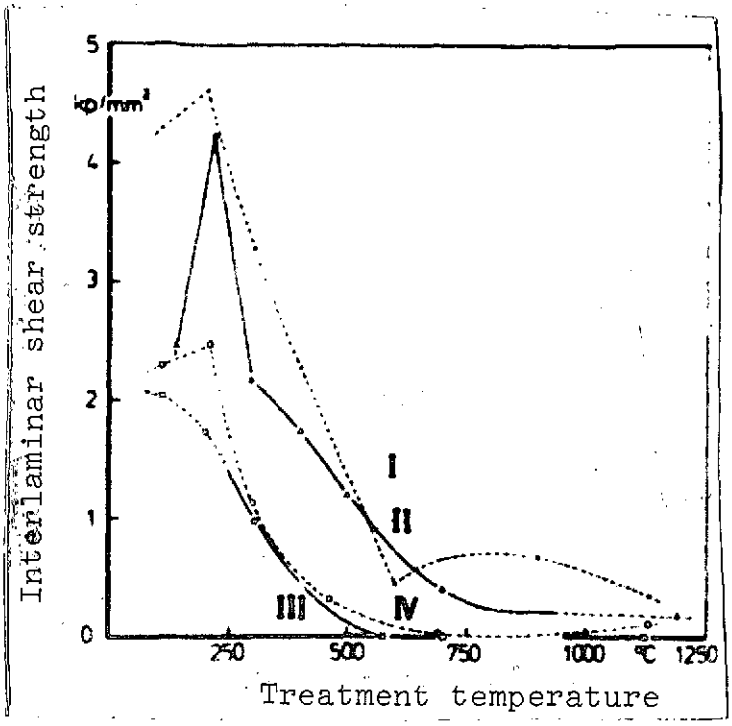

Fig. 35. Interlaminar shear strength of composites I - IV as a function of treatment temperature (determined in fiber direction at room temperature). ——— Delamination; ---------- No delamination.

referred to the fully cured state, can be seen from Table 27. The results are plotted as a function of treatment temperature in Fig. 36. In contrast to Table 27, these data refer to the initially cured state.

As can be seen from the measured data, the composites continually lose weight as thermal decomposition progresses. The sharp rise in the weight loss curves between 300 and 550°C coincides exactly with the high weight loss of the unreinforced matrices in this temperature range (see Section 4.133). During the further course of pyrolysis to 1200°C, the behavior of the pure matrix is reflected only in the weight loss curves of composites with the Thornel fibers. The composites reinforced with VYB fiber experience an increased weight loss which, as calculations show, can be caused only by recoking of the fiber in the composite. This conclusion is also supported by the finding, described in Section 7.221, that VYB fiber not imbedded in a matrix loses 17.6% of its weight during thermal treatment to 1000°C.

A consideration of the total weight lost by composites with Thornel fibers pyrolyzed to 1200°C shows that the measurements yield 4.5% lower values than calculated. Thus the imbedded carbon fibers contribute to an increase in the carbon yield of the thermoset matrix. /133

In contrast to the unreinforced thermoset matrices (see Section 4.133), the fully cured composites experience only minimal linear shrinkage in the fiber direction during thermal decomposition, due to the low compressibility of the carbon fibers. The greatest longitudinal contraction is to be observed in composites with VYB fiber. Yet it is less than 0.25% throughout the pyrolysis range. If we include curing shrinkage,

TABLE 27. WEIGHT LOSS AND LONGITUDINAL CONTRACTION IN THE FIBER DIRECTION OF FULLY CURED COMPOSITES I - IV DURING PYROLYSIS TO 1200°C (DETERMINED AT ROOM TEMPERATURE)

Type of composite	Treatment temperature [°C]	Weight loss [%]		Longitudinal contraction in fiber direction [%]
		measured	calculated	
I (PH-VYB)	305	0	0	0
	350	1.4	2.4	- 0.03
	400	3.1	3.9	0.11
	600	13.9	12.3	0.21
	900	15.6	13.5	0.21
	1190	19.9	15.2	- 0.38
II (EO-VYB)	300	0	0	0
	400	0.9	1.2	- 0.01
	500	11.3	4.0	0.15
	600	12.7	6.3	0.22
	700	-	7.3	0.22
	1190	15.8	7.9	0.11
III (PH-Thornel 25)	305	0	0	0
	575	14.2	13.8	0
	700	14.9	15.1	0.04
	1120	16.3	15.7	0.02
IV (PH-Thornel 50)	300	0	0	0
	460	8.1	5.6	0.02
	690	15.8	13.9	- 0.01
	1130	15.1	14.7	0

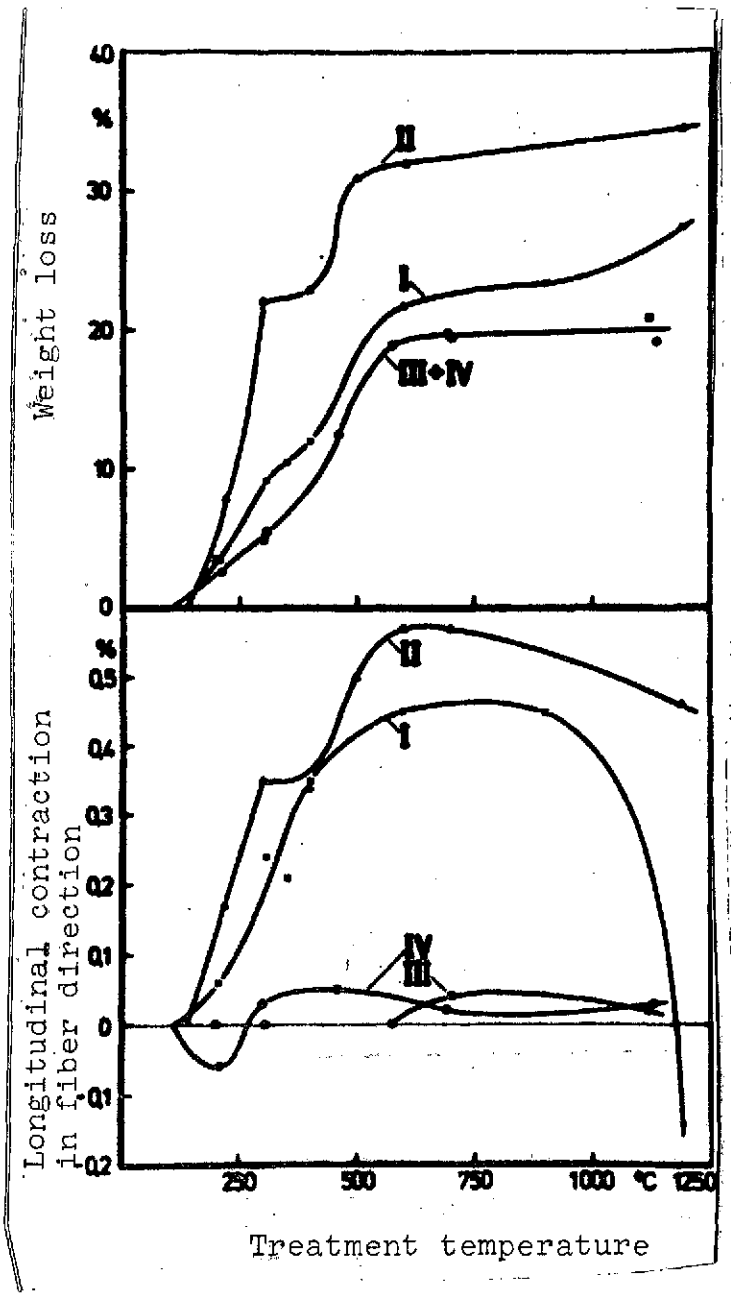

Fig. 36. Weight loss and longitudinal contraction in fiber direction of composites I - IV as functions of treatment temperature (determined at room temperature)

we obtain values of less than 0.6%. The obstructed shrinkage is compensated for, and even overcompensated for, by the development of cracks perpendicular to the fiber (see Section 7.23), as the composites with VYB fiber clearly show above 700°C.

7.23. Structure of the pyrolyzed composites

As can already be observed quantitatively from the strength behavior of thermally decomposed composites (see Section 7.22), pyrolysis shrinkage of the matrix causes extensive destruction of the composite structure, already damaged by curing shrinkage. Light and scanning electron microscopy studies performed on pyrolysis residues provide information regarding the overall extent of shrinkage damage.

Figs. 37 to 39 show photomicrographs of sections of composites I, II and IV after coking to temperatures of 1100 - 1200°C; composites reinforced with Thornel 25 and 50 fibers (types I and IV) are similar in appearance. The shrinkage behavior of the matrix and the surface character of the fiber largely determine the structure of the thermally decomposed composites.

Transverse microsections of /134
composites I and II (see Figs. 37 and 38, top) indicate that the epoxy resin matrix, in particular, is capable of forming a coherent composite structure. The reasons for this behavior are that epoxy resin experiences 6% less linear /135
shrinkage than phenolic resin in the unreinforced state and that the volume shrinkage prevented in the composite can in part be

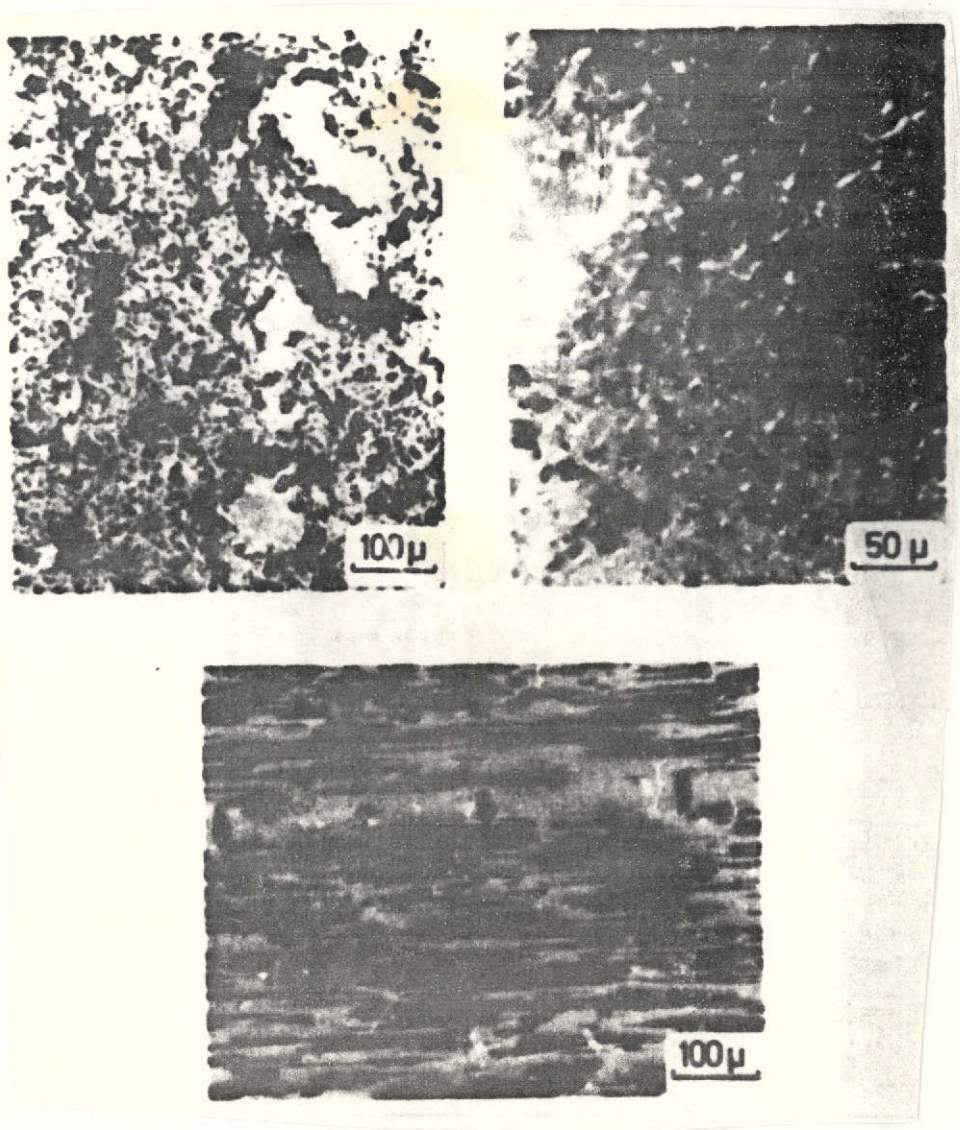

Fig. 37. Photomicrographs of a carbon-carbon composite of type I (PH -VYB), treatment temperature 1190°C; top: cross section; bottom: longitudinal section.

compensated for by spherical pores (see Sections 6.24). A comparison of composites I and IV (see Figs. 37 and 39, top) shows the effect of fiber surface area on the composite /136
structure. While the large specific surface area of VYB fiber ensures that the monofilaments are linked together by the thermally decomposed phenolic resin matrix, in the case of Thornel fiber there is no firm bonding among the filaments by the carbon matrix, due to their small specific surface area.

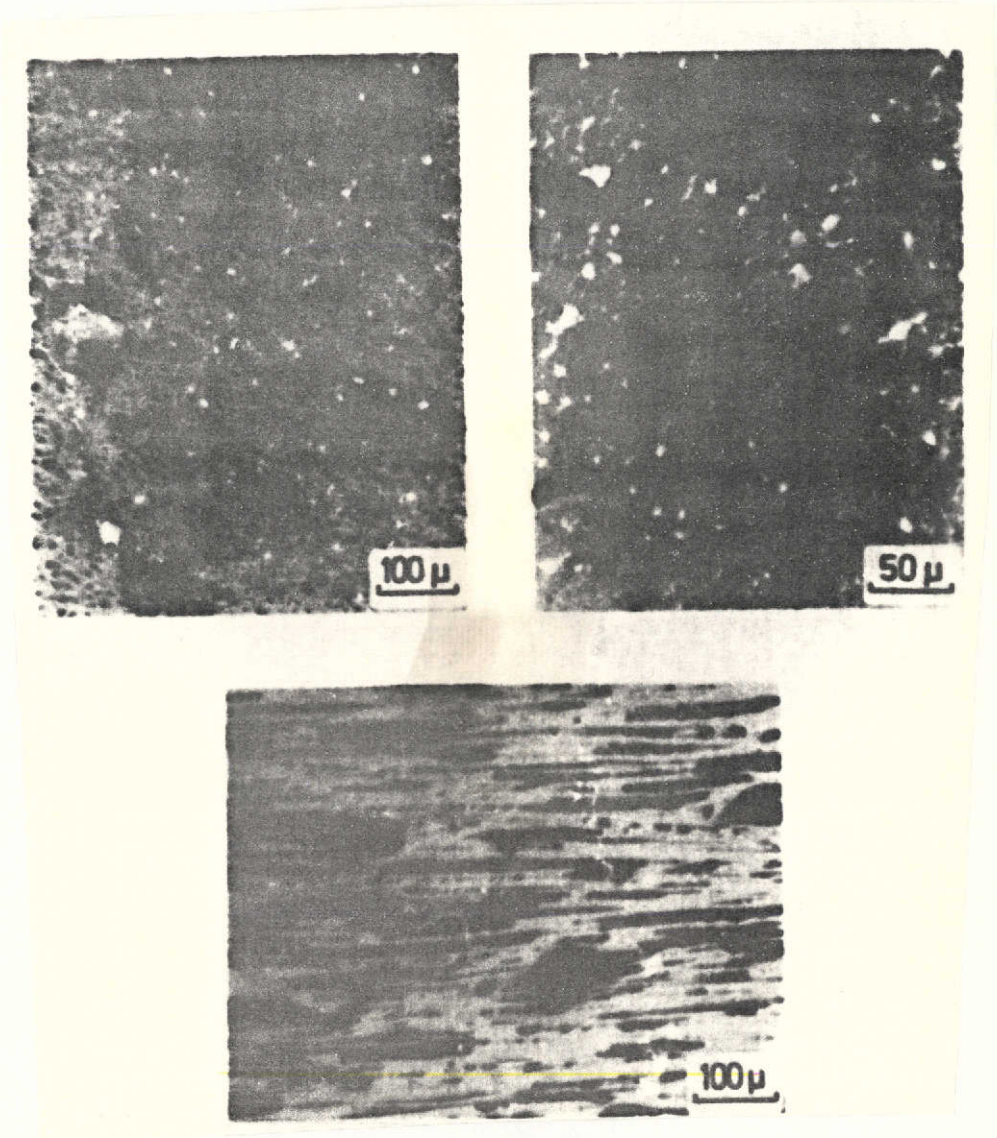

Fig. 38. Photomicrographs of a carbon-carbon composite of type II (EO-VYB), treatment temperature 1190°C; top: cross section; bottom: longitudinal section.

Longitudinal microsections of pyrolysis residues from composites I through IV, and even the unprepared surface of the composites, show damage to the composite structure by the cracks perpendicular to the reinforcing component. The transverse cracks are found primarily in the fiber-free areas of matrix bordering on the fiber bundles and exhibit a lenticular configuration (see Figs. 37 and 39, bottom). Crack formation commences even in the early stage of pyrolysis, at temperatures of 350 to 400°C, and begins in the marginal /137

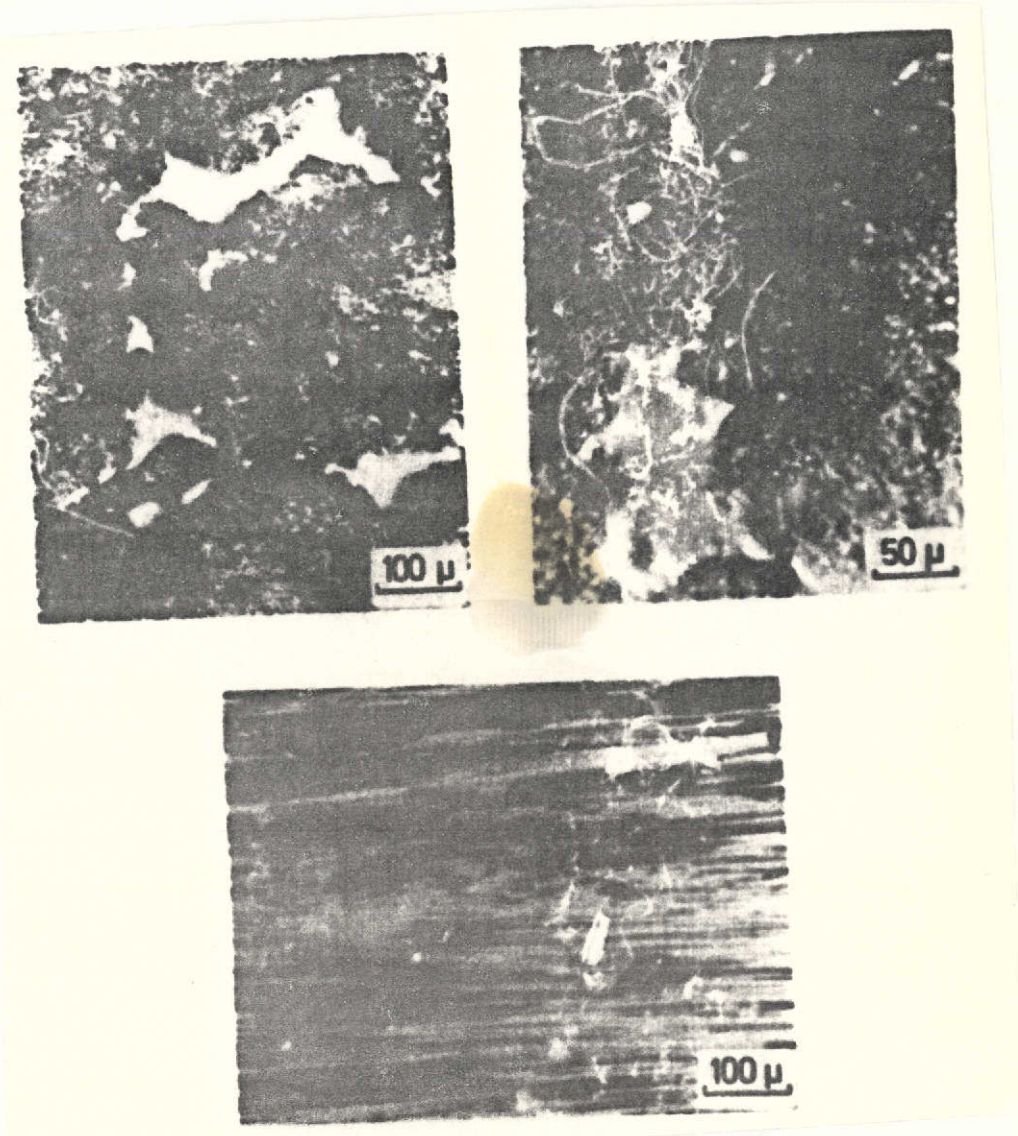

Fig. 39. Photomicrographs of a carbon-carbon composite of type IV (PH-Thornel 50), treatment temperature 1130°C; top: cross section; bottom: longitudinal section.

zones of the fiber bundles, since maximum shrinking stress in the fiber direction occurs here because of complete wetting of the fibers by the liquid resin matrix. Damage to the carbon fibers by shrinking stresses can be observed only in composite I, based on phenolic resin and VYB fiber. In the other carbon-carbon composites, particularly in composite II, of epoxy resin and VYB fiber, the conclusion arrived at on the basis of tensile testing (see Section 7.221) is not supported by the optical findings.

A scanning electron microscope study of the pyrolysis residues does not show the total extent of structural damage, but does represent a supplement to the light microscope studies. Fig. 40 gives an impression of the surface character of the carbon-carbon composites, with type I serving as an example. /138 The surfaces of the composites exhibit numerous shrinkage cracks transverse and longitudinal with respect to fiber orientation which, in conjunction with shrinkage damage within the composites, determine the poor strength characteristics of these materials.

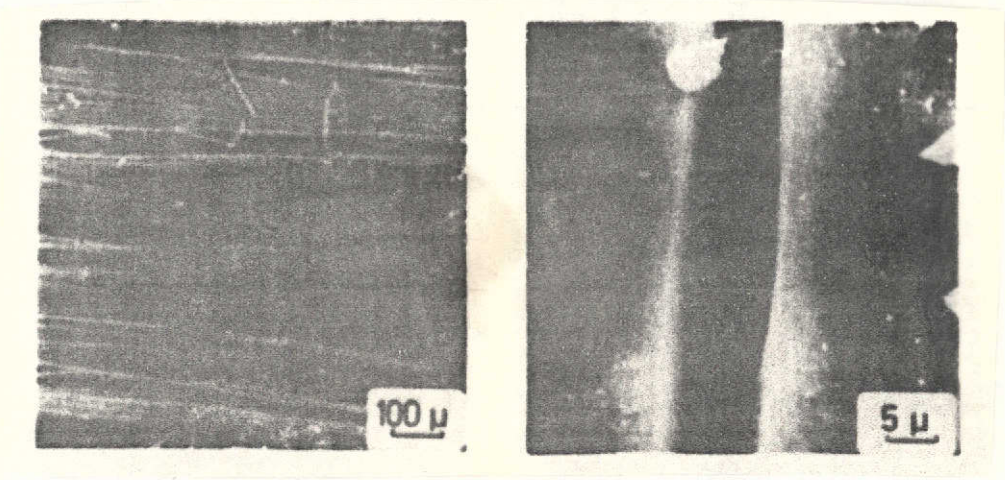

Fig. 40. Scanning electron micrographs of the surface of a carbon-carbon composite, type I (PH-VYB), treatment temperature 1190°C.

Figs. 41 and 42 show fracture surfaces, from tensile testing, of composites I and II pyrolyzed to 1190°C. The fracture behavior of such composites is quite brittle. Only a small number of VYB fibers project from the cracked and porous carbon matrix, based on phenolic resin or epoxy resin, respectively; this indicates the monofilaments to be held together strongly by the matrix. Brush-like tips are obtained from composites III and IV, reinforced with Thornel fiber, since adequate bonding does not exist between fiber and matrix. Scanning electronmicrographs of such fracture surfaces could not be prepared, for reasons involving preparation techniques.

7.24. Reimpregnation of thermally decomposed carbon-fiber-reinforced thermosets /140

The effect on the strength behavior of thermally decomposed carbon-fiber-reinforced thermosets caused by impregnation with new polymer matrix followed by coking was studied using the example of carbon-carbon composites based on Phenodur PR 373

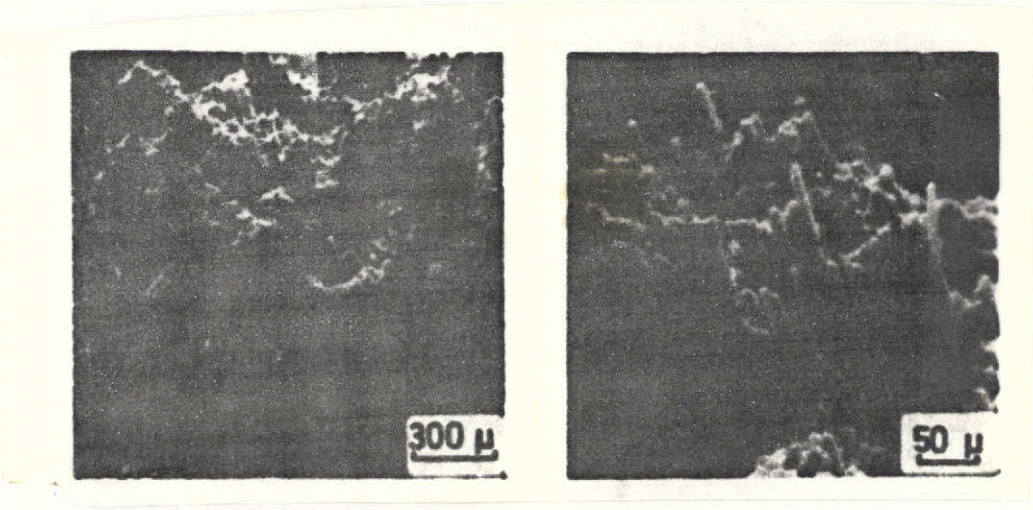

Fig. 41. Scanning electron micrographs of fracture surfaces of composite I (PH-VYB) from tensile test, treatment temperature 1190°C.

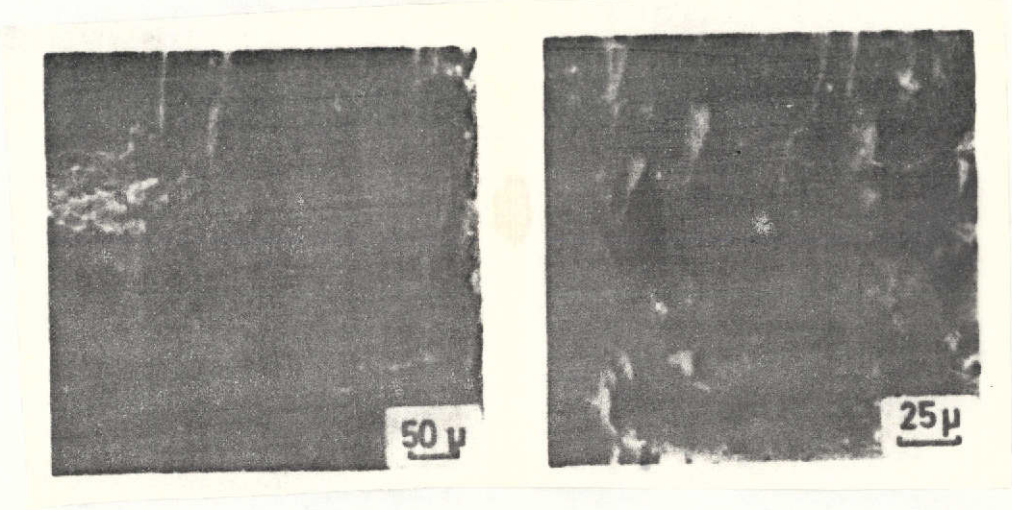

Fig. 42. Scanning electron micrographs of fracture surfaces of composite II (EO-VYB) from tensile test, treatment temperature 1190°C.

phenolic resin and Thornel fiber (composites III and IV; see Sections 7.22 and 7.23). Composites I and II, with VYB fiber, were not included in the studies, since the VYB fiber imbedded in the matrix is damaged too severely by the first coking treatment, as can be seen from the tensile strength data on the pyrolysis residues (see Section 7.221).

The carbon-carbon composites were impregnated with a 20 wt.% phenolic resin solution in methanol under a water-aspirator vacuum. Four impregnations of 10 min. each have proven usable. After each impregnation step, the specimens were heat treated for half an hour in the drybox at 90°C in order to evaporate the solvent and initially cure the resin. After the fourth impregnation step, the composites were cured at 110°C for 6 h and then heated to 1130°C in an ultrapure nitrogen atmosphere at a heating rate of 12°C/h. The impregnation and carbonization process was repeated several times to achieve high composite densities.

The weight change in composites III and IV can be seen from Table 28 and Fig. 43 as a function of the number of impregnations and carbonizations. It is found that the porous and cracked structure of the composites is almost completely sealed at the surface after four impregnation steps. New routes of access to the interior are created only by carbonization, making repeated impregnation possible. The specimens are already sealed to such an extent after three or four impregnation and recarbonization processes that an additional treatment cycle no longer yields an appreciable gain in weight. /141

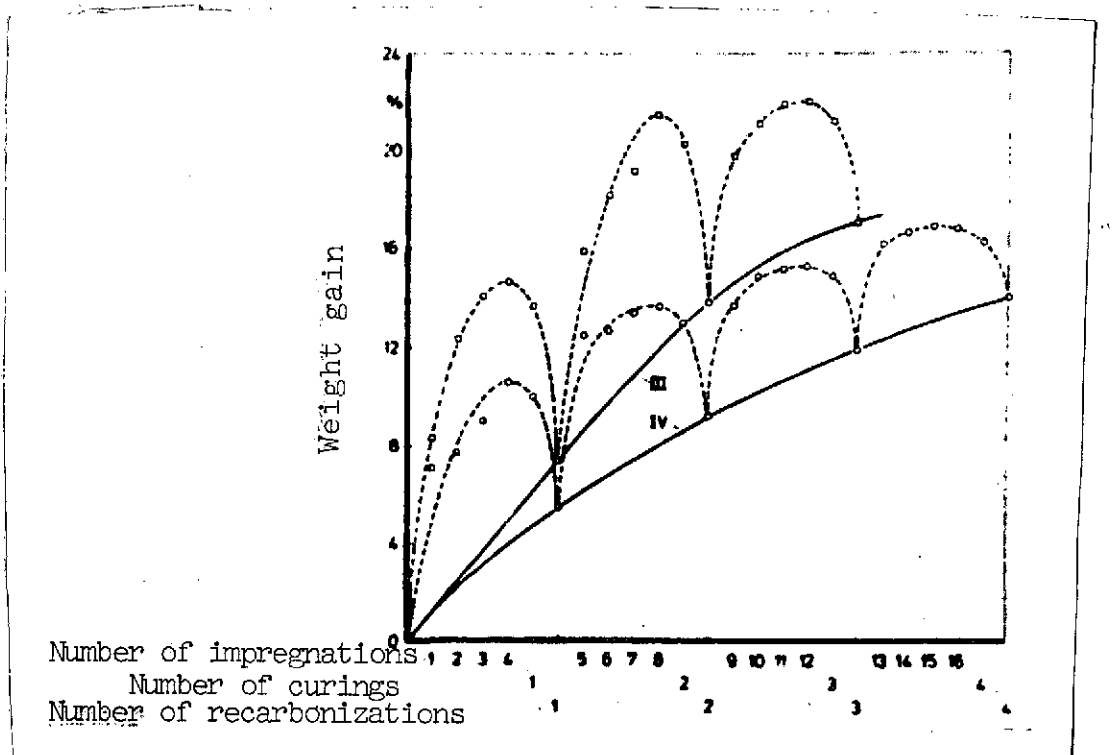

Fig. 43. Weight change in resin-impregnated and recarbonized carbon-carbon composites, type III (PH-Thornel 25) and IV (PH-Thornel 50) (determined at room temperature), recarbonization temperature 1130°C.

TABLE 28. WEIGHT GAINS BY IMPREGNATED AND RECARBONIZED COMPOSITES III AND IV RELATIVE TO THE UNIMPREGNATED STATE (DETERMINED AT ROOM TEMPERATURE)

Number of impregnations	Number of curings	Number of recarbonizations	Weight gain [%]	
			Composite III (PH-Thornel 25	Composite IV (PH-Thornel 50)
0			0	0
1			8.3	7.1
2			12.3	7.7
3			14.1	9.0
4			14.7	10.6
	1		13.7	10.0
		1	7.4	5.5
5			15.9	12.5
6			18.2	12.7
7			19.2	13.4
8			21.5	13.7
	2		20.3	13.0
		2	13.8	9.2
9			19.8	13.7
10			21.1	14.9
11			21.9	15.2
12			22.0	15.3
	3		21.2	14.9
		3	17.1	11.9
13			-	16.2
14			-	16.7
15			-	16.9
16			-	16.8
	4		-	16.3
		4	-	14.0

The mechanical properties of recarbonized resin-impregnated carbon-carbon composites are shown in Table 29 and Fig. 44. The composites' tensile strength and moduli of elasticity are improved relatively little by their repeated impregnation and carbonization. On the other hand, bending strength and interlaminar bending shear strength, which respond largely to the state of fiber/matrix bonding, increase considerably. /142

Fig. 45 shows scanning electron micrographs of the fracture surface of a resin-impregnated carbon-carbon composite (type III) from tensile testing after the third recarbonization.

TABLE 29. MECHANICAL PROPERTIES OF RESIN-IMPREGNATED COMPOSITES III AND IV AFTER RECARBONIZATION (DETERMINED IN FIBER DIRECTION AT ROOM TEMPERATURE)

Material	Number of impregnations and recarbonizations	Tensile strength [kp/mm²]			Young's modulus [kp/mm²]			Bending strength [kp/mm²]			Interlaminar bending strength [kp/mm²]
		measured	calculated	achieved [%]	measured	calculated	achieved [%]	measured	calculated	achieved [%]	
Composite III (PH-Thornel 25)	0 Impreg. 1 Recarbon.	28.9	67	44	6940	9950	70	≤1.1	67	≤2	<0.01
	4 Impreg. 1 Recarbon.	29.2	67	44	7020	9950	71	-	-	-	0.20
	8 Impreg. 2 Recarbon.	32.5	67	49	7710	9950	78	-	-	-	0.46+
	12 Impreg. 3 Recarbon.	35.7	67	54	8090	9950	82	26.7	67	43	0.83+
Composite IV (PH-Thornel 50)	0 Impreg. 1 Recarbon.	40.5	99	41	14800	17890	83	≤1.8	99	≤2	0.11+
	4 Impreg. 1 Recarbon.	40.4	99	41	18500	17890	104	4.9	99	5	0.39+
	8 Impreg. 2 Recarbon.	-	-	-	-	-	-	12.8	99	13	0.65+
	12 Impreg. 3 Recarbon.	-	-	-	-	-	-	32.1	99	33	0.87+
	16 Impreg. 4 Recarbon.	50.2	99	51	18400	17890	103	34.4	99	35	0.83+

+ Specimens did not delaminate

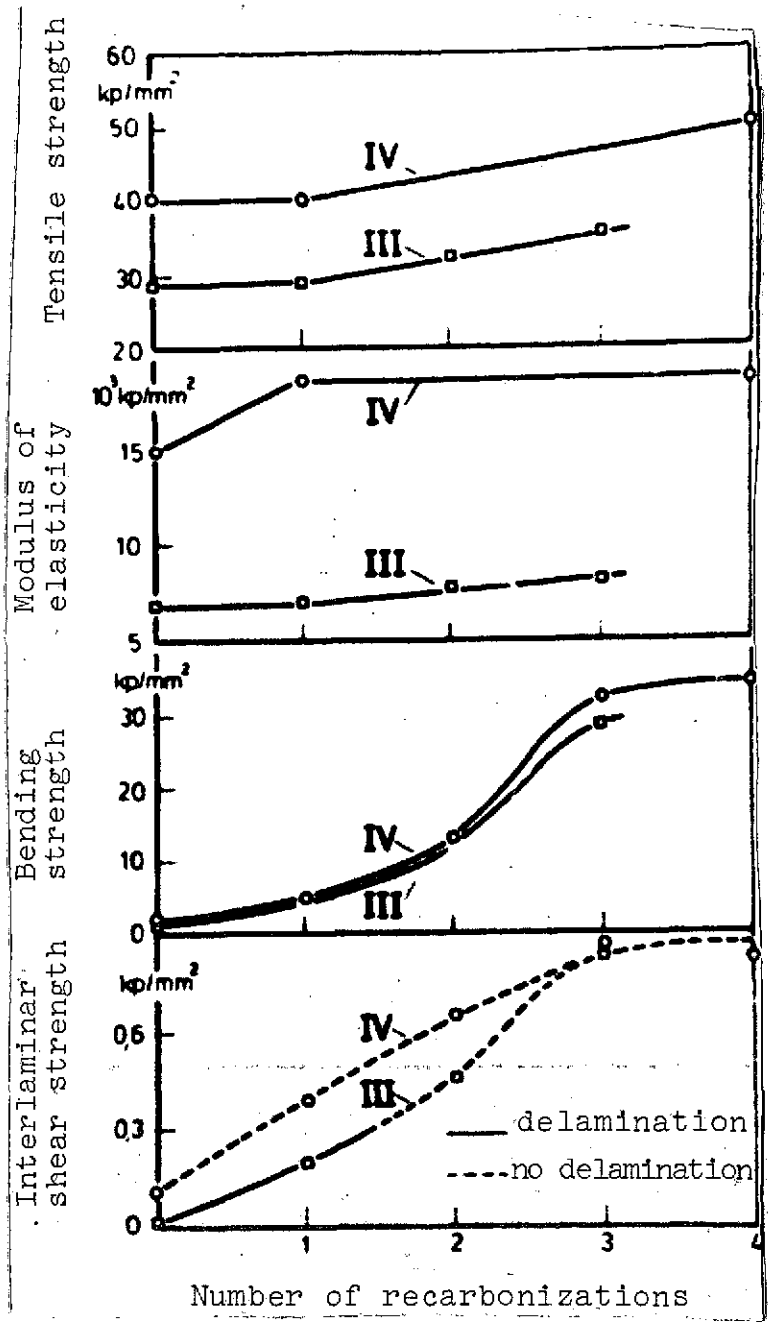

Fig. 44. Mechanical properties of recarbonized resin-impregnated carbon-carbon composites, type III (PH-Thornel 25) and IV (PH-Thornel 50) (determined in fiber direction at room temperature, recarbonization temperature 1130°C.

Imbedding of the Thornel 25 fiber in the carbon matrix is excellent. Adhesion between fiber and matrix can also be considered good, as indicated by the small number of fiber tips projecting from the matrix surface. Micrographs of the ground surface of composite IV after the fourth recarbonization (see Fig. 46) show that the composite structure is still relatively porous in the interior. This condition can be attributed to the fact that the marginal zones are already sealed before the cavities within can be completely filled. /145

7.25. Attempts /146 to produce crack-free carbon-carbon composites based on thermosets

7.251. Thermal decomposition of polyacrylonitrile fiber reinforced thermosets.

If we consider that carbon fibers are produced by the thermal decomposition of synthetic organic fibers, it appears feasible to use polymer-fiber-reinforced thermosets as starting material for carbon-carbon composites. Since polymer fibers are likewise subject to shrinkage during carbonization,

Fig. 45. Scanning electron micrographs of fracture surfaces of composite III (PH-Thornel 25) from tensile test after three impregnations and recarbonizations, recarbonization temperature 1130°C.

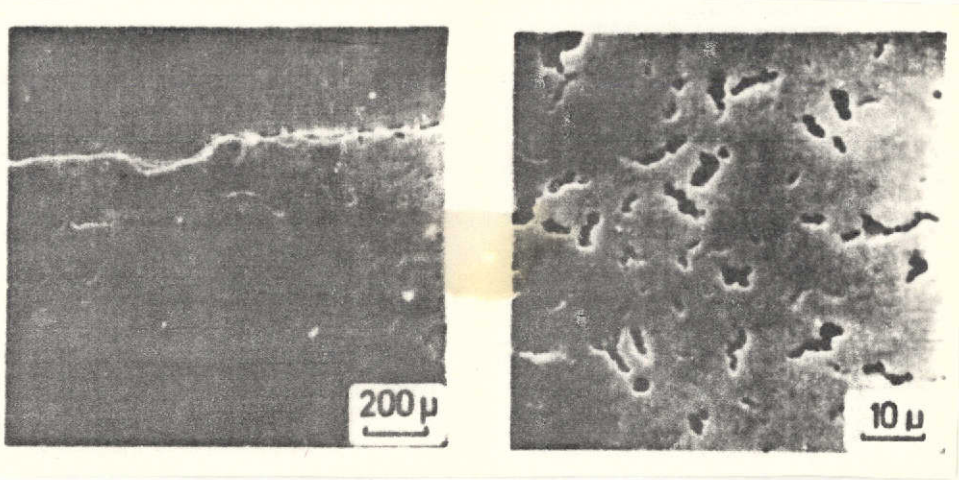

Fig. 46. Scanning electron micrographs of composite IV (PH-Thornel 50) after four impregnations and recarbonizations, recarbonization temperature 1130°C; cross section.

it appears feasible to coke polymeric composites without cracking. Cocoking of the reinforcing material is only usable, however, if its fiber character is not impaired and the decomposed fiber still possesses sufficiently high strength.

Highly stretched polyacrylonitrile (PAN) fibers, trademarked Dralon T, produced by Bayer, Dormagen, which are also employed as starting material for the production of carbon fibers [96], were used for the cocoking experiments. The PAN fibers (see Table 30) were supplied in the form of endless yarn consisting of 384 individual fibers.

TABLE 30. PROPERTIES OF PAN FIBER (Dralon T)

Tensile strength	[kp/mm^2]	45
Modulus of elasticity	[kp/mm^2]	800
Diameter	[μ]	16.5
Density	[g/cm^3]	1.17
Melting point	[°C]	320 ± 5 (97)

Preliminary experiments indicated that the fiber structure of the uncrosslinked PAN fibers is lost to a large extent during thermal decomposition in a matrix of furfuryl alcohol / formaldehyde resin (see Fig. 47). The volatile dissociation products /147 of the resin matrix do not make complete crosslinking of the fibers possible. The uncrosslinked fiber areas fuse and are subject to liquid-phase pyrolysis, leaving cavities behind. PAN fibers which have previously been crosslinked in air for long periods (15 days) at 200°C retain their fiber character during cocoking, however (see Fig. 48). The crosslinked fibers no longer possess appreciable strength, however, as qualitative studies made evident. Parallel experiments with Phenodur PR 373 phenolic resin indicated that the PAN fibers do not have to be previously crosslinked in this case. The dissociation products from the phenolic resin matrix ensure adequate crosslinking of the fibers, so fiber structure is not impaired by thermal decomposition.

Once the conditions under which the fiber character of the PAN fibers is retained could be determined in preliminary experiments, a quantitative study was made as to how cocoking of /148

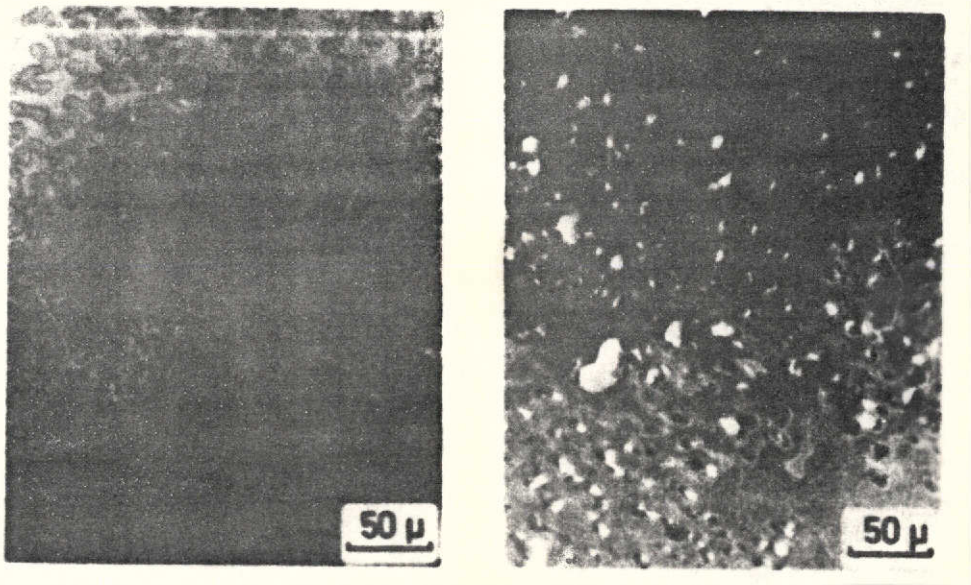

Fig. 47. Photomicrographs of a composite of furfuryl alcohol / formaldehyde resin and uncrosslinked PAN fiber; left: after curing at 120°C; right: after carbonization to 1000°C.

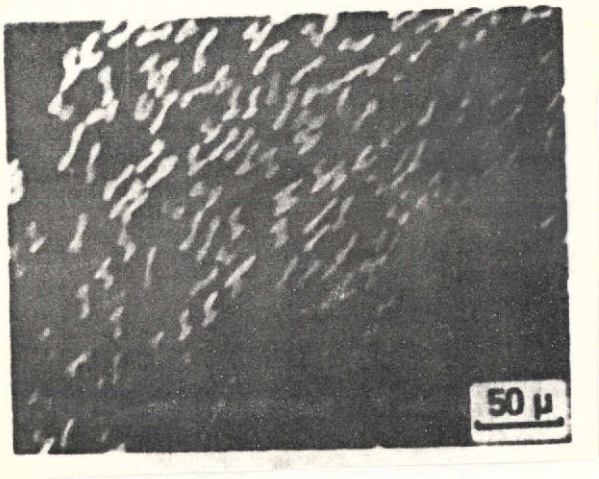

Fig. 48. Photomicrograph of a carbon-carbon composite of furfuryl alcohol / formaldehyde resin and crosslinked PAN fiber, treatment temperature 1200°C.

the reinforcing material affects the composite. Unidirectionally reinforced composites based on Phenodur PR 373 phenolic resin and uncrosslinked PAN fiber were prepared for this purpose by the wet winding method (see Table 31), and their properties in various stages of curing and pyrolysis were studied. The measured data are summarized in Table 32 and plotted in Figs. 49 and 50 as functions of treatment temperature.

It can be seen from the mechanical properties of the cured and pyrolyzed composites that the uncrosslinked PAN fiber contributes to a reinforcement and stiffening of the phenolic resin matrix only up to a treatment temperature of about

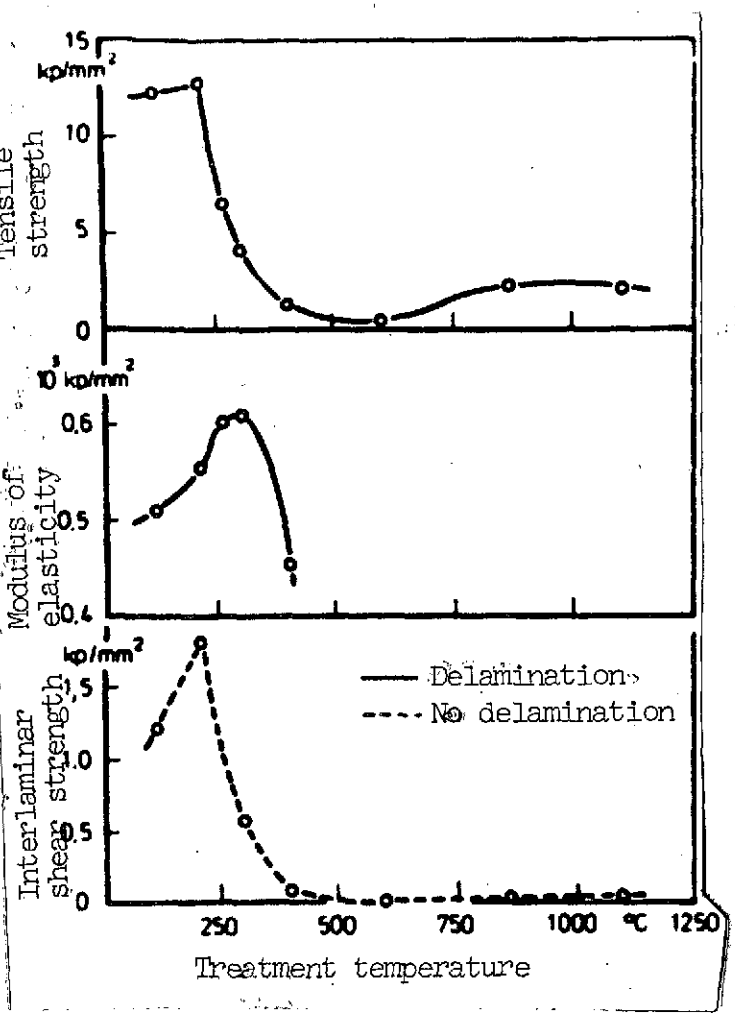

Fig. 49. Mechanical properties of a Phenodur PR 373 phenolic resin laminate reinforced with uncrosslinked PAN fibers as a function of treatment temperature (determined in fiber direction at room temperature)

250°C. The fiber has completely lost its initial strength by the end of curing at 300°C. After the loss of PAN fiber strength, the composite exhibits strength behavior similar to that of reinforced polymer matrix throughout the entire pyrolysis range, if we take the non-load-bearing fiber cross section and a certain degree of damage to the composite structure into consideration. For reasons involving measurement technique, composite modulus of elasticity could no longer /149 be determined beyond 400°C. Thus it is impossible to make a comparison with matrix containing no fibers in the temperature range between 400 and 1200°C.

Bending shear strength has a curve similar to the tensile strength of the composites. No delamination occurred in any specimen; this corresponds directly to the poor fiber strength. Weight loss increased by 6 to 7% relative to that of the pure matrix after thermal treatment to 1100°C, due to cocoking of the PAN fiber. Linear shrinkage (in fiber direction) is reduced by 5 to 6%, on the other hand.

Fig. 51 shows scanning /151 electron micrographs of fracture surfaces of the composites from tensile testing before and after their thermal decomposition. Imbedding of the fiber in the matrix is excellent in both cases. Unexpectedly, however, the pyrolyzed composites exhibit cracks in the fiber direction. This fact indicates that the volatile dissociation products of the PAN fibers cannot diffuse outward through the matrix rapidly enough. /152 Stresses build up which result in crack formation within the composites.

TABLE 31. DATA ON THE PREPARATION OF UNIDIRECTIONALLY REINFORCED COMPOSITES BASED ON PHENODUR PR 373 PHENOLIC RESIN AND UNCROSSLINKED PAN FIBER

Fiber tension [p]	400
Fiber advance per winding core turn [mm]	0.50
Number of winding layers	5
Curing conditions	20 h at 70°C 2 h at 100°C, Pressure: 0.03 kp/cm² 25 h at 100°C) 50 h at 110°C) Pressure: 4.3 kp/cm² 110 - 300°C Heating rate: 12°C/h in N_2 atmosphere
Composite thickness (after curing at 110°C) [mm]	1.80
Fiber content by volume (after curing at 110°C) [%]	42.3

7.252. Coking carbon-fiber-reinforced thermosets with fillers

An attempt was made to prevent the destructive effects of matrix shrinkage during the thermal decomposition of carbon-fiber-reinforced thermosets by incorporating both infusible fillers and fillers fusible within the temperature range of interest into the thermoset matrices. /154

Natural graphite (Kropfmühl, finely powdered graphite) was used for the nonfusing leaning material, since the shrinkage of thermosets can be influenced to within wide limits by the addition of this filler [34].

In a preliminary experiment, a unidirectionally reinforced carbon-fiber-laminate based on furfuryl alcohol / formaldehyde resin, graphite powder and VYB fiber (filler content was 17 wt.% in the liquid resin) was pyrolyzed to 1200°C and then studied by light microscopy. Fig. 52 shows micrographs of the laminate before and after coking. The flakes of natural graphite occur only in the matrix between the cords of fiber, not within the

TABLE 32. PROPERTIES OF UNIDIRECTIONALLY REINFORCED COMPOSITES BASED ON *PHENODUR* PR 373 PHENOLIC RESIN AND UNCROSSLINKED PAN FIBER AS FUNCTIONS OF TREATMENT TEMPERATURE (DETERMINED IN FIBER DIRECTION AT ROOM TEMPERATURE)

Treatment temperature [°C]	Tensile strength [kp/mm²]	Young's modulus [kp/mm²]	Interlaminar bending shear strength [kp/mm²]	Weight loss [%]	Linear shrinkage [%]
110	12.3	510	1.22+	0	0
210	12.8	555	1.82+	3.6	5.6
260	6.5	605	-	9.5	9.6
300	4.1	610	0.58+	13.8	10.0
400	1.3	455	0.09+	42.8	21.9
600	0.4	-	< 0.01+	46.4	17.3
865	2.2	-	0.02+	50.8	20.0
1100	2.1	-	0.03+	54.8	21.0

+ Specimens did not delaminate

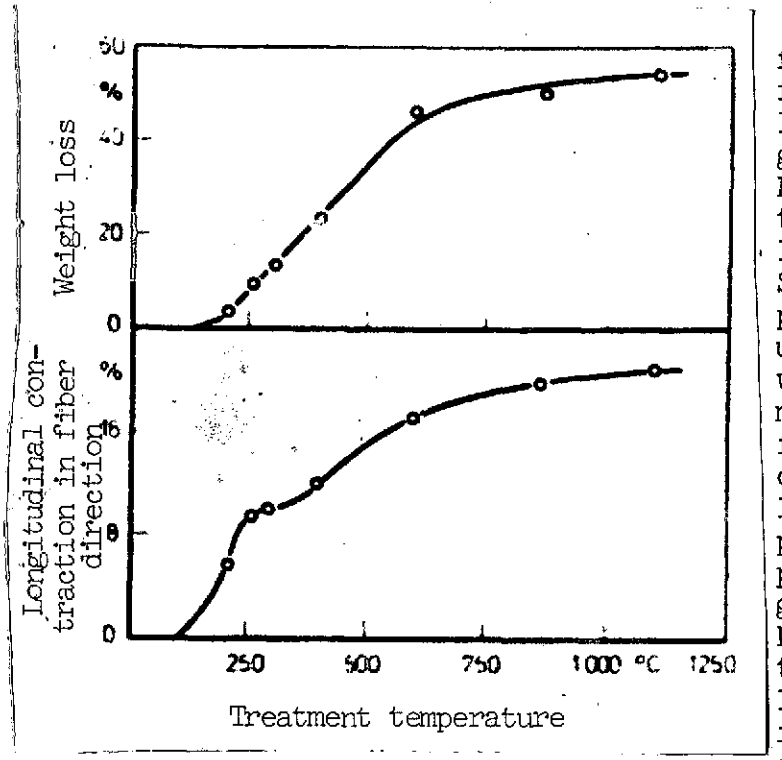

Fig. 50. Weight loss and longitudinal contraction in fiber direction of a Phenodur PR 373 phenolic resin laminate reinforced with uncrosslinked PAN fibers (determined at room temperature)

fiber bundles. The reasons for this are the relatively large grain size of the graphite powder, on the one hand, and, on the other, the method by which the laminate was prepared. Since the reinforcing component is wound on the core under pretension in the winding method used, the monofilaments in the individual fiber cords lie close to one another. Although the liquid matrix material can penetrate into the densely packed fiber bundle, the graphite particles are kept back. The structure of the thermally decomposed laminate, damaged by cracks, indicates that the extent of shrinkage damage obtained with carbon-carbon composites without filler (see Section 7.23) cannot be visibly reduced by the addition of graphite flakes. Since the imbedding of solid fillers in fiber-reinforced thermoset matrices does not promise a satisfactory solution to the shrinkage problem, studies in this direction were not pursued further.

Preliminary experiments with a fusible filler were more successful. A finely ground alkali glass with a melting point of about 550°C was used. Composites of furfuryl alcohol / formaldehyde resin (45 wt.%), glass powder (30 wt.%) and 2 to 3 cm long VYB carbon fibers (25 wt.%) did exhibit occasional /156 cracks and bubbles at the surface after heat treatment to 1200°C. In the interior, however, the composites were largely free of cracks and pores (see Fig. 53). During heat treatment, the molten glass filled the pores and cracks which were present and prevented the formation of new defects, so the heat-treated composites possess a compact structure at room temperature. To be sure, the glass serving as filler has the great disadvantage that when fused at even higher temperatures, it attacks the unprotected fibers chemically, thereby reducing their strength.

On the basis of the satisfactory results yielded by the preliminary experiments with low-melting glass powder, studies

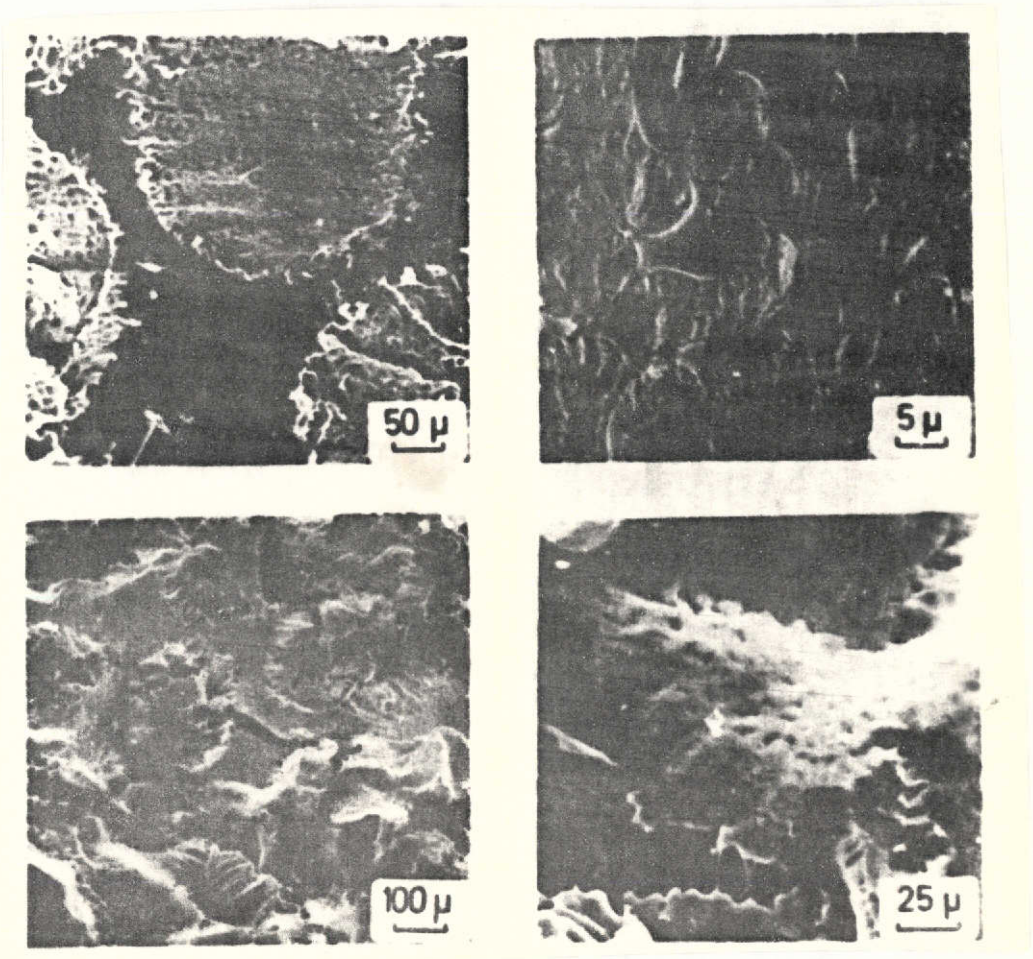

Fig. 51. Scanning electron micrographs of fracture surfaces of a Phenodur PR 373 phenolic resin laminate reinforced with uncrosslinked PAN fibers, from tensile test; top: after initial curing at 110°C; bottom: after coking to 1100°C.

were now performed with pitch as the fusible filler component. Results obtained by MacKay [15] are already available concerning the use of an epoxy resin modified with pitch as a matrix precursor for carbon-carbon composites (see Section 7.1). /157

In the present work, a soft pitch (see Table 33) was used which is particularly compatible with Phenodur PR 373 phenolic resin. The phenolic resin was modified with soft pitch with the aid of solvent, a 60 wt.% resin solution in n-butanol being mixed with a 25 wt.% solution of soft pitch in benzene. After

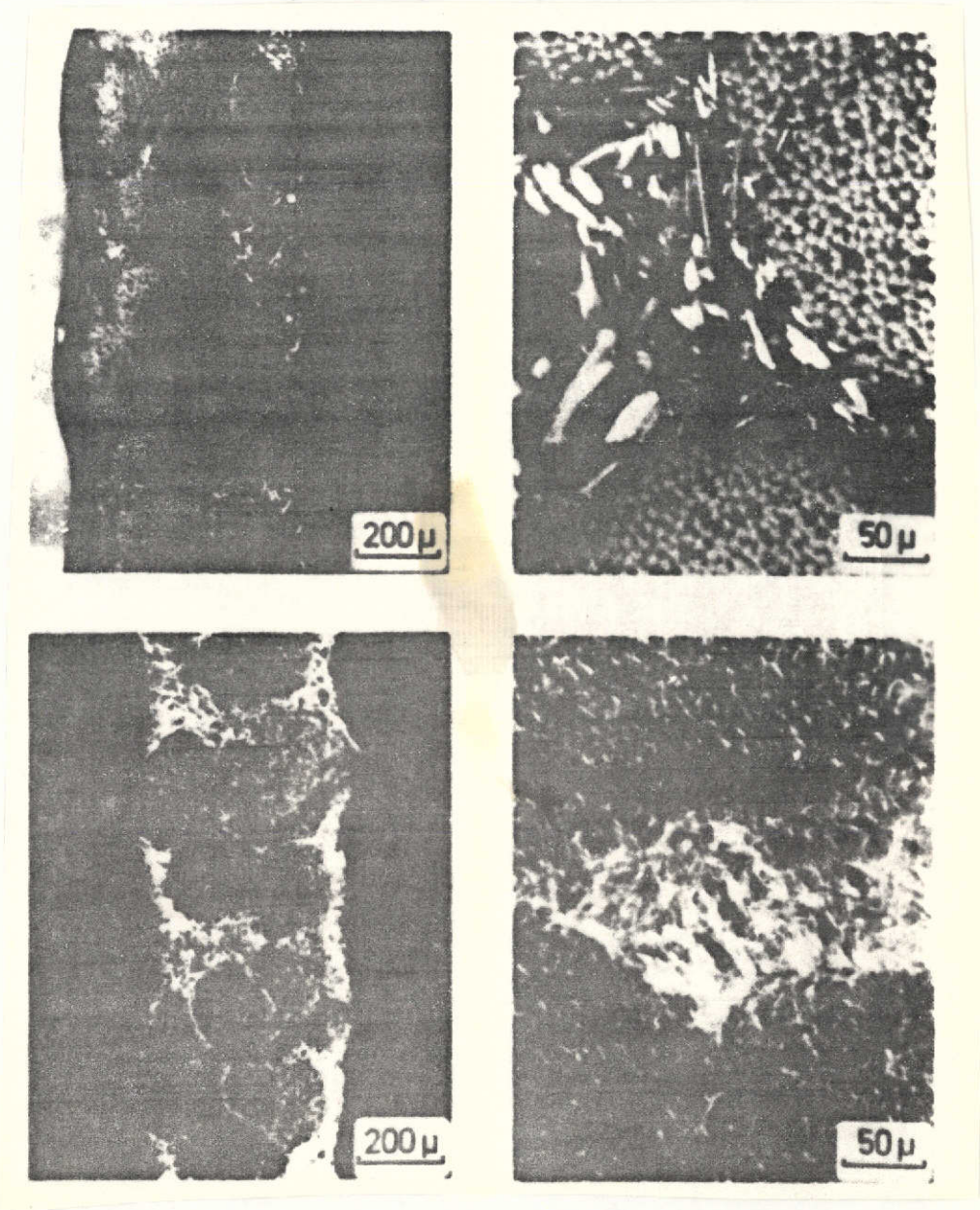

Fig. 52. Photomicrographs of a laminate of furfuryl alcohol / formaldehyde resin, graphite powder and VYB carbon fiber; top: after curing at 130°C; bottom: after thermal decomposition to 1190°C.

the removal of 50 wt.% solvent, a mixed solution was obtained which was still quite castable at room temperature. The soft pitch content of the modified phenolic resin was 25 wt.% in the solvent-free state.

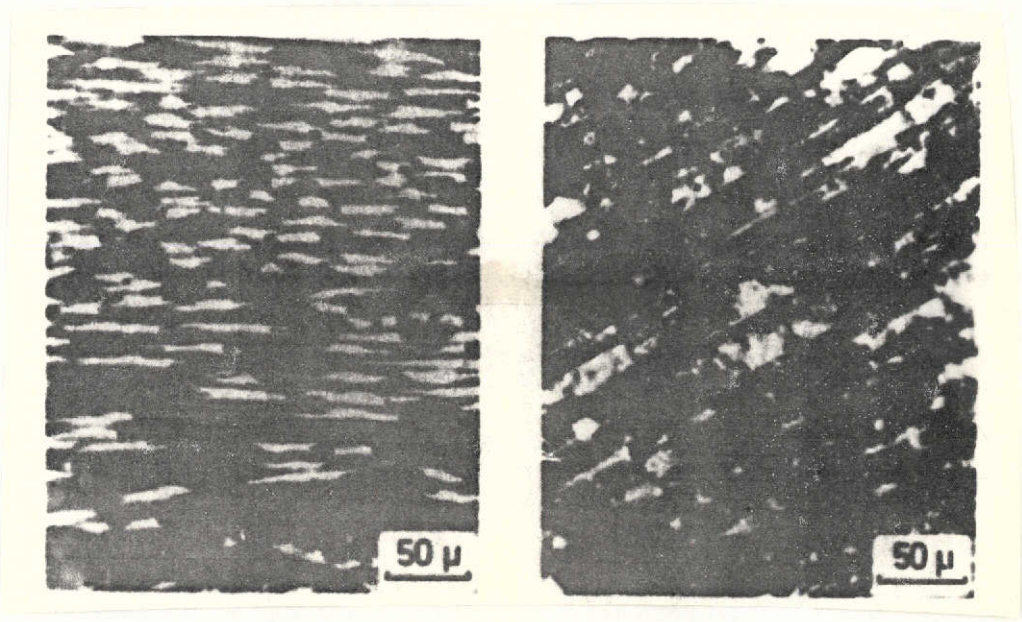

Fig. 53. Photomicrographs of a composite of furfuryl alcohol / formaldehyde resin, glass powder and VYB carbon fiber; left: after curing at 190°C; right: after heat treatment to 1190°C (polarized light)

TABLE 33. PROPERTIES OF THE SOFT PITCH

Softening point (from Kraemer-Sarnow)	[°C]	55
E-coke yield (Electro-kemisk process)	[%]	46
Insoluble in quinoline	[%]	4
Insoluble in pyridine	[%]	10
Insoluble in tuolene	[%]	23

In order to quantitatively determine the effect of the soft pitch component on the composite, unidirectionally reinforced composites based on Phenodur PR 373 phenolic resin, EP 55 soft pitch and VYB fiber were prepared by the wet winding method (see Table 34) and their properties studied in various

curing and pyrolysis stages. VYB fiber was chosen for these studies because the greatest shrinkage occurred in composites with VYB fiber and thus a particularly effect was expected. The results are shown in Table 35 and plotted in Figs. 54 and 55 as a function of treatment temperature.

TABLE 34. DATA ON THE PREPARATION OF UNIDIRECTIONALLY REINFORCED COMPOSITES BASED ON PHENODUR PR 373 PHENOLIC RESIN, EP 55 SOFT PITCH AND VYB FIBER

Fiber tension [p]	250
Fiber advance per winding core turn [mm]	1.00
Number of winding layers	4
Curing conditions	15 h at 70°C 2,5 h at 80°C; Pressure: 0,3 kp/cm² 25 h at 80°C) 65 h at 100°C) Pressure: 2,9 kp/cm² 20 h at 110°C 110 - 300°C Heating rate: 12°C/h in N_2 atmosphere
Composite thickness (after curing at 110°C) [mm]	1,20
Fiber content by volume (after curing at 110°C) [%]	56,4

A comparison of the results with the properties of composites based on Phenodur PR 373 phenolic resin and VYB fiber (composite I; see Section 6.23 and 7.22) shows that the soft pitch has produced no improvement. On the contrary, interlaminar bending shear strength is considerably impaired by the addition of pitch to about 600°C. In addition, the composites now delaminate to about 700°C. Due to the poor adhesion between fiber and matrix, lower values are also obtained for bending strength to about 500°C. The weight loss curve is higher in the curing range and early pyrolysis stage, but largely coincides with the weight loss curves of composites without added pitch above 500°C. /158

Scanning electron micrographs of fracture surfaces on the cured and carbonized composites from tensile tests (see Fig. 56) provide information about their structure. The vitreous /161

TABLE 35. PROPERTIES OF UNIDIRECTIONALLY REINFORCED COMPOSITES BASED ON PHENODUR PR 373 PHENOLIC RESIN, EP 55 SOFT PITCH AND VYB FIBER, AS A FUNCTION OF TREATMENT TEMPERATURE (DETERMINED IN FIBER DIRECTION AT ROOM TEMPERATURE)

Treatment temperature [°C]	Tensile strength [kp/mm²]	Young's modulus [kp/mm²]	Bending strength [kp/mm²]	Interlaminar bending shear strength [kp/mm²]	Weight loss [%]	Longitudinal contraction [%]
110	37.8	2140	25.6	1.08	0	0
225	38.1	2240	24.0	0.96	10.8	0.10
300	32.8	2100	-	0.55	11.3	0.15
480	28.4	2160	-	0.27	20.1	0.35
600	21.1	2200	11.0	0.25	21.0	0.31
700	12.5	2520	3.9	-	23.0	0.31
865	6.2	2770	2.2	0.36+	22.5	0.39
1100	4.0	2810	≤ 0.9	0.21+	27.5	0.21

+ Specimens did not delaminate

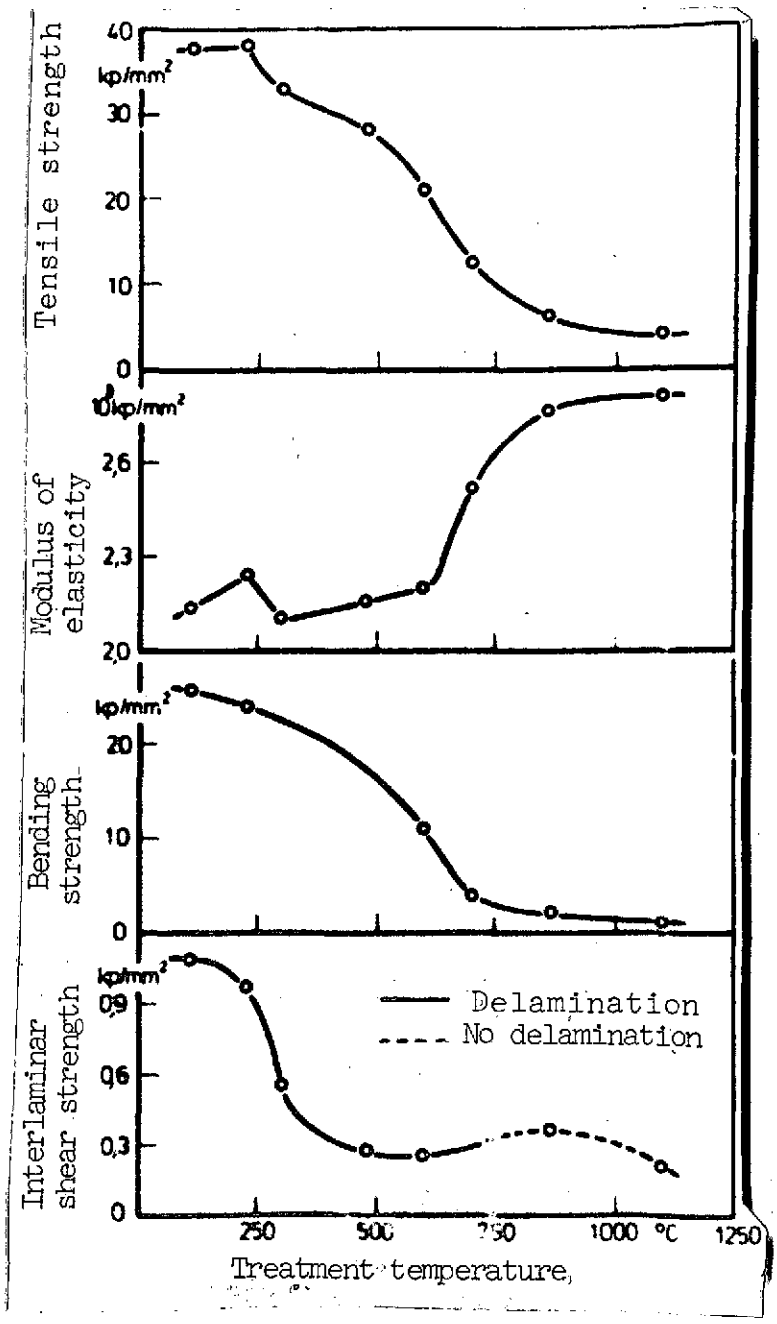

Fig. 54. Mechanical properties of a laminate of Phenodur PR 373 phenolic resin, EP 55 soft pitch and VYB carbon fiber as a function of treatment temperature (determined in fiber direction at room temperature).

structure of the phenolic resin (see Section 6.24, Figs. 20 - 23) is lost because of the addition of pitch. The resin/pitch matrix, when initially cured to 110°C, exhibits a granular fracture behavior and adheres poorly to the VYB fiber as shown by the loose grouping of fiber at the fracture end. After carbonization, the composites exhibit the same structure as the carbon-carbon composites without added pitch (see Section 7.23, Fig. 41). The extent of shrinkage damage can be described as equivalent in the two types of composites, explaining their similarity in strength behavior. Additional attempts to plasticize the thermosets in the critical pyrolysis range were therefore not undertaken. Reference has already been made several times to the successful use of resin-free pitch matrices in concurrent work at the Institute [26].

7.253. Pyrolysis of carbon-fiber-reinforced thermosets under mechanical pressure /162

The thermal decomposition of carbon-fiber-reinforced thermosets under mechanical pressure offers another possibility for preventing the composite damage caused by matrix shrinkage. This method appears promising in that /163 the thermosets are

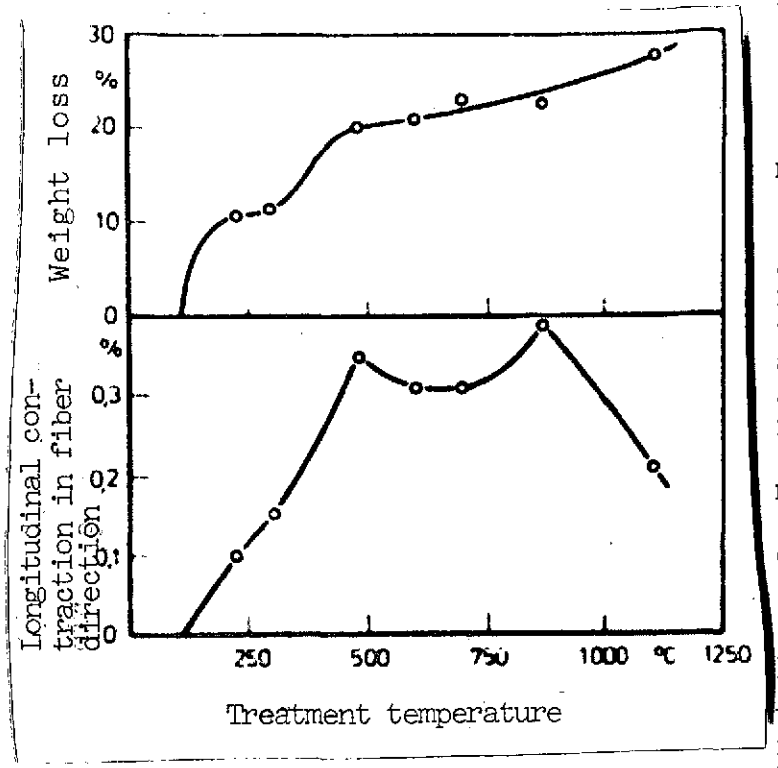

Fig. 55. Weight loss and longitudinal contraction in fiber direction of a laminate of Phenodur PR 373 phenolic resin, EP 55 soft pitch and VYB carbon fiber (determined at room temperature).

plastically deformable to about 550°C (see Section 4.135) and have already undergone more than half of their total shrinkage in this pyrolysis stage.

In preliminary experiments, 1 cm long carbon fibers of the WYB type, impregnated with furfuryl alcohol / formaldehyde resin, were pressed into tablet-shaped pieces with a diameter of 20 mm and a thickness of 3 mm. The resin content of the composites was intentionally made high -- 80 wt.% -- in order to avoid the danger of the fiber's coming in contact with one another as the matrix flows away perpendicular to the pressing direction under pressure as the result of its plasticity. The specimens, cured to 130°C, were then heated to 600°C at 12°C/h under high mechanical pressure (30 kp/mm^2) in a heatable cylindrical mold of Nimonic 90 with a bore diameter of 20 mm. Micrographs of the polished surface of the pressure-coked composites (see Fig. 57) show that although the material is highly compacted under the molding pressure, crack formation perpendicular to the direction of pressing cannot be suppressed. Because of the unpromising results of the preliminary experiments, further studies in this direction were not pursued. /164

7.254. Thermal decomposition of thermosets with thermally aftertreated carbon fibers

The necessity of subjecting carbon fibers heat treated at low temperatures, such as VYB fiber, to thermal aftertreatment before they are used to producedcarbon-carbon composites has already been reported on in the literature [23]. The purpose of this measure is to reduce the weight loss and shrinkage of the composites during pyrolysis.

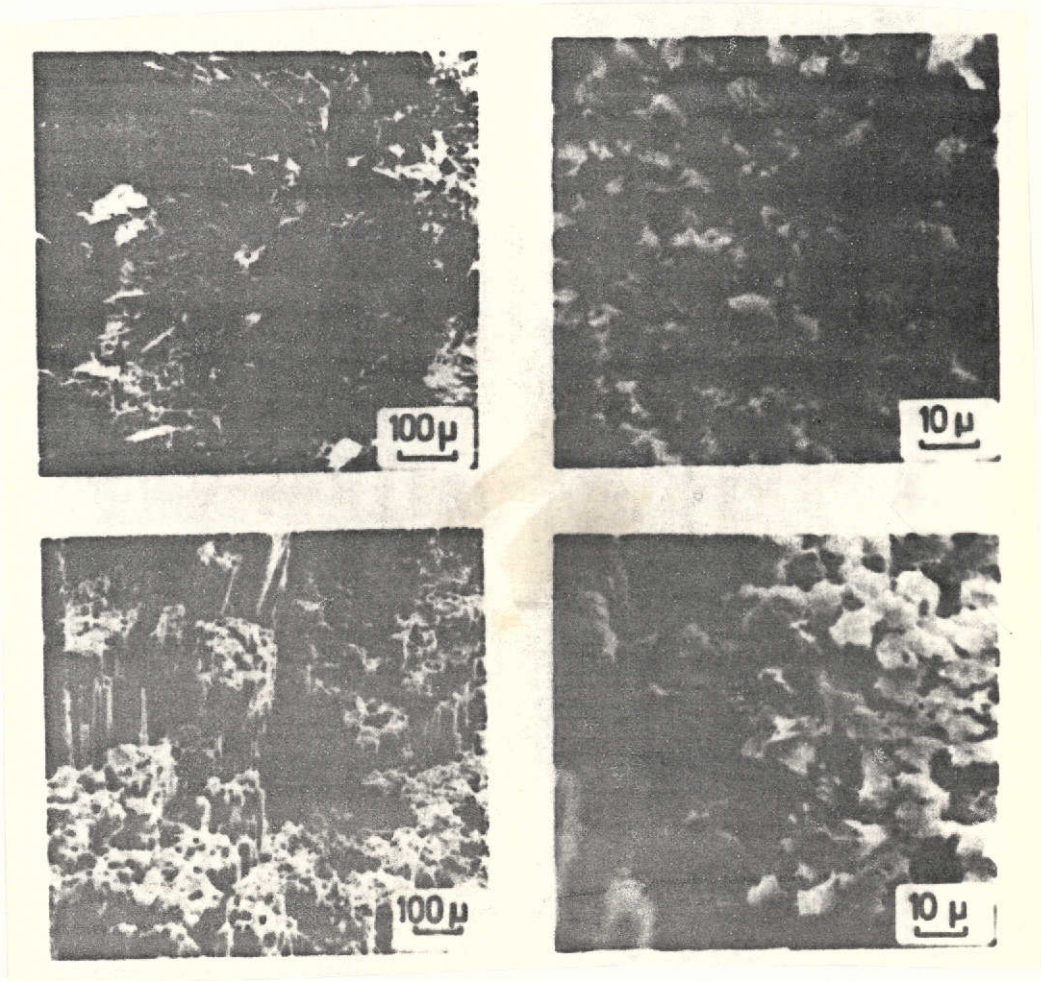

Fig. 56. Scanning electron micrographs of fracture surfaces of a laminate based on PR 373 phenolic resin, EP 55 soft pitch and VYB carbon fibers, from tensile test; top: after initial curing at 110°C; bottom: after thermal decomposition to 1100°C.

The effect of the thermal aftertreatment of carbon fibers on the strength properties of carbon-carbon composites was studied using the Phenodur PR 373 phenolic resin / VYB fiber composite system.

The fiber was recoked to 1150°C in ultrapure nitrogen at 12°C/h. During the heat treatment, the fiber loses 18.9% of its weight; its density increases from 1.53 to 1.64 g/cm^3.

The composites with recoked VYB fiber were prepared and cured under the same conditions as for the composite material

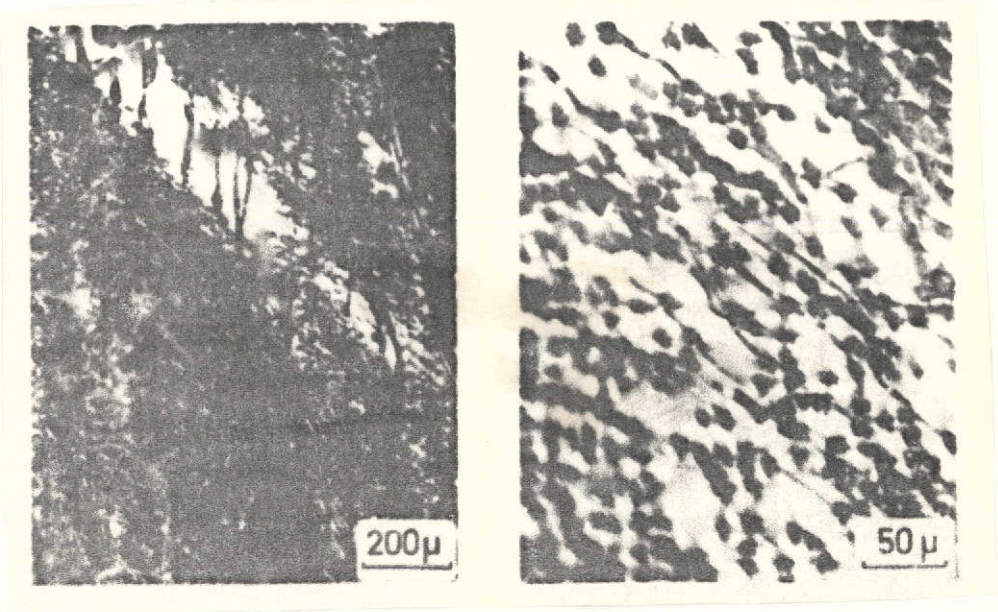

Fig. 57. Photomicrographs of a pressure-coked composite of furfuryl alcohol / formaldehyde resin and WYB carbon fiber, treatment temperature 600°C, pressure 30 kp/mm^2.

with untreated fiber (see Section 6.22). Pyrolysis conditions (heating rate 12°C/h, ultrapure nitrogen atmosphere) were likewise the same. The properties of the cured and pyrolyzed composites are compiled in Table 36. Characteristic values for the composite with VYB fiber not thermally aftertreated are included for comparison.

It can be seen from the tensile strength and modulus of elasticity data on the two composites in the curing stage that the mechanical properties of VYB fiber are improved somewhat by thermal aftertreatment. Adhesion between matrix and fiber is considerably impaired, on the other hand, as the shear strengths show. The cause of the impairment of adhesion can be assumed to be that the heat treatment and the associated high fiber weight loss destroy adhesive centers on the fiber surface and reduce the surface roughness of the fiber (see Table 3, Section 3.21). /166

The strength properties (tensile and bending strength) of the pyrolyzed composites indicate that the recoked fiber is damaged less severely by pyrolysis shrinkage of the matrix. Due to reduced adhesion in the curing stage, impairment of free matrix shrinkage along the fiber commences during an advanced

TABLE 36. PROPERTIES OF CURED AND PYROLYZED COMPOSITES BASED ON PHENODUR PR 373 PHENOLIC RESIN REINFORCED WITH THERMALLY AFTERTREATED VYB FIBER+ (DETERMINED IN FIBER DIRECTION AT ROOM TEMPERATURE)

	Fiber aftertreated	Fiber not aftertreated	Fiber aftertreated	Fiber not aftertreated
Treatment temperature [°C]	210	205	1100	1190
Fiber content by volume [%]	42.9	47.5	44.6	50.7
Tensile strength [kp/mm²]	42.0	39.8	12.0	5.9
Young's modulus [kp/mm²]	2105	1920	2830	2910
Bending strength [kp/mm²]	29.9	29.8	4.6	≤ 0.7
Interlaminar bending shear strength [kp/mm²]	3.39++	4.62++	0.59	0.35++
Weight loss [%]	2.7	3.4	21.8	27.3
Longitudinal contraction [%]	0	0.06	0	- 0.14

+ The fiber was thermally aftertreated to 1150°C under ultrapure nitrogen at 12°C/h.

++ 50% of specimens did not delaminate

+++ 100% of specimens did not delaminate

stage of pyrolysis, so the reinforcing component is not subjected to such high mechanical stresses up to the end of pyrolysis at 1100°C.

The above measure is of subordinate interest from an economic standpoint, since we can employ fibers of low specific surface area directly. The results of this study do provide a contribution to the confirmation of earlier assumptions regarding relationships between adhesion and fiber damage, however.

7.3. Pyrolysis of carbon-fiber-reinforced polyimides

7.31. Properties of the thermally decomposed composites

Carbon-fiber-reinforced polyimides, like the carbon-fiber reinforced thermosets, were thermally decomposed at a heating rate of 12°C/h in ultrapure nitrogen. The strength properties, weight losses and longitudinal contractions of the pyrolyzed composites are shown in Table 37. /167

It can be seen from the results of the strength measurements that Kerimid 601 polyimide is not suitable as a matrix for solid carbon-carbon composites. The pyrolysis shrinkage of this polymer matrix causes extensive destruction of the fiber-reinforced composite. The strength and fracture behavior of Kerimid 601 / Thornel 50 fiber composite decomposed thermally to 1030°C is almost identical to that of the carbon-carbon composite based on Phenodur PR 373 and Thornel 50 fiber (see Section 7.22 and 7.23).

The preliminary decomposition experiments with composites based on P 13 N polyimide resin and Thornel 50 fiber, limited to measurement of the interlaminar bending shear strength of pyrolysis residues, likewise yield no satisfactory results. The shear strength of the composites pyrolyzed to 1050°C, 0.45 to 0.65 kp/mm^2, is not appreciably higher than the 0.40 kp/mm^2 value for the carbon-carbon composite based on Kerimid 601 polyimide resin and Thornel 50 fiber.

In contrast to these two types of polyimides and the thermosets studied, QX-13 polyimide resin proves to be particularly suitable as a binder for carbon-carbon composites. The pyrolyzed composites based on QX-13 and Thornel 50 fiber exhibit high bending strength and interlaminar shear strength, indicating good fiber/matrix bonding. Their bending strength, 23 to 32 kp/mm^2, is also achieved with Phenodur PR 373 phenolic resin as the matrix precursor, but only after several impregnations and recarbonizations of the composite (see Section 7.24). The interlaminar shear strengths of 1.4 to 2.5 kp/mm^2 cannot be achieved with the impregnation method, however.

TABLE 37. PROPERTIES OF THERMALLY DECOMPOSED CARBON-FIBER-REINFORCED POLYIMIDES (DETERMINED IN FIBER DIRECTION AT ROOM TEMPERATURE)

Resin-fiber system	Pyrolysis temperature [°C]	Fiber content by vol. [%]	Tensile strength [kp/mm²] measured	Tensile strength [kp/mm²] calculated+	Tensile strength [kp/mm²] achieved [%]	Young's modulus 10^{-3} [kp/mm²] measured	Young's modulus 10^{-3} [kp/mm²] calculated+	Young's modulus 10^{-3} [kp/mm²] achieved [%]	Bending strength [kp/mm²] measured	Bending strength [kp/mm²] calculated+	Bending strength [kp/mm²] achieved [%]	Interlaminar bend. shear strength [kp/mm²]	Weight loss [%]	Longitudinal contraction [%]
KERIMID 601/ Thornel 50	1030	42.6	33.8	85	40	12.0	14.9	81	≤0.79	85	≤ 1	0.40	26.7	0
P13N/Thornel 50	1050	20.0	-	-	-	-	-	-	-	-	-	0.47++	-	-
		24.8	-	-	-	-	-	-	-	-	-	0.51++	-	-
		27.6	-	-	-	-	-	-	-	-	-	0.65++	-	-
		34.8	-	-	-	-	-	-	-	-	-	0.62++	-	-
QX-13/Thornel 50	1000	42.6	34.1	85	40	15.5	14.9	104	32.0	85	38	2.48+++	26.5	-0.01
	1100	57.8	46.1	116	40	14.8	20.2	73	23.5	116	20	1.41	24.1	0

\+ Matrix component was neglected

++ 100% of specimens did not delaminate

+++ 50% of specimens did not delaminate

Fiber damage due to matrix shrinkage during pyrolysis can also be detected in the case of QX-13 polyimide resin. Thermal /169 decomposition reduces the measured tensile strength of composites of low fiber content (30 vol.%) cured at 300°C from 62 to 40% of the calculated value and that of composites of high fiber content (46 vol.%) from 74 to 40%, too. The calculated modulus of elasticity is achieved 104% by the low-fiber composite, as opposed to an earlier 95%, and 73% by the high-fiber composite, as opposed to an earlier 93%. In the case of bending strength, the strength of the fiber used is utilized 38 and 20%, as opposed to 35 and 43% in the fully cured state. Thus the higher fiber content contributes to more severe damage to the structural integrity of the carbon=carbon composites.

7.32. Structure of thermally decomposed composites

Photomicrographs of ground surfaces and scanning electron micrographs of fracture surfaces of the carbon-carbon composite based on QX-13 polyimide and Thornel 50 fiber (see Figs. 58 and 59) provide information which agrees with results of the strength studies. In contrast to earlier thermally decomposed polymers reinforced with Thornel 50 fibers, this composite possesses a relatively compact structure. Bonding of the fibers is good, and the short fiber tips projecting from the fracture surfaces indicate good adhesion between matrix and fiber. The matrix shrinkage prevented in the longitudinal direction of the fibers by the good adhesion is compensated for by the formation of cracks perpendicular to the fibers.

Both the strength properties and the structure of this carbon-carbon composite show the superiority of QX-13 polyimide resin over the polymer matrices studied earlier as a matrix precursor. A consideration of the shrinkage behavior and plastic/170 deformability of the matrix materials during thermal decomposition contributes to an understanding of this situation.

As the measurements in Section 4.133 show, the longitudinal /171 shrinkage of molded thermosets after thermal decomposition to 1100°C falls between 21 and 27%, depending upon the type of resin; that of molded QX-13 specimens is about 17% (see Section 4.222). Ball impression diameter is between 0 and 0.75 mm for thermosets pretreated to 515°C (see Section 4.135); that for QX-13 polyimide after pretreatment to 550°C is 0.96 mm (surface load 1.33 kp/mm^2), as shown by a preliminary study.

These two properties of the polyimide resin, both the low pyrolysis shrinkage and the high plasticity in the advanced decomposition stage, allow the preparation of relatively strong carbon-carbon composites.

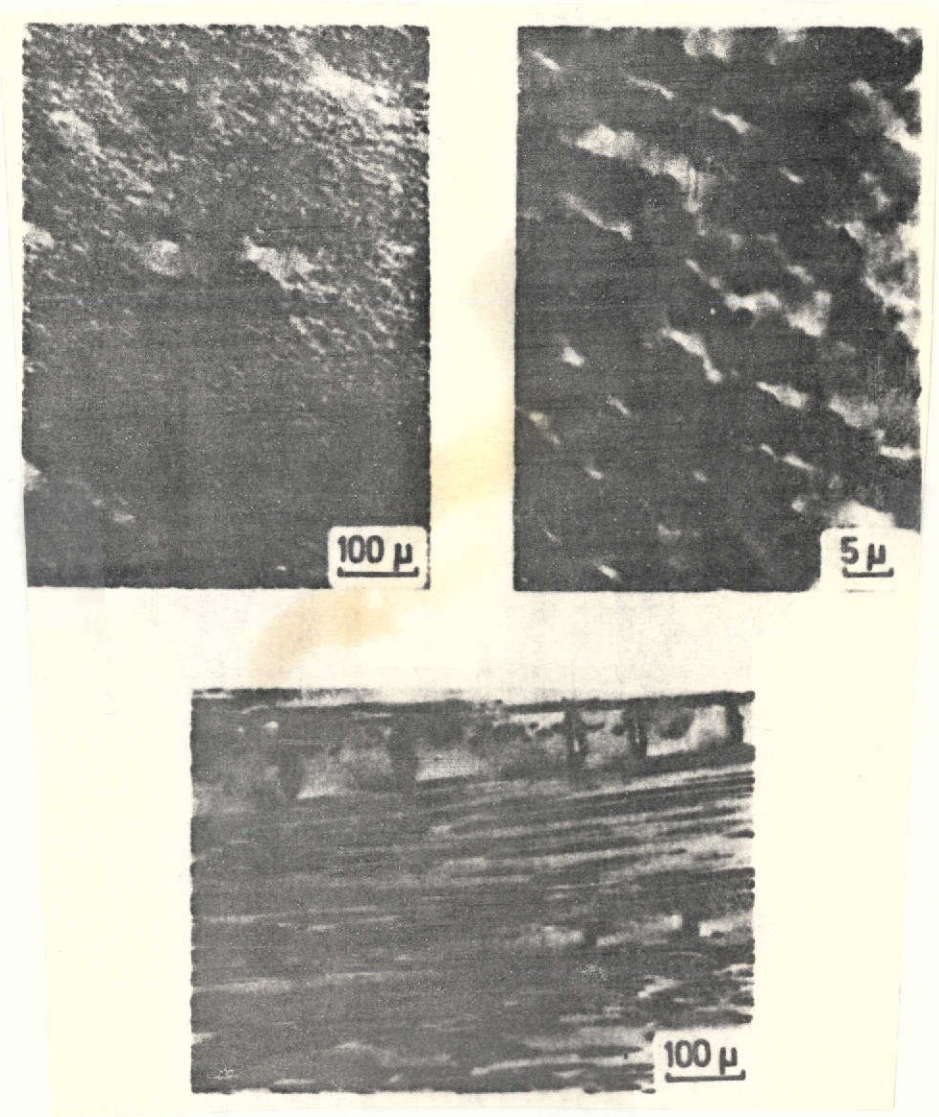

Fig. 58. Photomicrographs of a carbon-carbon composite based on QX-13 polyimide and Thornel 50 fibers, treatment temperature 1000°C, fiber content 42.6 vol. %; top: cross section; bottom: longitudinal section.

8. Summary of results /172

As set forth in the introduction, carbon-fiber-reinforced composites with polymeric matrix materials were developed in this work for the highest possible utilization temperatures. Of the potential approaches for solving this task, emphasis was placed on studying not only the chemical modification of conventional laminating resins (epoxy resins) and the use of new high-temperature-resistant polymers but also the thermal

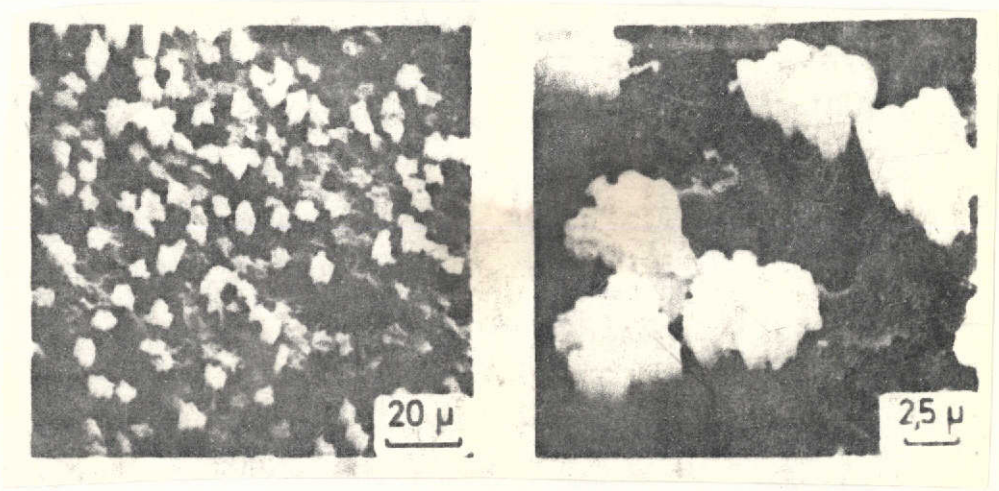

Fig. 59. Scanning electron micrographs of the fracture surface of a carbon-carbon composite based on QX-13 polyimide and Thornel 50 fiber, from tensile test, treatment temperature 1000°C, fiber content 42.6 vol. %.

aftertreatment of polymers, from curing to complete thermal decomposition to pure carbon.

The experimental study was broken down into two parts. The first part covered curing and the thermal decomposition of unreinforced polymer matrices and a study of their physical properties. The second part covered the preparation and testing of unidirectionally fiber-reinforced composites and their thermal decomposition to produce carbon-fiber-reinforced specimens of pure carbon.

Part I: Matrix materials

A conventional phenolic resol (Phenodur PR 373) and a furfuryl alcohol / formaldehyde (developed at this Institute; cf. [34]) were used as matrix materials; it was already known that they can be cured without cracks and pores and decomposed thermally to produce vitreous carbon. In addition, a special epoxy resin was developed which was based on a mixture of two conventional epoxy resins (Epikote 828 and Epikote 1031) and contained considerable amounts of pyromellitic dianhydride as a hardener and secondary component. New high-temperature-resistant polyimides were also incorporated into this study -- three commercially available types: P 13 N (Ciba-Geigy), QX-13 (ICI) and Kerimid 601 (Rhône-Poulenc).

With the exception of Kerimid 601 polyimide resin, all of the resins used proved to be suitable as precursors for /173

compact specimens of vitreous carbon. The weight loss of resin specimens decomposed in inert gas was between 44 (QX-13) and 63 wt. % (Kerimid 601). Longitudinal contraction during thermal decomposition to carbon was between 17% (QX-13) and 27% (Kerimid 601 and phenolic resin).

Thermogravimetric analysis has confirmed the superior thermal stability of the polyimides (with the exception of Kerimid 601) with respect to the thermosets. The latter break down just above 200 to 250°C, whereas P 13 N and QX-13 polyimides only show signs of decomposing above 400 to 450°C in inert gas.

Phenolic resin was used as an example to show that pyrolysis shrinkage is completely isotropic and independent of the geometry of the specimens. In addition, it was possible to demonstrate for the first time that the highly crosslinked thermosets are plastically deformable to a limited degree up a pyrolysis temperature of about 500°C. In the example of furfuryl alcohol / formaldehyde precursor, it was thus possible to convert the isotropic shrinkage of the pyrolysis specimen -- through the application of mechanical pressure during pyrolysis -- into a unidimensional shrinkage in the direction of the applied pressure while maintaining shape transverse to the pressure. In addition, the tensile strengths and moduli of elasticity of the thermosets were determined at various stages of curing and pyrolysis. Crosslinking curing is accompanied by a rise in tensile strength. Maximum tensile strengths of 7 kp/mm^2 are achieved for molded specimens of unreinforced epoxy resin and furfuryl alcohol / formaldehyde resin after curing to about 200°C. Tensile strengths of 11 kp/mm^2 were achieved for molded specimens of phenolic resin after curing to 300°C.

It was possible to show that if the treatment temperature is raised beyond the optimum curing temperatures, room temperature tensile strengths drops to minima of about 3 to 4 kp/mm^2 after final temperatures of 500°C; if the temperature is increased further, however, it increases again and reaches values between 10 and 12 kp/mm^2 after carbonization at 1100°C. /174

The modulus of elasticity shows a dependence upon treatment temperature similar to that of tensile strength. Moduli of elasticity of 300 to 500 kp/mm^2 correspond to the maximum strengths of 7 to 11 kp/mm^2. The modulus of elasticity is increased to about 3000 kp/mm^2 by carbonization to 1200°C. A pronounced minimum in the modulus of elasticity was not observed in the early pyrolysis stage (final temperature 500°C).

Part II: Composites

The polymers studied in the first part were reinforced unidirectionally with endless carbon fibers made from rayon precursor. A nongraphitized fiber of high specific surface area

(VYB) and two stretch-graphitized fibers of low specific surface but very good mechanical properties (Thornel 25 and 50) were chosen as reinforcing components. All fibers were used without special surface treatment to increase interlaminar shear strength, so as to avoid effects which could not be checked during thermal decomposition.

Part IIa: Composites with polymer matrix

All fiber types were not treated with all polymers coming under consideration as matrix material, however; rather, only typical combinations were studied. The selected combinations of individual fiber types with the various matrix polymers were based on the availability or new development of different materials during this several-year study and on results obtained in the meantime. Thus VYB fiber was combined with epoxy resin and with phenolic resin, and Thornel 25 only with phenolic resin. The improved stretched-graphitized Thornel 50 fiber was used for reinforcement for both the phenolic resin and the two polyimides Kerimid 601 and QX-13 which had become commercially available.

The unidirectionally reinforced composites were generally /175 prepared by the wet winding method, followed by pressure curing. This process could not be applied in the case of P 13 N and QX-13 polyimides; these matrices were therefore reinforced by pressing thermally pretreated resin-impregnated fibers (yarns consisting of 1440 monofilaments each). The composites were fully cured uniformly to maximum temperatures of 300°C for the sake of greater comparability.

Tensile strength, Young's modulus and bending strength were used to characterize the mechanical properties of the carbon-fiber-reinforced polymer composites, and interlaminar shear strength (short beam test) was used as a measure of adhesion between matrix and fiber.

The results are discussed in terms of the effect of the various fiber types on adhesion to the polymer matrices, in terms of the effect of curing temperatures, and in terms of utilization of the fiber reinforcing component in the polymers with respect to the strength of molded specimens.

It was found that the composites with a matrix of phenolic resin, epoxy resin or Kerimid 601 polyimide experience a reduction in strength even during full curing and, to a greater degree, during hot aging. On the other hand, composites made of QX-13 polyimide with Thornel 50 fibers proved to be considerably more resistant to heat.

The effect of the various fibers on the strength properties of composites can be summarized as follows: Throughout the entire curing range, composites with Thornel 25 and Thornel 50 fibers

do yield the highest absolute values for tensile strength, Young's modulus and bending strengths, but the lowest values for interlaminar shear strength. Good utilization of the strength properties provided by the fibers occurs only in the case of tensile strength and Young's modulus. In the case of bending strength, which is enhanced by adhesion between matrix and fiber, poor utilization of fiber strength occurs as the result of inadequate adhesion. /176

Better adhesion between fiber and matrix was observed for composites with VYB fibers, i.e., the reinforcing component with the greatest specific surface area. This is manifested in the highest interlaminar shear strength values and in better utilization of fiber properties in the bending strength of the composites.

The measured shear strength values and their comparison with literature data show that equivalent and sometimes even better shear strength can be achieved with phenolic resin than with epoxy resin, although the latter exhibits the better wetting prior to full curing, as was determined by contact angle measurements. It is concluded from this that in the case of surface-treated fibers with phenolic resin, too, shear strengths can be achieved which are just about as good as those already known for epoxy resins (10 to 12 kp/mm^2).

Part IIb: Composites with thermally decomposed matrix

It could already be seen from studying the pyrolysis behavior of unreinforced polymers that the major problem in preparing carbon-fiber-reinforced carbon composites by the thermal decomposition of fiber-reinforced polymers would come from pyrolysis shrinkage. The interactions between fiber and matrix caused by matrix shrinkage were therefore studied with model composites of particularly low fiber content with the aid of scanning electron microscopy. These studies were performed with all three fiber types (VYB, Thornel 25 and Thornel 50) in combination with phenolic resin as the matrix precursor.

It was possible to show that the good adhesion between fiber and matrix, as is absolutely necessary for high interlaminar shear strength of fiber-reinforced polymers, has particularly damaging effects in thermal decomposition of the composites. Primary adhesion impairs free matrix shrinkage in the fiber direction during pyrolysis, causing damage to the composites. Damage is limited here not just to the matrix component but also extends to the reinforcing fiber. /177

This qualitative finding was supported by systematic strength measurements performed on composites. It is found that the greatest drop in composite strength takes place during thermal

decomposition in the temperature range of severest matrix shrinkage. In the case of composites containing VYB fiber (good adhesion between matrix precursor and fiber, due to the high specific surface area of the fiber), the bending and tensile strengths of the completely decomposed composites drop below the strength of the unreinforced carbon matrix.

It was also found that fibers of low specific surface area (stretch-graphitized Thornel types) withstand thermal decomposition of the composite without appreciable damage to the fiber (pronounced drop in bending strength while tensile strength remains unchanged). This information opens up the possibility of preparing carbon composites by multiple reimpregnation and recarbonization. In this experimental study, the maximum bending strength of 34 kp/mm^2 for a carbon-carbon composite prepared in this manner was achieved after four recarbonizations, corresponding to about 35% utilization of the strength of the Thornel fiber used. The interlaminar shear strength of this composite reaches only 0.9 kp/mm^2, however.

The results of these systematic experiments show the necessity of plasticizing the matrix precursor during the decisive coking stage. Of the many possible approaches, the example of the particularly sensitive VYB fiber was used in a preliminary attempt to increase the plasticity of the phenolic /178
resin matrix by adding coal-tar pitch, but without success in terms of improving composite properties.

The rest of the work therefore concentrated on the more promising use of polyimide resins combined with high-strength Thornel 50 fiber, which exhibits a smoother surface, since these resins pass through an albeit narrow temperature range of plastic deformability.

With QX-13 polyimide resin as the matrix starting material and a fiber content of about 40 vol. %, it was possible to obtain a fiber-reinforced carbon-carbon composite with a specimen bending strength of 32 kp/mm^2 without any reimpregnation treatment after coking, corresponding to about 40% utilization of the strength of the fiber employed. Measuring the interlaminar shear strength of this composite yielded the surprisingly high value of 2.5 kp/mm^2. A few successive impregnation and recarbonization steps can be expected to yield carbon-carbon composites whose properties at least correspond to those of composites prepared by the expensive gas impregnation method.

It has been possible to indicate a promising pathway for the industrial production of carbon-fiber-reinforced carbon composites in this study on the various adhesion and pyrolysis behaviors of polymeric carbon-fiber composites. A contribution has perhaps thus also been made to the broader application of this new, very special class of materials.

REFERENCES

1. Hagen, H., Glasfaserverstärkte Kunststoffe [Fiberglass-reinforced plastics], 2nd Edition, Springer-Verlag, Berlin, Göttingen, Heidelberg, 1961.

2. Mc Creight, L. R., Rauch, H. W., Sr., Sutton, W. H., Ceramic and graphite fibers and whiskers, Academic Press, New York, London, 1965.

3. Frazer, A. H., High temperature resistant fibers, Interscience Publishers, New York, 1967.

4. Jahn, H., Raumfahrtforschung, (4), 169-174,(July/August 1969)

5. Wetter, R., Kunststoffe 60(10), 756-760 (1970).

6. Nowak, P., Kunststoffe 51(9), 480-488 (1961).

7. Charles, G., Le Floch, A., Villamayor, M., Characterizations of boron-aluminum composites, Paper 20 of the Conference on "Testing fibrous composites for mechanical properties," Materials and testing group and National Physical Laboratory, Teddington, England, July 1970.

8. van Rensen, E., Sahm, K. F., Entwicklung von borfaserverstärkten Leichtmetallen [Development of boron-fiber-reinforced light metals], Paper delivered at meeting of the "Composites" technical committee of the German Metallurgical Society, Konstanz, March 1972.

9. Pepper, R. T., Rossi, R. C., Upp, J. W., "Development of an aluminum-graphite composite," Report TR-0059 (9250-03)-1, The Aerospace Corp., El Segundo, Calif., August 30, 1970.

10. Morris, A. W. H., "The fabrication and evaluation of carbon-fiber-reinforced aluminum composites," Paper No. 17 of the International Conference on "Carbon fibres, their composites and applications," the Plastics Institute, London, February, 1971.

11. Ignatowitz, E., Dissertation, Chemical Engineering Institute, University of Karlsruhe, 1973.

12. Poremba, S. W., Niesz, D. E., Fleck, J. N., Kistler, C. W., Jr., "Control of composite microstructure through the use of coated filaments," AIAA Paper No. 67-175 of the 5th Aerospace Sciences Meeting, New York, January 23-26, 1967.

13. France, L. L., Kachur, V., Hengstenberg, T.F., "Mechanical behavior of a continuous filament carbon composite," SAMPE 10, B-81/B-93 (1966).

14. Pinoli, P., Bradshaw, W., Iosty, L., Heynen, A., "Glassy carbon composites," Proceeding of the 13th Annual Refractory Composites meeting, Seattle, Wash., 1967.

15. MacKay, H. A., "The characterization of carbon fabrics and filaments, carbonizing resins, carbon-carbon composites and processing techniques," Report SC-RR-68-651, Sandia Laboratories, Albuquerque, New Mexico, April 1969.

16. Mc Donald, J. E., "Composite technology and carbon/carbon materials," Proceedings of the 10th Annual Symposium of the New Mexico Section of ASME and University of New Mexico, College of Engineering, January 1970.

17. Union Carbide Corp., Carbon Products Div., New York, Prod. Eng. 41(14), 54 (July 6, 1970).

18. Mc Loughlin, J. R., Nature 227, 701 (August 15, 1970).

19. Parmee, A. C. "Carbon fibre/carbon composite: some properties and potential applications in rocket motors," Paris Air Show, 1971.

20. Newling, D. O., Walker, E. J., "High-performance graphitized carbon-carbon composites," Paper No. 37 of the International Conference on "Carbon Fibres, their Composites and Applications," The Plastics Institute, London, February 1971.

21. Terwiesch, B., Fitzer, E., Bürger, A., "The behaviour of carbon-fiber-reinforced plastics during heat treatment above 300°C," Paper No. 67 of the 161st meeting of the American Chemical Society, Div. of Organic Coatings and Plastics Chemistry, Los Angeles, March-April, 1971.

22. Stoller, H. M., Irwin, J. L., Granoff, B., Wright, G. F., Jr., Gieske, J. H., "Properties of flight-tested CVD/felt and CVD/FW carbon composites," Report SC-DC-71 4046, Sandia Laboratories, Albuquerque, New Mexico, June 1971.

23. Evangelides, J. S., Meyer, R. A., Zimmer, J. E., "Investigations of the properties of carbon-carbon composites and their relationship to nondestructive test measurements," Technical report AFML-70-213, Part II, Air Force Materials Laboratory, Wright-Patterson AFB, Ohio, August 1971.

24. Yamada, S., Tamada, K., "Graphitizing process of carbon fibre/glassy carbon composites," personal communication to E. Fitzer and coworkers, December 1971.

25. Fitzer, E., Terwiesch, B., "Carbon-carbon composites unidirectionally reinforced with carbon and graphite fibers," Carbon 10(4), 383-390 (August 1972).

26. Terwiesch, B., Dissertation, Chemical Engineering Institute, University of Karlsruhe, 1972.

27. Dt. Offenlegungsschrift [German disclosure] 1925009, United Kingdom Atomic Energy Authority, London, 1969.

28. Bowen, D. H., "Fiber-reinforced ceramics," Fibre Sci. & Tech. 1(2), 85-112 (October 1968).

29. Burger, A., Fitzer, E., Chem. Ing. Tech. 42(19) 1203-1209 (1970).

30. Fitzer, E., Burger, A., "The formation of carbon/carbon composites by thermally decomposing carbon-fibre-reinforced thermosetting polymers," Paper No. 36 of the International Conference on "Carbon Fibres, their Composites and Applications," The Plastics Institute, London, February 1971.

31. Graham, L. W., Watt, W., Johnson, W., Arragon, P. A. P., Price, M. S. T., "The development of low permeability graphite for the dragon reactor experiment," Proceedings of the Fifth Conference on Carbon, Pergamon Press, New York, Oxford, London, Paris, Vol.2, 387-404, 1963.

32. Kaesmacher, H., Kunstst. Rundsch. 7(6), 265-268 (June 1970).

33. Fitzer, E., Schäfer, W., Yamada, S., Carbon 7, 643-648 (1969).

34. Schäfer, W., Dissertation, Chemical Engineering Institute, University of Karlsruhe, 1969.

35. Fitzer, E., Schäfer, W., Carbon 8, 353-364 (1970).

36. Holister, G. S., Thomas, C., Fibre reinforced materials, Elsevier Publ. Co. Ltd., Amsterdam, London, New York, 1966.

37. Broutman, L.J., Krock, R. H., Modern composite materials, Addison Wesley Publ.Co., Reading, Mass., 1967.

38. Dow, N. F., "Study of stresses near a discontinuity in filament-reinforced composite metal," General Electric Co. Report TIS R63SD61, 1963.

39. Sutton, W. H., Chorne, J., "Potential of oxide-fiber reinforced metals" in: Fiber Composite Materials, American Society for Metals, Metals Park, Ohio, 1965.

40. Kelly, A., Tyson, W. R., J. Mech. Phys. Solids 13, 329-350 (1965).

41. Kelly, A., Davies, G. J., Met. Rev. 10(37), 1-77 (1965).

42. Conference on "Testing fibrous composites for mechanical properties," National Physical Laboratory, Teddington, England, July 15-17, 1970.

43. Sykes, R., "Determination of tensile strength of composites," Paper 2 of the Conference on "Testing Fibrous Composites for Mechanical Properties," National Physical Laboratory, Teddington, England, July 15-17, 1970.

44. Muller, J. Raumfahrtforschung (5), 224-227 (1969).

45. Menges, G., Kleinholz, R., Kunststoffe 59(12), 959-966 (1969).

46. Siebel, E., Handbuch der Werkstoffprüfung [Handbook of materials testing], 2nd Edition, Vol. I, Springer-Verlag, Berlin, Göttingen, Heidelberg, 1958, p. 81.

47. Read, B. E., Dean, G. D., "Experimental methods for composite materials," AGARD lecture series No. 55 on composite materials, May 1972, pp. 4-1 to 4-28.

48. Grüninger, G., Kochendörfer, R., Jahn, H., Kunststoffe 60(12) 1029-1036 (1970).

49. Lubin, G., Handbook of fiberglass and advanced plastics composites, Van Nostrand Reinhold Comp., New York, 1969, p. 696.

50. v. Meysenbug, C. M., Kunststoffkunde für Ingenieure [Plastics theory for engineers], Carl Hanser-Verlag, Munich, 1963.

51. Saechtling, H., Zebrowski, W., Kunststoff-Taschenbuch [Plastics handbook], 17th Edition, Carl Hanser-Verlag, Munich, 1967.

52. Vollmert, B., Kunststoffe 56(10), 680-694 (1966).

53. Behr, E., Hochtemperaturbeständige Kunststoffe [High-temperature-resistant plastics], Carl Hanser-Verlag, Munich, 71-139, 1969.

54. Lax, E., Synowietz, C., Taschenbuch für Chemiker and Physiker [Handbook for chemists and physicists], 3rd Edition, Vol. I, Springer-Verlag, Berlin, Heidelberg, New York, 772-782, 1967.

55. Foerst, W., Ullmanns Encyklopädie der technischen Chemie [Ullman's encyclopedia of industrial chemistry], 3rd Edition, Vol. 11, Urban & Schwarzenberg, Munich, Berlin, 1960, pp. 36-37.

56. Morgan, P., Glass Reinforced Plastics, 3rd Edition, Iliffe Books Ltd., London, 1961.

57. Duffin, D. J., Laminated Plastics, 2nd Edition, Reinhold Publ. Corp., New York, 1966, p. 21.

58. Diefendorf, R. J., "Fiber and matrix materials for advanced composites," AGARD Lecture Series No. 55 on Composite Materials, May 1972, pp. 2-15.

59. "Precision parts made of VESPEL," brochure from DuPont.

60. Fitzer, E., Fiedler, A. K., Müller, D. J., Chem. Ing. Tech. 43(16), 923-931 (1971).

61. Ruland, W., Umschau Wiss. Tech. 70(22), 717 (1970).

62. Hawthorne, H. M.,"Structure and properties of strain-graphitized glassy carbon fibres," Paper No. 13 of the International Conference on "Carbon Fibres, their composites and applications," The Plastics Institute, London, February 1971.

63. Prosen, S. P., Fiber Sci. Tech. 3, 81-104 (1970).

64. Brie, M., Cazard, J., Lang, F. M., Riess, Gl., Greffage de polymères sur fibres de carbone [Attachment of polymers to carbon fibers], Bull. Inform. Sci. Tech.(Comissariat A L'Energie Atomique) 155, 31 (1971).

65. Yamada, S., Sato, H., Nature 193, 261-262 (January 20, 1962).

66. Davidson, H. W., Nuclear Engineering 7, 159-161 (April 1972).

67. Yamada, S., "A review of glasslike carbons," DCIC report 68-2 (April 1968).

68. Chekanova, V. D., Fialkov, A. S.,"Preparation, properties and applications of vitreous carbon," Russ. Chem. Rev. 40(5), 413-428 (1971).

69. Tokai Electrode Mfg. Co., Ltd., Toyko, Japan, Catalog on "Glassy Carbon,"1965.

70. Davidson, H.W., Losty, H. H. W., Gen. Elec. J. 30(1), 22-30 (1963).

71. Cowlard, F. C., Lewis, J. C., J. Mat. Sci. 2(6), 507-512 (1967).

72. Sigri GmbH, Meitingen, FRG, brochure on "Sigradur," 1970.

73. Lockheed Missile & Space Co., Palo Alto, Calif., "LMSC glass-like carbon," Report 6-78-69-33, August 1969.

74. Terwiesch, B., Pyrolysis of molded polyimides, unpublished report, 1972.

75. Imperial Chemical Industries (ICI), private communication, 1972.

76. Neumann, A. W., Z. Phys. Chem. (New Series) 41, 339-352 (1964).

77. Neumann, A. W., Tanner, W.,"Examples of applied research," Jahrbuch 1966/1967 der Fraunhofer-Gesellschaft [1966/1967 yearbook of the Fraunhofer Society], pp. 39-42.

78. Neumann, A. W., Chem. Ing. Tech. 42(15), 969-977 (1970).

79. Wenzel, R. N., J. Phys. Coll. Chem. 53, 1466-1467 (1949).

80. Beyer, W., Glasfaserverstärkte Kunststoffe [Fiberglass-reinforced plastics], 3rd Edition, Carl Hanser-Verlag, Munich, 1963.

81. Rosato, D. V., Grove, C. S., Jr., "Filament winding: its development, manufacture, applications, and design," Interscience Publishers, New York, London, Sidney, 1964.

82. Peters, D. M., Design Eng. (September 1968).

83. Morganite Research and Development Ltd., London, "Modmor high modulus carbon fibres," New Products Data Sheet R25/10-68/5M, Reprint 10-69/2M.

84. Union Carbide Corp., Carbon Products Div., New York, Technical Information Bulletin No. 465-201 IF.

85. Ray, J. D., "Mechanical properties of high-performance plastics composites," Paper No. 29 of the International Conference on "Carbon fibres, their composites and applications," The Plastics Institute, London, February 1971.

86. Union Carbide Corp., Carbon Products Div., New York, Technical Information Bulletin No. 465-206 BI.

87. Simon, R. A., Barnet, F. R., "The mechanical properties of carbon-fibre composites," Paper No. 26 of the International conference on "Carbon fibres, their composites and applications," The Plastics Institute, London, February, 1971.

88. Morganite Research and Development Ltd., London, New Products Data Sheet No. M2. 6/69. G.

89. Fuhrmann, U., Garnish, E. W., Niederhauser, U., Kunststoffe 59(12), 865-869 (1969).

90. Courtaulds Ltd., Coventry, England, Data Sheet FSL2 (August 1968).

91. Imperial Chemical Industries (ICI), Welwyn Garden City, Herts, England, "Polyimide Resins: Laminating resin QX-13," Product Information (February 1970).

92. Rogers, K. F., Kingston-Lee, D. M., "Heat-resistant carbon-fibre/polyimide-resin composites," Paper No. 34 of the International conference on "Carbon fibres, their composites and applications," The Plastics Institute, London, February 1971.

93. Darmory, F. S., Hirsch, S. S., Kaplan, S. L., "P 13 N: polyimide laminated varnish," Proceeding of the Annual Institute of Printed Circuits Meeting, Washington, April 1971.

94. Union Carbide Corp., Carbon Products Div. in association with Case Institute of Technology and Bell Aerosystems Co., a Textron Co., "Integrated research on carbon composite material," Technical Report AFML-TR-66-310, Part I, Air Force Materials Laboratory, Wright-Patterson AFB, Ohio, October 1966.

95. Terwiesch, B., Private communication, 1972.

96. Müller, D. J., Dissertation, Chemical Engineering Institute, University of Karlsruhe, 1973.

97. Hinrichsen, G., Angew. Makromol. Chem. 20, 121-127 (November 1971).